Corticosteroid-Encapsulated Nanoparticles in Thermoreversible Gels for the Amelioration of Choroidal Neovascularization in Age-Related Macular Degeneration

Anjali Hirani

Dissertation submitted to the Faculty of the Virginia Polytechnic Institute and State University in partial fulfillment of the requirement for the degree of

Doctor of Philosophy
in
Biomedical Engineering

Yong W. Lee, Chair
Luke E. Achenie
Aaron S. Goldstein
Liwu Li
Vijaykumar B. Sutariya
Yashwant Pathak

April 1, 2015
Blacksburg, VA

Keywords: Choroidal Neovascularization, Age-Related Macular Degeneration, Sustained Drug Delivery

Corticosteroid-Encapsulated Nanoparticles in Thermoreversible Gels for the Amelioration of Choroidal Neovascularization in Age-Related Macular Degeneration

Anjali Hirani

Abstract

Age-related macular degeneration (AMD) is one of the leading causes of blindness in adults over the age of 60. Currently, at least 11 million patients in the United States have some form of macular degeneration and this number is projected to grow as the population ages. The more severe form of the disease – neovascular (wet) AMD, is characterized by intraocular neovascularization, inflammation, and retinal damage; however, the disease progression can be deterred through intraocular injections of anti-angiogenic agents. The complications and burden that arise from repetitive injections as well as the difficulty posed by targeting the posterior segment of the eye make this an interesting territory for the development of novel drug delivery systems. New methods for drug delivery are being investigated exploring the use of nanoparticles and other polymeric materials.

The goal of this project is to study the potential use of poly(lactide-co-glycolic acid)-polyethylene glycol (PLGA-PEG) nanoparticles in thermoreversible gels as localized sustained intraocular drug delivery. We prepared stable and reproducible corticosteroid-encapsulated nanoparticles in thermoreversible gels to inhibit vascular endothelial growth factor (VEGF) overexpression characteristic of neovascular AMD. We characterized the drug delivery system by obtaining size, shape, and drug encapsulation data. We also demonstrated that the polymer could be injected into the vitreous as a solution and transition to a gel phase based on the temperature difference between regular indoor environment and the vitreous body. The drug delivery system was tested on human retinal pigment epithelial cells (ARPE-19), for cytotoxicity, uptake and VEGF expression.

We also examined the drug delivery system's ability to mitigate the disease progression in a mouse model of choroidal neovascularization (CNV). The effect on blood vessel area was shown and the changes in the mRNA expression of angiogenesis mediators were analyzed by

real-time reverse transcription polymerase chain reaction (RT-PCR). These results indicate that the proposed drug delivery systems has the promise to be developed for retinal diseases, involving CNV, including neovascular AMD. Further studies are warranted in developing this promising intraocular drug delivery system for wet AMD and similar ophthalmic diseases.

Acknowledgements

This journey has been carried out with incalculable support and advice from numerous individuals. I would first like to express my gratitude and respect to my advisor, Dr. Yong Woo Lee, for your guidance and patience throughout my graduate studies. I will always admire your scientific expertise and analytical skills. Everything I have achieved is due to your influence and support.

I would like to acknowledge my committee members for their insight and their individual efforts in helping me through this process. I could not have completed this work without the help and expertise of Dr. Yashwant Pathak. You have taught me the true meaning of a guru and gave me a way to follow my dreams when I thought there were no other options available. I will always be grateful to you. Dr. Sutariya, thank you for opening your lab to me and giving me a position here. You have given me so many opportunities in such a short time and so much of the progress I made is due to you. You have reignited my interest in research and I have looked forward to coming in and working each and every day.

Dr. Luke Achenie, I have learned so much from you on other projects over the past several years. Your passion for science and academia is inspiring. Dr. Aaron Goldstein, thank you for your willingness to guide me in the projects I have worked on over the years. It has been a pleasure to learn from you. Dr. Liwu Li, you are truly an expert in your field and I appreciate your advice.

Additionally, another professor who provided tremendous support is Dr. Radouil Tzekov. Your willingness to take time out of your hectic schedule to teach a student who blindly reached out to you is humbling. It has truly been a pleasure working with you and I will aspire to guide and connect with others as you have done with me.

I would like to thank my fellow lab members, both at Virginia Tech and USF, who have become family to me: Hyung Joon Cho, Won Hee Lee, Aditya Grover, Aum Solanki, Chia Tha Thach and Xingxiao (Shelly) Li. We have created a dynamic environment together and it has been a joy to work with you on a daily basis.

No degree could be completed successfully without the support of the administrative staff and I am especially grateful to Tess Sentelle and Pam Stiff who have both been so helpful and cheerful along the way.

Most importantly, I need to thank my sister, parents and extended family members. You have supported me from the beginning, prayed for me, pushed me and even pulled me back on track when I was discouraged. My mother and father have been my rock and inspiration. I am so blessed to have my sister, Arti, in my life. Everyone should be so lucky to have their own personal cheerleader dancing alongside them in their journey.

Table of Contents

List of Abbreviations

AMD: Age-related macular degeneration

BRB: Blood retinal barrier

CNV: Choroidal neovascularization

DDS: Drug delivery system

EE: Encapsulation efficiency

ELISA: Enzyme linked immunosorbent assay

ICAM-1: Intercellular adhesion molecule-1

LE: Loteprednol etabonate

NP: Nanoparticle

PBS: phosphate-buffered saline

PDI: Polydispersity index

PDT: Photodynamic laser therapy

PEG: Polyethylene glycol

PLGA: Poly(lactide-co-glycolic acid)

RPE: Retinal pigment epithelium

RT-PCR: Reverse transcription polymerase chain reaction

TA: Triamcinolone acetonide

TEM: Transmission electron microscopy

VEGF: Vascular endothelial growth factor

List of Figures and Tables

Chapter 1. Introduction

1.1 Problem Statement

Based on the 2010 U.S. Census, it was estimated that 38.2 million people over the age of 40 are affected by vision loss due to ocular diseases in the United States (1). Age-related macular degeneration (AMD) affects the posterior segment of the eye. Specifically, the central part of the retina, responsible for the subject's ability to see fine details – the macule, is damaged by abnormal growth of blood vessels in the choroid which can penetrate into the retina itself. These newly-formed blood vessels have increased permeability and that leads to sub- and/or intestinal edema which could affect negatively central vision (2). While the exact cause is unknown, lack of nutrient supply for the macula and UV exposure are believed to contribute to the progression. Therapeutic intervention is limited due to the physiological barriers of the eye that limit potential routes of drug administration (3).

While drugs are available clinically to delay or even stop the progression of posterior segment ocular diseases, they are limited by the need for repeated intravitreal administration to maintain the therapeutic levels. The development of new drugs is time consuming and expensive; therefore, more efficient and safer drug delivery systems would benefit disease treatment. Thermoreversible hydrogels are a unique delivery vehicle for the eye. They are a type of *in situ* gels that can be administered as a solution and undergo gelation with a change in temperature (4, 5). PLGA-PEG-PLGA thermoreversible polymers can be tuned to induce gelation at body temperature (6). Additionally, nanoparticles incorporated in thermoreversible gel for use in drug delivery offer novel strategies for sustained intraocular delivery.

1.2. Background and Significance

1.2.1 Age-related macular degeneration

Age-related macular degeneration (AMD) is a sight-threatening disease that affects central vision. It is localized mostly in the central region of the retina known as the macula, which is responsible for fine vision. One of the main characteristics of AMD is the formation of subretinal deposits, called drusen. Advanced AMD can be evolve into two forms – a non-neovascular (‘dry’) form, characterized by an atrophy of the RPE and outer retina (‘geographic atrophy’) and a neovascular (‘wet’) form, characterized by choroidal neovascularization (CNV), the growth of abnormal blood vessels below or extending into the retina (7). Defects in the membrane separating the (retinal pigment epithelium) RPE and choroid (Bruch’s membrane) could lead to fluid and blood leakage into the subretinal space, leading to irregularities of the retina structure and affecting retinal function (Figure 1.1).

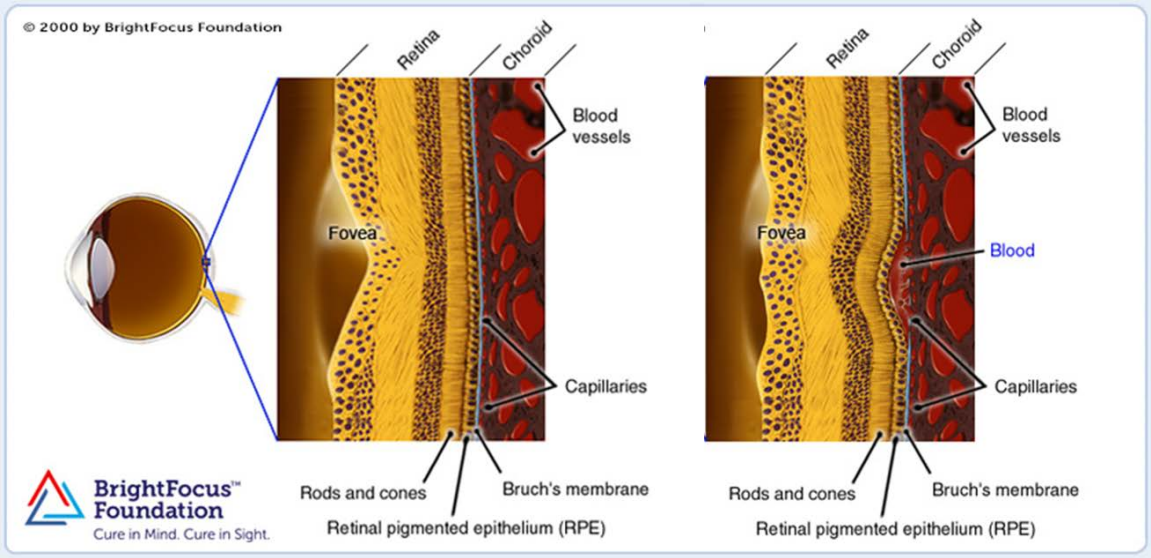

Figure 1.1: Cross section of macula at normal state (left) and with wet AMD (right) (Medical illustration courtesy of Macular Degeneration Research, a BrightFocus Foundation program (8)).

1.2.2 Vascular endothelial growth factor (VEGF)

Due to the neovascularization present in AMD, anti-angiogenic therapy is useful to slow the progression of the disease (9, 10). Vascular endothelial growth factor (VEGF) is recognized for its role in the pathogenesis of neovascular AMD as a promoter of angiogenesis and vascular permeability (11-13). The VEGF family includes VEGF-A, VEGF-B, VEGF-C, VEGF-D, VEGF-E, as well as placenta growth factor (PIGF) (14). VEGF-A is the prototype member and

commonly referred to as VEGF. VEGF is produced by many sources, including endothelial cells, photoreceptors and RPE (14). VEGF levels in the vitreous are elevated in human CNV when compared to healthy controls (14). Elevated VEGF levels lead to the breakdown of the blood retinal barrier (BRB) (13, 15) and can also increase inflammation *via* induction of inflammatory mediators like intercellular adhesion molecule-1 (ICAM-1). Therefore, VEGF is a potential pharmaceutical target for the treatment of AMD (16-18).

1.2.3 Current therapies and challenges

1.2.3.1 Anti-angiogenic drugs

Due to the implication of VEGF in the progression of AMD, anti-angiogenic drugs have been recently pursued to block the development and leakage of newly formed, abnormal blood vessels. Three anti-angiogenic drugs are currently used in the treatment of neovascular AMD: ranibizumab (Lucentis, Genentech Inc., San Francisco, CA), bevacizumab (Avastin, Genentech Inc.), and pegaptanib sodium injection (Macugen, OSI Pharmaceuticals Inc., Melville, NY) (7). Ranibizumab is a human recombinant antibody fragment that displays high binding affinity towards all VEGF-A isoforms. Clinical trials have shown that ranibizumab helps maintain stable vision without further progression of the disease in many patients with wet AMD; however, because of the high cost of the drug, the use of the drug worldwide is limited (19). Bevacizumab is a recombinant humanized monoclonal antibody, which binds all VEGF-A isoforms. It is FDA approved for colorectal, lung, and breast cancer, but is used in clinical trials for AMD and in clinical practice off-label due to lower cost. Pegaptanib is a pegylated aptamer, a single strand of nucleic acid that binds with specificity to a particular target, in this case, VEGF and thus, acts as an anti-VEGF agent. It binds the $VEGF_{165}$ isoform and inhibits angiogenesis, although less effectively than either bevacizumab or ranibizumab, which led to a considerable decline in use in recent years (20, 21). Several large, randomized, multicenter clinical trial have demonstrated that the other two drugs, bevacizumab and ranibizumab, although having different molecular structure and pharmacokinetic profile, show equivalent efficacy and safety profiles in AMD (22) and in diabetic macular edema (23). For these anti-angiogenic drugs, the biggest challenges are the route of administration and duration of action. Intravitreal injections allow for the most direct approach; however, the chronic nature of the disease requires repeated injections for the rest of

the patient's life, resulting in rare, but sight-threatening side-effects such as retinal detachment, endophthalmitis and cataract formation (24).

1.2.3.2 Corticosteroids

Corticosteroids are commonly used for treatment of various ophthalmic diseases due to their anti-inflammatory (25, 26), angiostatic, antipermeable and antifibrotic properties (27). Two of the most common used corticosteroids, especially for treatment of posterior ocular inflammatory diseases are triamcinolone acetonide and dexamethasone, often used in combination with other treatments. They act by binding steroid receptors in cells to induce or repress targeted genes, thereby inhibiting inflammatory symptoms like edema and vascular permeability (28). Corticosteroids act on VEGF by inhibiting both VEGF secretion, formation of prostaglandins, and cytokines (IL-1, IL-3, TNF-α) (26, 29). Corticosteroids can also inhibit other pro-angiogenic and inflammatory factors, like basic fibroblast growth factor, transforming growth factor-beta, and ICAM-1 and decrease VEGF levels that are evident in neovascularization (30, 31).

Ophthalmic steroids are rated by the potency of their anti-inflammatory properties. Table 1.1 gives a comparison chart of common steroids used for ophthalmic purposes.

Table 1.1: Corticosteroid comparison chart (32)

Steroid	Equivalent Glucocorticoid Dose (mg)	Anti-inflammatory potency relative to Hydrocortisone	Duration of action (hours) Half-life
Low potency			
Cortisone	25	0.8	8-12
Hydrocortisone	20	1	8-12
Upper mid strength potency			
Prednisone	5	4	12-36
Prednisolone	5	4	12-36

Triamcinolone Acetonide	4	5	12-36
High potency			
Dexamethasone	.75	25	36-54

Despite their wide clinical use, steroids can have some drawbacks. High doses of steroids can lead to adverse effects such as raised intraocular pressure and cataract formation, the later due to formation of covalent adducts with steroid and lysine residues on the lens capsule (33).

1.2.3.3. Laser therapy

Thermal laser therapy uses a target laser beam to destroy CNV formation by photocoagulation. The laser energy is absorbed mainly by melanin pigment granules in RPE cells. Thermal energy released by the heating of the melanin granules coagulates and destroys surrounding CNV areas. Clinical trials have shown the efficacy of this treatment for sub-foveal CNV with patients showing a reduction in risk of vision loss (15). While this treatment is simple and relatively inexpensive, bystander RPE cells and overlying photoreceptors also get damaged, and relatively high rates of recurrence have been observed (15).

1.2.3.4. Photodynamic laser therapy (PDT)

Verteporfin (Visudyne) is a light-sensitive drug that is absorbed by abnormal blood vessels. The dye is activated with a low-intensity laser light (wavelength 689 nm). In the illuminated area, the drug generates highly reactive short-lived singlet oxygen and free radicals that damage abnormal vessels while having a relatively small effect on the overlaying RPE and retina. However, it was found that when applied in full fluency, the damaging effect is not limited to the treated area and the newly formed blood vessels only, but can extend beyond it and affect the healthy nearby retina (34). This led to the instruction of protocols of reduced laser intensity (reduced-fluence) photodynamic therapy (35). Furthermore, the treatment is expensive and side effects include transient visual disturbances, adverse effects at site of injection, and photosensitivity reactions (13). Additionally, eyes with larger CNV lesions and good visual acuity do not benefit from PDT (13).

1.2.4 Routes of drug administration

The posterior segment of the eye consists of the retina, vitreous, choroid and sclera. While the anterior segment of the eye can be readily accessed for topical treatment, multiple physical barriers and clearance mechanisms prevent easy access to the posterior segment. The topical route is a convenient method of drug delivery; however, there is poor bioavailability due to nasolacrimal drainage and systemic absorption (36). A model of transient diffusion has shown that less than 5% of a lipophilic drug and 0.5% of a hydrophilic drug reach the anterior chamber (37). The amount of available drug transported further decreases across the sclera, choroid, and retinal pigment epithelium (RPE) (38). Permeability *via* sclera is reduced with cationic and lipophilic solutes, and the RPE has tight intercellular junctions for hydrophilic molecules (38). Additionally, the lymphatic system, blood vessels and active transporters all work to clear drugs administered through transscleral routes. Drug delivery *via* systemic routes requires high doses to obtain a therapeutic concentration in the posterior eye due to the tight barrier of the RPE. Intravitreal injections circumvent physiological barriers and maintain therapeutic doses without damage to bystander tissues. However, due to the liquefaction of the vitreous body related to aging, drug delivery can be non-uniform across different retinal areas (39). Furthermore, frequent injections can lead to sight-threatening complications like retinal detachment, increase in intraocular pressure, hemorrhage and endophthalmitis (40). Given the presence of these physiological barriers, the development of therapies that efficiently deliver drugs and extend drug release to the posterior segment of the eye would be beneficial to the progression of ocular disease treatment.

1.2.5 Drug delivery systems for posterior segment ocular disorders

Age-related macular degeneration is one of the most prevalent posterior segment disorders and its chronic nature results in a challenging drug delivery problem. It currently requires multiple injections to maintain therapeutic concentrations, which can increase the risk of sight-threatening complications. Sustained drug delivery devices offer alternatives to reduce the frequency of administration and, as a result the burden on the patient and the physician. The use of drug delivery systems (DDS) provides an effective method to deliver drugs to the posterior segment of the eye for extended periods of time (several months or even years). By preparing

drug/polymer ophthalmic formulations, drug release can be controlled over an extended duration (41). For any DDS therapy to be effective, it should fulfill three major goals:

1. Drug release must be targeted to the site of action,
2. Drug release should be controlled at an optimal rate to reduce toxicity,
3. Drug should maintain therapeutic efficacy at adequate dosage levels to eliminate need for repeated administration (42).

Drug delivery systems can provide strategies to circumvent physiological barriers and provide sustained release with minimal systemic side effects, thereby expanding current disease therapy and repurposing presently used drugs and extending their patent life. Several DDS being investigated to enhance therapeutic profiles of current drug therapies are described below.

1.2.5.1 Ocular implants

Recently, ocular implants have been used to provide platforms for sustained release of steroids. They are implanted either into the vitreous or on the sclera for intravitreal or transscleral delivery. Biodegradable implants degrade in the eye and do not require surgical removal; however, the degradation process can result in inconsistent drug release profiles (3). Ozurdex™ (Allergan Inc. Irvine, CA) is composed of poly(lactide-co-glycolic acid) (PLGA) and releases dexamethasone intravitreally over a period of 4 to 6 weeks. Currently, this DDS is approved by FDA for macular edema following branch retinal vein occlusion, central retinal vein occlusion, for diabetic macular edema and for uveitis. Results have shown an improvement in intraocular inflammation for up to six months; however, surgery is required for placement and removal of the implant (3, 43). Non-biodegradable implants provide more accurate control of drug release, but also require surgical removal. Polymers such as silicone, polyvinyl alcohol, and ethylene vinyl acetate are typically used in these implants (3). Several implants are in clinical use and clinical trials; however, studies have shown that while they reduce disease symptoms, they increase intraocular pressure and cataract progression (3).

1.2.5.2 Nanoparticles

Nanoparticles have been studied extensively as drug carriers in ocular pharmaceuticals (44-47). They can be made from biodegradable, polymeric materials in which the drug can be

dissolved, entrapped, or adsorbed (48). The major benefits for implementing nanoparticles for ocular drug delivery are:

1. Ease of administration *via* injection due to size of particle.
2. Smaller particles are tolerated well in the eye.
3. Particles at the nanometer range have shown increased solubility, surface area, and drug dissolution.
4. Nanoparticles can be manipulated by polymer's weight and hydrophilicity to allow sustained drug release.
5. Particles approximately 200 nm in size can be localized in RPE cells.

Recent studies have shown that after intravitreal injection, a majority of nanoparticles were localized at the RPE within 6 hours and cytoplasmic concentrations of the NP remained elevated for as long as 4 months in rats (49).

PLGA is an FDA-approved polymer that has been studied for biocompatibility and toxicity. The rate of degradation can be manipulated by the polymer's molecular weight, hydrophilicity, and ratio of lactide to glycolide in order to extend the release time of drugs (50). Polyethylene glycol (PEG) also has a slow clearance from blood, allowing increased drug release. PEG reduces uptake by reticulo-endothelial system in blood compared with unmodified PLGA RES system clearance (51-53). When bevacizumab, an anti-VEGF antibody, was incorporated in PLGA-PEG, it showed sustained release for up to 60 days (54). In another study, when corticosteroid triamcinolone acetonide was encapsulated by PLGA, inflammation associated with ocular diseases was reduced. The drug/polymer ratio was shown to affect the entrapment efficiency and release profiles (47).

1.2.5.3 Thermoreversible gels

Thermoreversible hydrogels are a subtype of *in situ* gels that can be administered as a solution and undergo gelation with specific stimuli (4, 5). Specifically, thermoreversible gels are biodegradable, water-soluble polymers that undergo phase transition upon temperature elevation (36, 55). The gel can be loaded with bioactive macromolecules and pharmacological agents irrespective of their solubility properties. Since the gel forms quickly *in vivo*, it can be used to achieve localized and sustained release. They are attractive due to their ease of administration

and improved bioavailability. Studies have shown synthesis of an ABA-type block copolymer, poly(ethylene glycol)-poly(serinol hexamethylene urethane), to release bevacizumab (55, 56). The drug release profile demonstrated a sustained release over 17 weeks *in vitro*. Such therapy treatment could potentially reduce intravitreal injection frequency (55). Additional studies of thermo gels based on PLGA and PEG were able to deliver 45kDa protein across the sclera to the retina for up to 14 days (42). An alternative formulation includes Pluronic F 127 as the thermoreversible polymer and methylcellulose as a release-controlling agent. This formulation has been used to deliver nonsteroidal anti-inflammatory drugs for conjunctivitis (57) as well as selective inhibitors for glaucoma treatment (58).

1.3 Hypothesis and Specific Aims

I hypothesize that sustained-release of corticosteroid-nanoparticles incorporated in thermoreversible gels can improve the therapeutic profiles of corticosteroids for choroidal neovascularization in wet age-related macular degeneration by reducing the frequency of intravitreal injections. The hypothesis is tested by the following three specific aims:

1. Preparation and characterization of corticosteroid-encapsulated nanoparticles incorporated into thermoreversible gels. Nanoparticles including corticosteroid are prepared by an emulsion solvent evaporation technique and incorporated into a thermoreversible gel. The drug delivery system is characterized by obtaining size, shape, drug encapsulation, gelation properties and *in vitro* sustained release profiles.
2. Examination of the effects of the corticosteroids, nanoparticles, and thermoreversible gel on cytotoxicity, VEGF expression, and cellular uptake in ARPE-19 cells.
3. Determination of the effect of corticosteroid-nanoparticles incorporated in thermoreversible gel on chemically induced choroidal neovascularization in mice. The effects of the drug delivery system on the size of choroidal neovascularization area in a mouse model are examined.

This study examines the potential of a sustained drug delivery system to reduce the frequency of intravitreal injections in the treatment of choroidal neovascularization. The drug delivery system utilizes a dual approach with a PLGA-PEG-PLGA triblock thermoreversible polymer to suspend corticosteroid nanoparticles. The thermoreversible polymer will hold the drug-encapsulated nanoparticles at the site of administration and allow for controlled release of the corticosteroids over a longer duration. This work can help lead to the development of more effective therapies for age-related macular degeneration.

Chapter 2. Triamcinolone Acetonide Nanoparticles Incorporated in Thermoreversible Gels for Age-Related Macular Degeneration

Anjali Hirani[1,2], Aditya Grover[1], Yong W. Lee[2], Yashwant Pathak[1], Vijaykumar Sutariya[1*]

[1] Department of Pharmaceutical Sciences, USF College of Pharmacy, University of South Florida, Tampa, FL 33612

[2] School of Biomedical Engineering and Sciences, Virginia Tech-Wake Forest University, Blacksburg, VA 24061

Manuscript published in Pharmaceutical Development and Technology 2014 Sep 26:1-7. [Epub ahead of print]

2.1. Abstract

Age-related macular degeneration (AMD) is one of the leading causes of blindness in the US affecting millions yearly. It is characterized by intraocular neovascularization, inflammation, and retinal damage which can be ameliorated through intraocular injections of glucocorticoids. However, the complications that arise from repetitive injections as well as the difficulty posed by targeting the posterior segment of the eye make this interesting territory for the development of novel drug delivery systems. In the present study, we described the development of a drug delivery system composed of triamcinolone acetonide-encapsulated PEGylated PLGA nanoparticles incorporated into PLGA-PEG-PLGA thermoreversible gel and its use against VEGF expression characteristic of AMD. We found that the nanoparticles with mean size of 208±1.0 nm showed uniform size distribution and exhibited sustained release of the drug. We also demonstrated that the polymer can be injected as a solution and transition to a gel phase based on the biological temperature of the eye. Additionally, the proposed drug delivery system was non-cytotoxic to ARPE-19 cells and significantly reduced VEGF expression by 43.5 ± 3.9% as compared to a 1.53 ± 11.1% reduction with triamcinolone. These results suggest the proposed

drug delivery system will contribute to the development of novel therapeutic strategies for age-related macular degeneration.

2.2. Introduction

Triamcinolone acetate (TA), a synthetically-modified glucocorticoid, is utilized for its anti-inflammatory and immunomodulatory effects against a number of diseases (59). TA is commonly used in conjunction with other drugs and acts by binding steroid receptors in cells and subsequently inducing or repressing target genes. This leads to an inhibition of inflammatory processes, such as edema and vascular permeability (59, 60). TA and similar glucocorticoids also act on vascular endothelial growth factor (VEGF) by inhibiting its secretion and inhibiting cytokine production (61). Such drugs can also inhibit basic fibroblast growth factor (bFGF) along with decreasing the VEGF levels characteristic of neovascularization (62). TA was shown to inhibit laser-induced choroidal neovascularization in rats as well as improve visual acuity when injected intravitreally (63, 64). However, high doses of TA and similar steroids may lead to adverse effects such as increased intraocular pressure and the formation of cataracts (65). TA is clinically used intravitreally against neovascularization in age-related macular degeneration (AMD) (59).

AMD, a progressive, inflammatory eye disease, is one of the leading causes of blindness (66). It was estimated that 36.8 million people suffered from some sort of vision loss due to eye diseases in the United States in 2010 (32). AMD affects the posterior segment of the eye through damage to retinal pigment epithelium (RPE) cells and leads to a loss of central, focused vision through the abnormal growth of blood vessels damaging the macula of the retina, the area responsible for fine vision (67, 68). The presence of intraocular debris may induce an inflammatory response which may cause further damage to the retina through the induction of a sustained immune response (69). Advanced AMD is characterized by choroidal neovascularization (CNV), the growth of abnormal blood vessels beneath the RPE or between the RPE and retina, accompanied by fluid and blood rupturing Bruch's membrane into the subretinal space and leading to retinal irregularities (70). Physical ocular barriers and routes of treatment pose limitations to therapeutic intervention in treating AMD (71).

Anti-angiogenic therapy is useful in slowing the progression of AMD due to the neovascularization characteristic of the disease. Vascular endothelial growth factor A (VEGF-A)

is the most potent promoter of angiogenesis and vascular permeability and its role in the pathogenesis of neovascular AMD is well recognized (72, 73). VEGF-A levels are elevated in human CNV and its vitreous levels have been reported to be increased when compared to healthy controls (15). VEGF is a potential pharmaceutical target; elevated VEGF levels can increase inflammation *via* inducing inflammatory mediators like intercellular adhesion molecule-1 (ICAM-1) and subsequently lead to the breakdown of the blood retinal barrier (BRB) (74, 75).

The anatomy of the eye is a challenging part of the body for drug delivery. The posterior segment of the eye consists of the retina, vitreous, and choroid. Topical treatment can easily access the anterior portion of the eye; however, multiple physical barriers and clearance mechanisms prevent easy access to the posterior segment of the eye. The topical route is the most favored and convenient for drug delivery, but nasolacrimal drainage and systemic absorption results in a poor drug bioavailability (76). A model of transient diffusion has shown that less than 5% of a lipophilic drug and 0.5% of a hydrophilic drug reach the anterior chamber (74). The bioavailability of the drug further decreases across the sclera, choroid, and RPE (75). Drug permeability through the sclera is reduced with cationic and lipophilic solutes and RPE have tight intercellular junctions to prevent the permeation of hydrophilic molecules (75). Furthermore, the lymphatic system, blood vessels, and active transporters all work to clear drugs administered through transscleral routes. Drug delivery through systemic administration requires high doses to obtain a therapeutic concentration in the posterior segment of the eye due to the tight barriers in RPE. Intravitreal injections circumvent the physiological barriers and maintain therapeutic doses without damaging bystander tissue; however, frequent injections can lead to complications like retinal detachment, increase in ocular pressure, and hemorrhage (40). Given the presence of these physiological barriers, the development of therapies that efficiently deliver drugs and extend drug release to the posterior segment of the eye would be beneficial to the progression of ocular disease treatment.

Although current therapies exist to slow the progression of AMD, alternative drug delivery systems (DDS) are needed to enhance the therapeutic profiles of these drugs. Nanoparticles (NP) have been studied as drug carriers in ocular pharmaceuticals (77-80). They can be made from biodegradable, polymeric materials in which drugs can be dissolved, entrapped, or adsorbed (81). The major benefits for implementing NPs for ocular drug delivery are: 1) Ease of administration *via* injection due to the size of the particle, 2) smaller particles are

well tolerated in the eye, 3) particles of the nanometer range have shown increased solubility, surface area, and drug dissolution, 4) NPs can be manipulated by polymer's weight and hydrophilicity to allow sustained drug release, and 5) particles approximately 200 nm in size can be localized in RPE cells. In addition, recent studies have shown that after intravitreal injections, a majority of NPs were localized at the RPE within 6 hours and cytoplasmic concentrations of the NP remained elevated for as long as 4 months (82).

Poly(lactide-co-glycolic acid) (PLGA) is an FDA-approved polymer that has been studied due to its biocompatibility and toxicity. The rate of degradation can be manipulated by the polymer's molecular weight, hydrophilicity and ratio of lactide to glycolide to extend the release time of associated drugs (83). PLGA NPs have been shown to have controlled drug release, low cytotoxicity, and few side effects (84, 85). Polyethylene glycol (PEG) has a slow clearance from the blood, allowing an increased drug release and reducing PLGA NP uptake by the reticulo-endothelial system (RES) when chemically conjugated to the PLGA vector as compared to non-conjugated PLGA (84-86). PEGylated PLGA NPs of bevacizumab, an anti-VEGF antibody, showed sustained release of the drug over 60 days (87). In another study, TA encapsulated in PLGA NPs revealed a decrease in inflammation associated with ocular diseases (80).

Thermoreversible hydrogels (TR gels) are a subtype of *in situ* gels that can be administered as a solution and undergo gelation with specific stimuli (88, 89). Specifically, TR gels are biodegradable, water soluble polymers that undergo phase transitions upon temperature elevation (76, 90). The gel can be loaded with bioactive macromolecules and pharmacological agents irrespective of their solubility properties. Localized and sustained release can be achieved due to the gel's quick formation *in vivo*. Their improved bioavailability and ease of administration make them an attractive DDS. Studies have shown the synthesis of an ABA-type block copolymer, poly(ethylene glycol)-poly(serinol hexamethylene urethane), to release bevacizumab. The *in vitro* drug release profile achieved a longer therapeutic window over 17 weeks. Such treatments could potentially reduce the frequency of intravitreal injections (90). An alternative formulation includes Pluronic F 127 as the thermoreversible polymer and methyl cellulose as a release controlling agent. This formulation has been used to deliver nonsteroidal anti-inflammatory drugs for conjunctivitis as well as selective inhibitors for glaucoma (91, 92).

The present study described the preparation of TA encapsulated PLGA-PEG NPs incorporated into TR gel to improve the therapeutic profile of TA in AMD. We showed that the NP size is appropriate for intracellular uptake, the NPs and TR gel demonstrate a sustained release of the drug over 10 days, the NP and TR gel vectors are nontoxic in ARPE-19 cells, and the NP and TR gel DDS is able to reduce VEGF levels in ARPE-19 cells. These results suggest that the proposed DDS has the potential to significantly improve current therapies against AMD.

2.3. Materials and Methods

2.3.1. Materials

Poly(lactic-co-glycolic acid) (PLGA) conjugated with polyethylene glycol (PEG) (PEG-PLGA) (5050 DLG, mPEG 5000, 5wt% PEG) was purchased from Lakeshore Biomaterials (Birmingham, AL). Triamcinolone acetonide was purchased from Alfa Aesar (Ward Hill, MA). Poly(lactide-co-glycolide)-b-Poly(ethylene glycol)-b-Poly(lactide-co-glycolide) [PLGA-PEG-PLGA (Mn ~ 1,100:1,000:1,100 Da, 3:1 LA:GA) (25% PEG)] thermogelling polymer was purchased from Polyscitech (West Lafayette, IN). Phosphate buffered saline (PBS) solution was purchased from Mediatech, Inc (Manassas, VA). Thiazolyl blue tetrazolium bromide (MTT reagent), acetone and methanol were purchased from Sigma Aldrich (St. Louis, MO). All other chemicals used in the study were of analytical grade and were used without any further purification unless specified.

2.3.2. Nanoparticle synthesis

TA NPs were prepared using a previously reported nanoprecipitation method (80, 84). Briefly, 22 mg of TA and 110 mg of PEGylated PLGA were dissolved in 2 mL acetone (organic phase) and the resulting solution was added dropwise to 20 mL of deionized H_2O (40^o C) spinning at 300 rpm overnight to allow the full evaporation of the organic phase and the formation of the NP suspension. The NPs were separated by centrifugation at 3,000 rpm for 10 minutes and resuspended in fresh deionized H_2O.

2.3.3. Nanoparticle characterization

The NP parameters were studied by measuring the particle size and polydispersity index (PDI). The effect of loading TA into the NPs on these parameters was studied by comparing TA NPs to blank NPs. Particle size and PDI were measured using the Dynamic Pro plate reader (Wyatt Technology Corporation, Santa Barbara, CA). The NP samples were diluted 1:5 in deionized water to fit instrument specifications.

2.3.4. Drug encapsulation efficiency

Drug encapsulation efficiency was determined by using a previously reported method (84). 1 mL of the NP solution was centrifuged at 12,000 rpm for 5 minutes. The supernatant was removed and was replaced with 1 mL of methanol and stored at 4^{o} C overnight. The supernatant of the NP/methanol solution was diluted 1:5 times and measured by UV spectroscopy at a wavelength of 240 nm (λ_{max}). The supernatant was analyzed and compared to a series of standard dilutions of TA in methanol (r^2=0.99764). Encapsulation efficiency was determined using the following equation:

$$\%\ Entrapment\ Efficiency\ = \frac{Actual\ drug\ amount}{Theoretical\ drug\ amount} \times 100$$

2.3.5. Preparation of thermoreversible gels

TR gels were prepared using the cold method (93). To prepare 20% w/v gel, 100 mg of PLGA-PEG-PLGA gel was solubilized in deionized H_2O overnight at 4^{o} C. Different percentages of the gel (10, 15, 20, 25, 30% w/v) were screened for the most optimal gelation temperature.

2.3.6. Determination of gelation temperature

Gelation temperature was detected by visual inspection using a previously published method (89, 94). Aqueous solutions of the gel (10, 15, 20, 25, 30% w/v) were prepared in distilled deionized H_2O and 500 µL of each solution was heated from 10^{o} C to 60^{o} C. At each 1^{o} C interval, the tubes were inverted to investigate flow properties. Solutions were considered to be in the gel state if no flow was observed following tube inversion.

2.3.7. *In vitro* release

NPs: The rate of TA release from the NPs was measured by adapting a previously reported method (95). Dialysis membrane tubing, MWCO 10,000 Da. (Spectrum Laboratories, Rancho Dominguez, CA) was soaked in deionized H_2O overnight. 1 mL of the NP suspension was added to the dialysis membrane tubing after being briefly sonicated, and were placed into 100 mL of PBS covered and stirring at 100 rpm at 37^o C. 1 mL samples were removed at predetermined intervals over 10 days and replaced with fresh PBS. Samples were analyzed using UV spectroscopy at a wavelength of 240 nm (λ_{max}) and compared to standard dilutions of TA in PBS (r^2=0.989) to determine the percentage of drug released over 10 days.

TR gel: The rate of TA release from the TR gel was measured by dispersing TA NPs in 200 µL of 20% w/v polymer solution and allowed to gel by placing in incubator at 37°C for 5 minutes. After gelling, release was initiated by adding 2.5 mL PBS. 1 mL samples were removed at predetermined intervals over 10 days and replaced with fresh PBS (94).

2.3.8. Cell culture

Human retinal pigment epithelium, ARPE-19, cells (ATCC # CRL-2302) were grown in 1:1 Dulbecco's Modified Eagle's Medium and Ham's F12 Medium (Mediatech, Inc., Manassas, VA) with 10% fetal bovine serum and 100 U/mL penicillin/streptomycin (Sigma Aldrich, St. Louis, MO). The cultures were maintained in a humid environment at 5% CO_2 and 37^o C.

2.3.9. Cytotoxicity

The cytotoxicity of the DDS was assessed in ARPE-19 cells by the 3-(4,5-dimethylthiazol-2-yl)-2,5-diphenyltetrazolium bromide salt (MTT) assay. Briefly, cells were seeded in 24-well plates at a density of 5 x 10^4 cells/mL for 24 hours to achieve confluency before treatment. Cells were exposed to free TA, TA NPs, and TA NP-TR gel at varying concentrations (0, 1, 10, 100 µM) for 24 hours after which the MTT assay was performed. Cell culture media were aspirated and 500 µL of MTT reagent solution (1 mg/mL) was added to each well. Cells were incubated at 37^o C and 5% CO_2 for 4 hours, after which the MTT reagent solution was aspirated and 1 mL of DMSO was added to each well. Plates were allowed to shake gently for 10 minutes before being read by Synergy H4 plate reader (Biotek Industries, Inc., Winooski, VT) at absorbance of 570 nm.

2.3.10. VEGF secretion

ARPE-19 cells were seeded onto 24-well plates at 5 x 10^4 cells/mL and allowed to grow until confluence. On the day of study, cell culture media were replaced with 1% FBS experimental media and allowed to remain in quiescence for 12 hours. The cellular monolayers were incubated with varying treatment concentrations of free TA solution (1, 10, 100 μM), TA NPs (10, 100 μM), and TA NP-TR gel (10, 100 μM). Culture media were collected at 12 and 72 hours. Secreted VEGF in collected culture media was quantified by the ELISA method (Human VEGFA ELISA kit, Thermo Scientific, Waltham, MA). The cell protein content was assayed using the BCA protein assay kit after lysing the cells and VEGF secretion was normalized to total protein. Samples were read by using the Synergy H4 plate reader (Biotek Industries, Inc., Winooski, VT) with absorbance at 450 nm minus absorbance at 550 nm.

2.3.11. Statistical analysis

Statistical analyses were performed using GraphPad Prism (GraphPad Software, Inc., San Diego, CA). Comparisons of the effect of free TA solution, TA NPs, and TA NP-TR gels on cell viability and VEGF expression were assessed using paired t-tests with a significance level (p) of 0.05. All experiments were carried out in triplicates (n=3) and shown as mean values ± SD.

2.4. Results

2.4.1. Nanoparticle characterization

Dynamic Pro plate reader was used to determine the size and PDI of the blank and TA-loaded NPs. The TA NPs were larger in size than the blank NPs. PDI data revealed that all NP formulations had a narrow average size distribution (Table 2.1).

Table 2.1: NP characterization data carried out in triplicates (n=3) and represented as the mean value ± SD.

NP Type:	Particle size (nm):	PDI:
Blank NP	125.10 ± 43.89	0.014 ± 0.004
TA NP	208.00 ± 1.00	0.005 ± 0.001

2.4.2. Drug encapsulation efficiency

UV spectroscopy was used to determine the encapsulation efficiency of TA by comparing the absorbance in methanol to standard dilutions of TA in methanol (r^2=0.99764) at 240 nm (λ_{max}). It was found that 42.4 ± 0.09% of the TA added during formulation was taken up by the NPs.

2.4.3. Determination of gelation temperature

Phase transition studies revealed that the 15% w/v aqueous solution of the polymer converts to the gel phase at 40^o C and remains in a gel state until 47^o C. The gel phase is broader with higher % w/v solutions. The 20% w/v gel solution demonstrated an optimal transition within physiological conditions and was employed for future studies. Figure 2.1 shows the temperature at which each gel formulation transitioned from the solution state to gel state. Figure 2.2 gives a visual depiction of the phase change from a solution at 4^o C to a gel at 37^o C with the 20% w/v polymer.

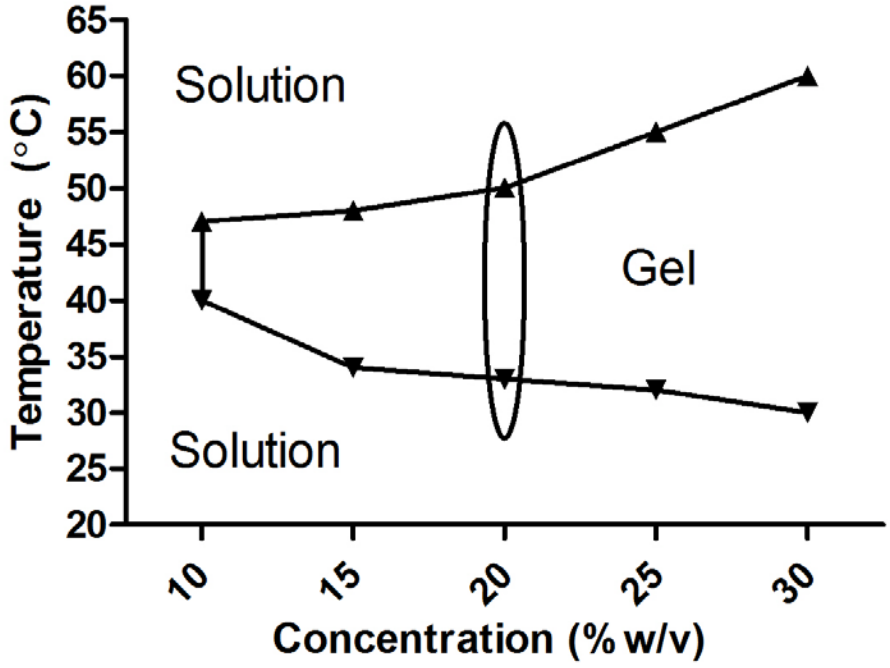

Figure 2.1: Temperature-dependent phase transitions in PLGA-PEG-PLGA thermoreversible gels based on w/v concentration of gel in aqueous solution. The 20% w/v thermoreversible gel was chosen for further studies because its phase transition occurs over physiologically relevant temperatures.

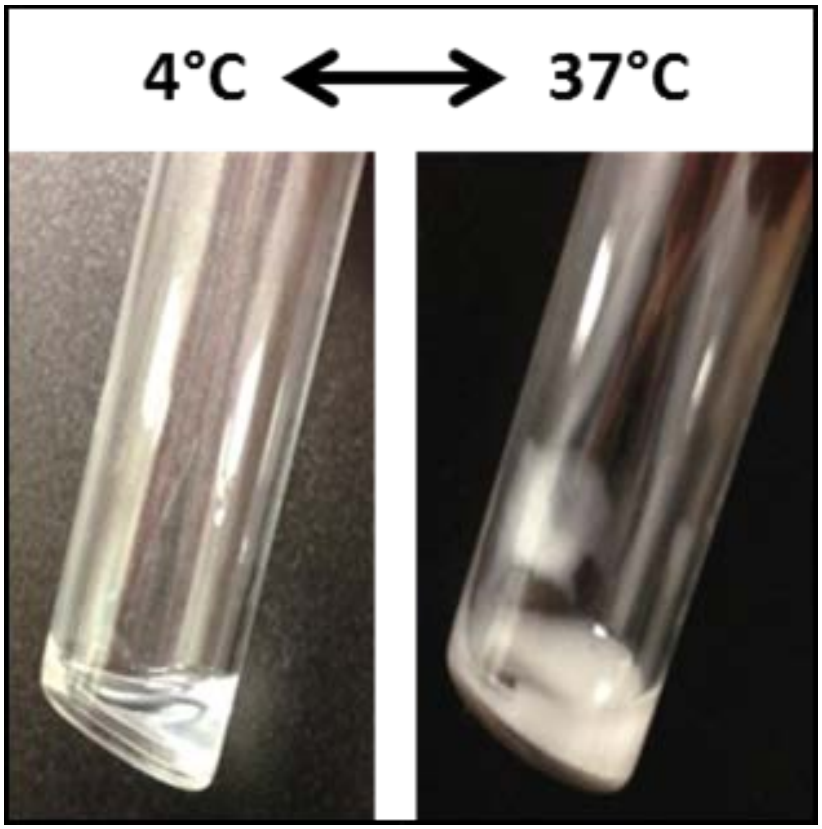

Figure 2.2: Pictorial representation of the temperature-dependent phase change exhibited by the 20% w/v PLGA-PEG-PLGA thermoreversible gel. The gel solution exists in the liquid state at 4° C and transitions into a gel state at 37° C.

2.4.4. *In vitro* release

The release of TA from NPs and TR Gel was investigated in 100 mL of PBS and 37° C. Figure 2.3 shows the cumulative release profile of the TA NP formulation and TA NP Gel as compared to equal concentrations of the free TA solution. At 48 hours, free TA was fully released while the TA NPs released 48.9 ± 7.0% of encapsulated drug and the TA NP Gel released 23.24 ± 6.7% of drug. At 168 hours, the cumulative release of TA from the NP formulations was 94.17 ± 20.8%. There is a lack of initial burst release of drug from the NPs. TR Gel had released 31.49 ± 5.1% of drug at 10 days.

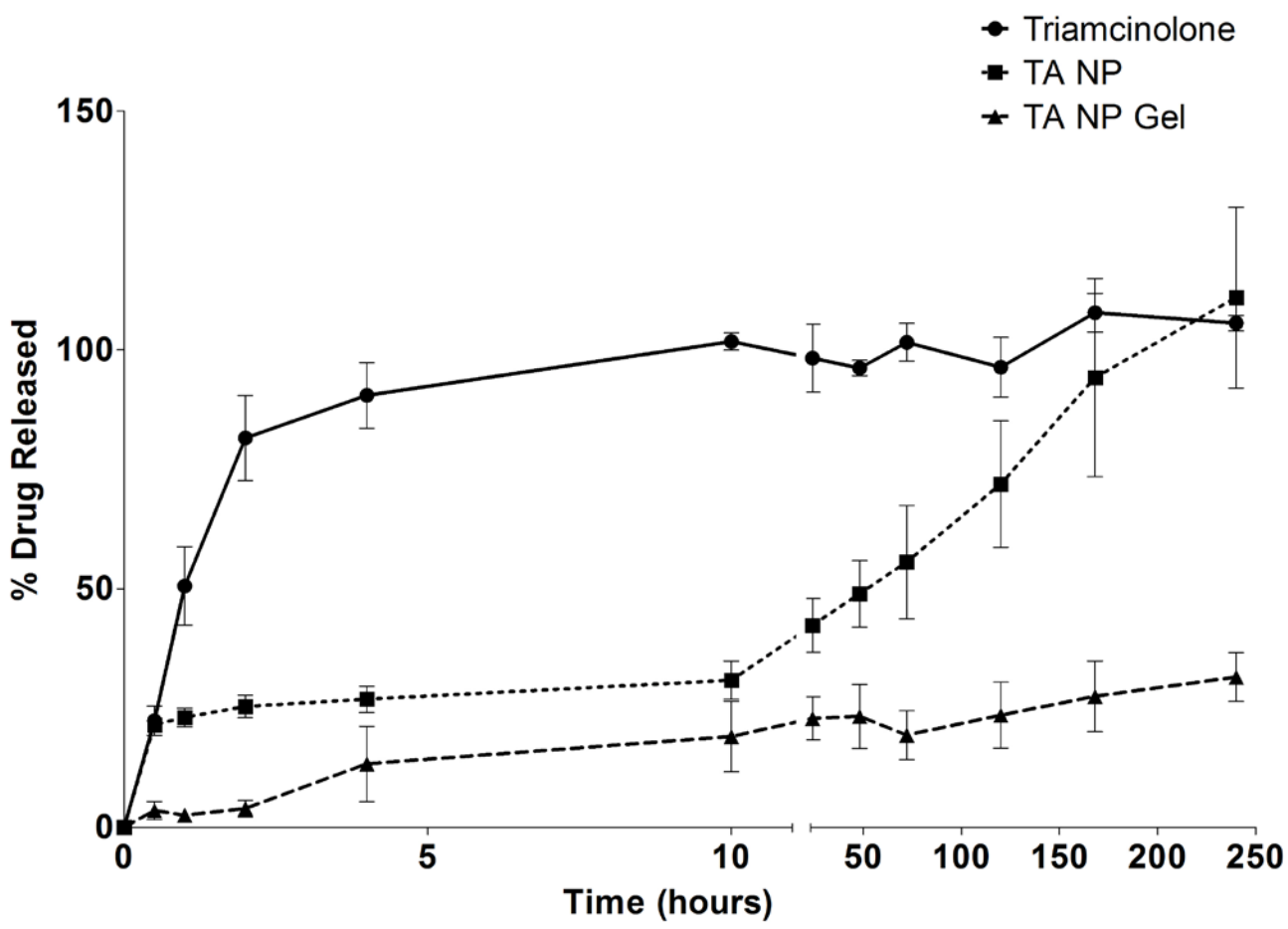

Figure 2.3: *In vitro* release data of the TA NP and TA NP Gel as compared to equal concentrations of the TA drug. Samples were analyzed by UV spectroscopy (240 nm, λ_{max}) at predetermined intervals over a 10-day period (*n*=3, mean value ± SD).

2.4.5. Cytotoxicity

The cytotoxicity of the DDS was investigated by MTT assay in the ARPE-19 cells to determine any possible harm related to its use. Figure 2.4 compares the cytotoxicity data of the free TA with equal concentrations (10 µM) of the different TA DDS's described in the present study: The blank NPs, TA NPs, the TA in 20% w/v TR gel, and the TA NP in 20% w/v TR gel. The free TA induced significant cell death in ARPE-19 cells as compared to the untreated control cells. All other treatments were not significantly cytotoxic in ARPE-19 cells.

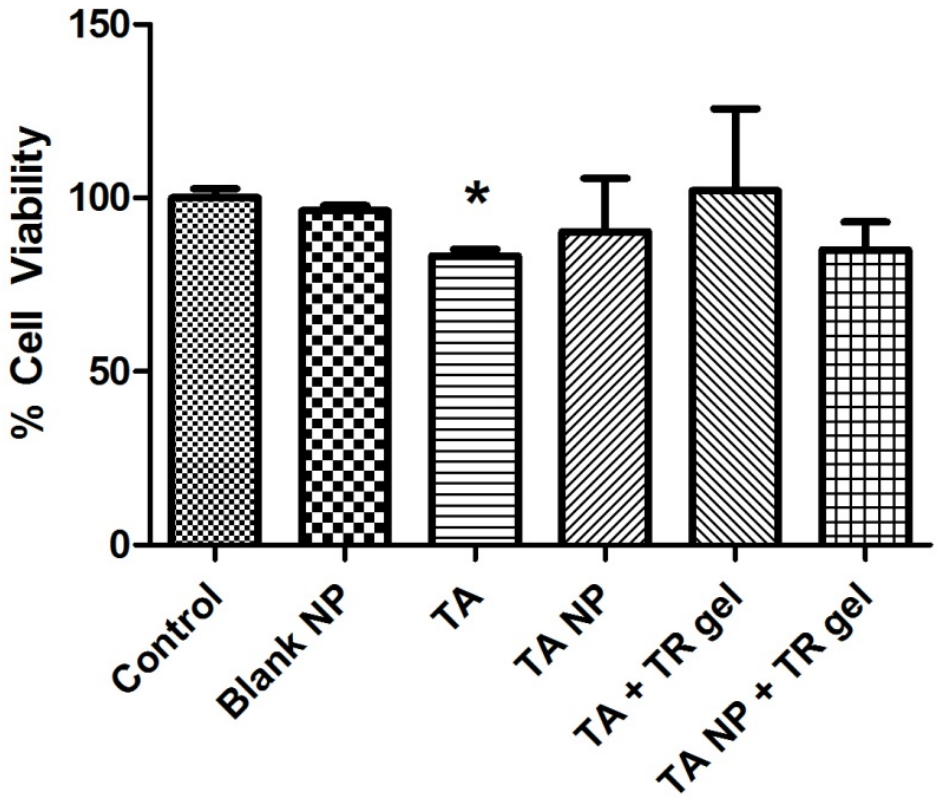

Figure 2.4: MTT cytotoxicity data in ARPE-19 cells of equal treatments (10 µM) of the following: Blank NP, TA free drug, TA NPs, TA drug in 20% w/v TR gel, and TA NPs in 20% w/v TR gel as compared to untreated control cells. Experiments were carried out in statistical triplicates (*n*=3) and quantified by absorbance reading at 570 nm (Synergy H4 Plate reader, Biotek Industries Inc.). Data is represented as mean number of viable cells ± SD. Statistical tests were carried out using paired t-test ($p \leq 0.05$).

2.4.6. VEGF secretion

The effect of the different TA NP formulations on VEGF secretion was studied in ARPE-19 cells. Cells were treated with different concentrations of free TA, TA NPs, TA in 20% w/v TR gel, and TA NP in 20% w/v TR gel, for 12 and 72 hours. Figure 2.5 compares the time-dependent suppression of VEGF expression among blank NPs, free TA, and TA NPs (100 µM) at 12 and 72 hours. The blank NPs did not reduce VEGF expression throughout the time periods tested. The free TA significantly reduced VEGF secretion in 12 hours, but TA NPs were not able to do it; however, at 72 hours, free TA was unable to significantly reduce VEGF secretion but TA NPs were able to reduce VEGF secretion. Figure 2.6 compares the effect of different DDS's

(10 µM) on VEGF expression at 72 hours: free TA, TA NPs, TA in 20% w/v TR gel, and TA NPs in 20% w/v TR gel. The TA NPs, TA in 20% w/v TR gel, and TA NPs in 20% w/v TR gel all significantly reduced VEGF expression after 72 hours, but the free TA alone had no significant effect.

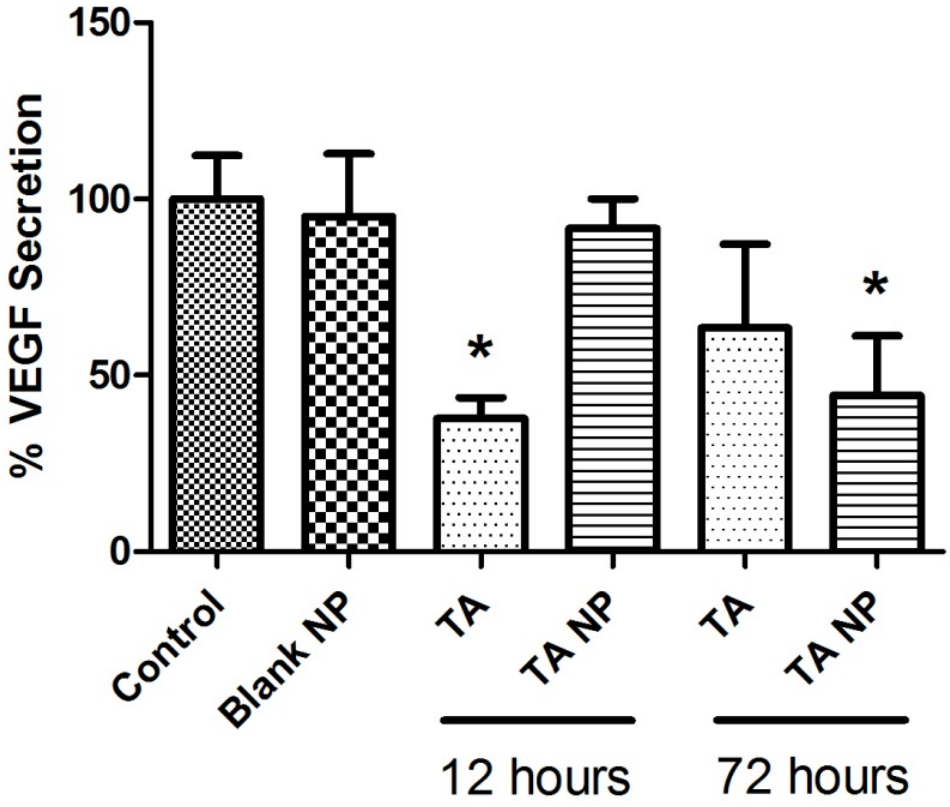

Figure 2.5: Time-dependent inhibition of VEGF secretion in ARPE-19 cells through equal concentration treatments (100 µM) of blank NPs, TA free drug, and TA NPs at 12 and 72 hours. Experiments were carried out using the ELISA method (Human VEGFA ELISA kit, Thermo Scientific) in statistical triplicates (*n*=3). Data is represented by amount of VEGF secretion normalized to untreated control levels ± SD.

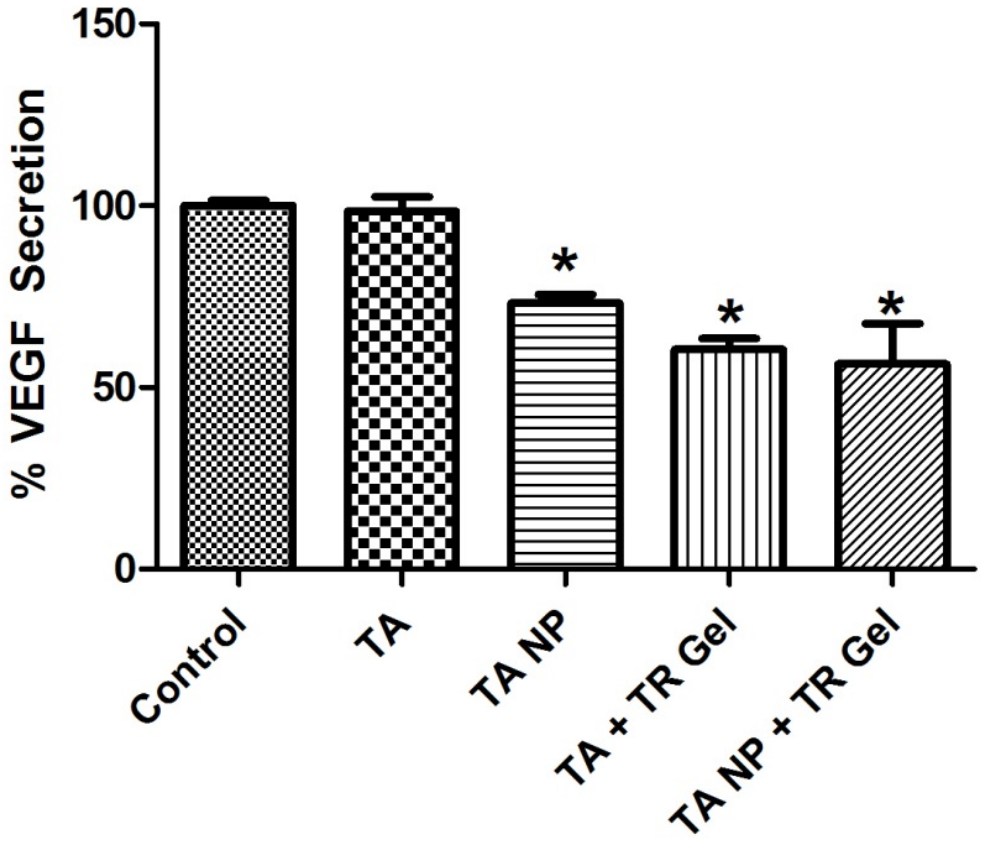

Figure 2.6: Comparative suppression of VEGF secretion in ARPE-19 cells through equal concentration treatments (10 µM) of TA free drug, TA NPs, TA drug in 20% w/v TR gel, and TA NPs in 20% w/v TR gel at 72 hours. Experiments were carried out using the ELISA method (Human VEGFA ELISA kit, Thermo Scientific) in statistical triplicates (*n*=3). Data is represented by amount of VEGF secretion normalized to untreated control levels ± SD.

2.5. Discussion

The emulsion solvent evaporation process was used in the formulation of the polymeric TA NP suspension. Multiple formulations revealed consistent reproducibility with respect to particle size and encapsulation efficiency (data not shown). Particle size data showed that the average size of the NPs increases with drug loaded into the NPs as compared to the blank NPs (180-208 nm). Each of the NP formulations exhibited a unimodal size distribution, suggesting a Gaussian distribution with respect to NP size in each formulation. Particle size, PDI, and encapsulation efficiency data were corroborated with previously published studies (80, 96-98).

The release of TA from the TA NPs and TR gel was measured in 37^{o} C PBS over 10 days as compared to the release of the free TA. TA remains stable in solution as demonstrated by release data previously reported (80, 99, 100). The free TA was completely released from the dialysis membrane in the first 48 hours; however, only approximately 48.9 ± 7.0% of the drug was released from each of the NP formulations in as much time. Almost all of the drug was released from the NPs by the end of the 10 day period. The lack of initial burst release suggests that the drug was well encapsulated by the PLGA NP during formulation and none of the drug exists on the surface of the NP. The NP formulation exhibited a sustained release over the 10 day period tested. The release of entrapped drug from a polymer matrix is believed to occur in two stages: The early stage of drug release occurs through diffusion in the polymer matrix while the latter phases occur through a combination of diffusion and polymer degradation (101). 31.49 ± 5.1% of the drug was released from the TR gel at 10 days. Similar results are reported in the literature where TR gels based on PLGA and PEG were able to deliver a 45 kDa protein across the sclera to the retina for up to 14 days (102).

The gelation temperatures of different % w/v formulations of the PLGA-PEG-PLGA TR gel were investigated. It was found that an increasing % w/v of the TR gel solution broadened the temperature range over which the TR gel changes phases from solution to gel to solution (sol-gel-sol). The temperatures over which the 20% w/v TR gel phase transitioned from sol-gel-sol were best in regards to physiological conditions. The 20% w/v TR gel transitions from solution to gel at approximately 32^{o} C, which is the optimum temperature for its easy intraocular injection and phase transition into the gel phase at physiological temperatures. The incorporation of a 10 μM treatment of TA NP formulation into the 20% w/v gel did not produce any cytotoxic effects on ARPE-19 cells, suggesting its safe use in *in vivo* settings.

NP cytotoxicity studies in ARPE-19 cells showed that the PLGA NP vector is not cytotoxic although treatments with 10 μM free TA are cytotoxic under similar conditions. It was also found that not only is the PLGA vector safe for use in ARPE-19 cells but also that the TA NP formulation and TR gel DDS (with incorporated TA NPs) are not significantly cytotoxic. Concentrations of TA needed to can inhibit VEGF secretion have been previously reported (103). Consistent with those values, our studies have shown the TA NPs and TR DDS formulations were able to significantly reduce VEGF expression in ARPE-19 cells at 10 and 100 μM over 72 hours more effectively than the free TA at equal concentrations. The free TA is able

to significantly reduce VEGF expression at the 100 µM concentration in 12 hours and similar concentrations take the TA NPs 72 hours to reduce VEGF expression, which may be due to the extended release properties of the TA NPs.

2.6. Conclusion

The present study describes the potential use of a novel DDS for the amelioration of the CNV exhibited in cases of AMD. The DDS consists of two parts: TA encapsulated NPs that are incorporated into 20% w/v TR gels. The TA NPs are spherical and the shape and sizes are compatible in the cells. The NPs exhibited an extended and sustained release of TA as is evident from *in vitro* release data. Furthermore, the TA NPs and NP-incorporated 20% w/v TR gel did not exhibit cytotoxicity in ARPE-19 cells in concentrations that are shown to significantly reduce ARPE-19 cell viability by free TA alone under the same conditions. The TA NP and NP-incorporated 20% w/v TR gel were able to significantly reduce the expression of VEGF in ARPE-19 cells over 72 hours at concentrations less than those required by free TA alone (10 µM TA-loaded DDS vs. 100 µM free TA). The biocompatibility and therapeutic potential of the proposed DDS makes it an effective model for further studies investigating the pathology and treatment of AMD.

Declaration of Interest:
The authors report no declarations of interest.

Chapter 3. Efficacy of Loteprednol Etabonate Drug Delivery System in Suppression of *in vitro* Retinal Pigment Epithelium Activation

Anjali Hirani[1,2], Yong W. Lee[2], Yashwant Pathak[1], Vijaykumar Sutariya[1*]

[1] Department of Pharmaceutical Sciences, USF College of Pharmacy, University of South Florida, Tampa, FL 33612

[2] School of Biomedical Engineering and Sciences, Virginia Tech-Wake Forest University, Blacksburg, VA 24061

Manuscript accepted in Pharmaceutical Nanotechnology.

3.1 Abstract

Choroidal neovascularization (CNV) is the growth of abnormal blood vessels in the choroid layer of the eye; it is a pathophysiological characteristic of wet age-related macular degeneration (AMD). Current clinical treatment utilizes frequent intravitreal injections, which can result in retinal detachment and increased ocular pressure. The purpose of the current study is to develop a novel drug delivery system of loteprednol etabonate-encapsulated PEGylated PLGA nanoparticles incorporated into the PLGA-PEG-PLGA thermoreversible gel for treatment of AMD. The proposed drug delivery system was characterized for drug release, cytotoxicity studies and vascular endothelial growth factor (VEGF) suppression efficacy studies using ARPE-19 cells. The nanoparticles showed uniform size distribution with mean size of 168.60 ± 23.18 nm and exhibited sustained drug release. Additionally, the proposed drug delivery system was non-cytotoxic to ARPE-19 cells and significantly reduced VEGF expression as compared to loteprednol etabonate solution. These results suggest the proposed drug delivery system can be

used for further work in an animal model of experimental AMD with reduced intravitreal administration frequency.

3.2 Introduction

Loteprednol etabonate (LE), a derivative of prednisolone was the first retrometabolically designed steroid. It is a site-active corticosteroid designed to transform into an inactive metabolite after exerting its therapeutic effect. It contains an ester group at the carbon 20 position instead of a ketone (104-108). Compared to prednisolone acetate, it is less likely to increase ocular pressure and does not lead to cataract formation. Therefore, it is commonly prepared as a suspension and used topically for anterior segment disorders such as allergy conjunctivitis, anterior uveitis, and postoperative inflammation (109, 110).

Physical barriers and routes of drug administration create serious limitations in treating AMD (71). The eye is extremely challenging for drug delivery. Physical barriers and clearance mechanisms prevent access to the posterior segment of the eye. The bioavailability of a drug further decreases across the sclera, choroid, and retinal pigment epithelium (RPE) (75). Moreover, the lymphatic system, blood vessels, and active transporters all work to clear drugs administered. As a consequence, most formulations have short residence times within the eye. Due to these barriers, the development of therapies that prolong ocular residence time and enhance drug delivery and release to the posterior segment of the eye would be beneficial to the progression of ocular disease treatment.

Currently, the most efficient method to administer therapeutics for AMD is by intravitreal injections. The vitreous is gelatinous in nature, which is capable of retaining drug molecules and also delivering them to nearby structures, such as the RPE or ciliary body. Intravitreal injections circumvent the physiological barriers and maintain therapeutic doses without damaging

bystander tissue; however, frequent injections are necessary and can lead to complications like retinal detachment, increase in ocular pressure, and hemorrhage (40). Therefore, alternative drug delivery systems (DDS) are needed to enhance the therapeutic profiles of these drugs. Nanoparticles (NPs) made from biodegradable, polymeric materials in which drugs can be dissolved, entrapped, or adsorbed (81) have been studied as drug carriers for effective drug delivery to the posterior segment in ocular pharmaceuticals (77-80). Recent research has shown that NPs can localize within the RPE and maintain therapeutic effect for up to 4 months (111-113). In one study, Bourges et al. have reported distribution of polylactic acid (PLA) NPs loaded with Rh-6G fluorochromes in RPE cells of the healthy rat after 24 hours. The fluorochrome was visible for 4 months after the single injection. Another report studied different nanosuspensions prepared of three insoluble glucocorticoids, such as hydrocortisone, prednisolone, and dexamethasone, and revealed higher bioavailability and therapeutic effects of the glucocorticoid action (114). Recently, poly(lactide-co-glycolic acid)-polyethylene glycol (PLGA-PEG) NPs have been shown to have controlled drug release, low cytotoxicity, and few side effects (84, 85). Chemical conjugation with PEG reduces clearance from the blood, allowing an increased drug release and reducing PLGA NPs uptake by the reticulo-endothelial system (RES) (84-86). PEGylated PLGA NPs of anti-VEGF antibodies have shown sustained release of the drug over 60 days (87). Other PLGA DDS that have been approved for ophthalmic applications include Ozurdex$^{TM;}$ this implant releases dexamethasone intravitreally over 4 to 6 weeks. Results have shown improvement in inflammation; however surgery is required for implant and removal (3, 43). Alternative PLGA biodegradable implants are being investigated for use in cytomegalovirus retinitis with the release of ganciclovir, and for proliferative vitreoretinopathy with the release of all-trans retinoic acid (115).

Thermoreversible hydrogels (TR gels) are biodegradable, water soluble polymers that undergo phase transitions upon temperature changes (76, 90). These polymers can be loaded with therapeutic agents and can give sustained drug release *in vivo*. They are effective for use as DDS due to their improved bioavailability and ease of administration. *In vitro* drug release profile of bevacizumab loaded in an ABA-type block copolymer have demonstrated a sustained drug release over 17 weeks (90). Moreover, PLGA-PEG TR gels have also been used to deliver proteins to the retina for up to 2 weeks (102).

The present study describes a drug delivery system consisting of loteprednol etabonate encapsulated PLGA-PEG NPs incorporated into TR gel to improve the therapeutic profile of loteprednol etabonate in AMD. The proposed DDS has the potential to significantly improve current therapies against CNV.

3.3 Materials and Methods

3.3.1 Materials

Poly(lactic-co-glycolic acid) (PLGA) conjugated with polyethylene glycol (PEG) (PEG-PLGA) (5050 DLG, mPEG 5000, 5wt% PEG) was purchased from Lakeshore Biomaterials (Birmingham, AL). Loteprednol etabonate was purchased from Selleckchem (Houston, TX). Poly(lactide-co-glycolide)-b-Poly(ethylene glycol)-b-Poly(lactide-co-glycolide) [PLGA-PEG-PLGA (Mn ~ 1,100:1,000:1,100 Da, 3:1 LA:GA) (25% PEG)] thermogelling polymer was purchased from Polyscitech (West Lafayette, IN). Phosphate buffered saline (PBS) solution was purchased from Mediatech, Inc (Manassas, VA). Thiazolyl blue tetrazolium bromide (MTT reagent), acetone and methanol were purchased from Sigma Aldrich (St. Louis, MO). All other

chemicals used in the study were of analytical grade and were used without any further purification unless specified.

3.3.2 Nanoparticle synthesis

Loteprednol etabonate -loaded NPs (LE NPs) were prepared using a previously reported nanoprecipitation method (80, 84). 8 mg of LE and 55 mg of PEGylated PLGA were dissolved in 4 mL acetone (organic phase) and added dropwise to 8 mL of deionized H_2O spinning at 300 rpm overnight to allow full evaporation of the organic phase and the formation of the NP suspension. The NPs were separated by centrifugation at 3,000 rpm for 10 minutes and resuspended in fresh deionized H_2O.

3.3.3 Nanoparticle characterization

Parameters of the NPs were studied by measuring the particle size and polydispersity index (PDI). The effect of loading LE into the NPs on these parameters was studied by comparing LE NPs to blank NPs. Particle size and PDI were measured using the Dynamic Pro plate reader (Wyatt Technology Corporation, Santa Barbara, CA). The NPs samples were diluted 1:5 in deionized water to fit instrument specifications.

3.3.4 Drug entrapment efficiency

Drug entrapment efficiency was determined by using a previously reported method (84). 1 mL of the NPs solution was centrifuged at 12,000 rpm for 5 minutes. The supernatant was removed and was replaced with 1 mL of methanol and stored at 4^o C overnight. The supernatant of the NPs/methanol solution was diluted 1:5 and measured by UV spectroscopy at a wavelength of 243 nm (λ_{max}). The supernatant was analyzed and compared to a series of standard dilutions of

LE in methanol (r^2=0.9981). Encapsulation efficiency was determined using the following equation:

$$\%\ Entrapment\ Efficiency\ = \frac{Actual\ drug\ amount}{Theoretical\ drug\ amount} \times 100$$

3.3.5 Scanning electron microscopy (SEM)

SEM was utilized to visualize the surface and physical integrity of LE NPs. JOEL JSM-6490LV (JOEL Industries, Tokyo, Japan) was used to visualize the samples. The samples were diluted according to instrumental specifications and loaded onto aluminum cylinders coated with an adhesive carbon polymer. NP formulations were viewed in 15,000x magnification and 5 kv acceleration voltage was used to visualize the drug loaded NPs.

3.3.6 Preparation of thermoreversible gels

TR gels were prepared using the cold method (93).. Briefly, the 20% w/v gel was prepared by solubilizing 100 mg of PLGA-PEG-PLGA gel in deionized H_2O overnight at 4^oC.

3.3.7 *In vitro* release

LE release rate from the NPs was measured by a previously reported method (95). Dialysis membrane tubing, MWCO 10,000 Da. (Spectrum Laboratories, Rancho Dominguez, CA), was soaked in deionized H_2O overnight. NPs solutions were sonicated, and 1 mL was added to the dialysis membrane tubing; tubing was placed into 100 mL of PBS and stirred at 100 rpm at 37^o C. 1 mL samples were removed at predetermined intervals over 7 days and replaced with fresh PBS. Samples were analyzed using UV spectroscopy at a wavelength of 243 nm (λ_{max}) and compared to standard dilutions of LE in PBS (r^2=0.9915) to determine the percentage of drug released over 10 days.

LE release from the TR gel was measured by allowing 200 μL of LE NPs in 20% w/v polymer solution to gel by placing in incubator at 37°C for 5 minutes. After gelling, release was initiated by adding 2.5 mL PBS. 1 mL samples were removed at predetermined intervals over 7 days and replaced with fresh PBS (94).

3.3.8 Cell culture

Human retinal pigment epithelium, ARPE-19, cells (ATCC # CRL-2302) were grown in 1:1 Dulbecco's Modified Eagle's Medium and Ham's F12 Medium (Mediatech, Inc., Manassas, VA) with 10% fetal bovine serum and 100 U/mL penicillin/streptomycin (Sigma Aldrich, St. Louis, MO). The cultures were maintained in a humid environment at 5% CO_2 and 37^{o}C.

3.3.9 Cytotoxicity

Cytotoxicity was assessed in ARPE-19 cells by the 3-(4,5-dimethylthiazol-2-yl)-2,5-diphenyltetrazolium bromide salt (MTT) assay. Briefly, cells were seeded in 24-well plates at a density of 5 x 10^4 cells/mL for 24 hours to achieve confluence before treatment. Cells were exposed to free LE solution, LE NPs, and LE NPs-TR gel at varying concentrations (0, 1, 10, 100 μM) for 24 hours after which the MTT assay was performed. Cell culture media were aspirated and 300 μL of MTT reagent solution (1 mg/mL) was added to each well. Cells were incubated at 37^{o}C and 5% CO_2 for 4 hours, after which the MTT reagent solution was aspirated and 500 μL of DMSO was added to each well. Plates were allowed to shake gently for 10 minutes before being read by Synergy H4 plate reader (Biotek Industries, Inc., Winooski, VT) at absorbance of 570 nm.

3.3.10 Intracellular uptake of coumarin-6-loaded NPs in ARPE-19 cells

Coumarin-6-loaded NPs were prepared by the method outlined above. In lieu of LE, 15 μL of coumarin-6 (1mg/ml acetone stock solution) was added (85). ARPE-19 cells were seeded at 10,000 cells per well in a four-well chamber slide. The cells were incubated for 24 hours to achieve 70% confluence. The medium was aspirated and cell monolayer was washed three times with PBS. 500 μL media containing 50 μg of coumarin-loaded NPs was added to the wells and incubated for 2 hours. After 2 hours, cells were washed with PBS three times, and treated with DAPI for nuclear staining and Cell Mask Deep Red for membrane staining. The slide was then examined by confocal microscopy with a magnification of 60x.

3.3.11 VEGF secretion

ARPE-19 cells were seeded onto 24-well plates at 5 x 10^4 cells/mL and allowed to grow until confluence. On the day of study, cell culture media were replaced with 1% FBS experimental media and allowed to remain in quiescence for 12 hours. The cellular monolayers were incubated with varying treatment concentrations of free LE solution (1, 10 μM), LE NPs (10 μM), and LE NPs-TR gel (10 μM). Culture media were collected at 12 and 72 hours. Secreted VEGF in collected culture media was quantified by the ELISA method (Human VEGFA ELISA kit, Thermo Scientific, Waltham, MA). The cell protein content was assayed using the BCA protein assay kit after lysing the cells and VEGF secretion was normalized to total protein. Samples were read by using the Synergy H4 plate reader (Biotek Industries, Inc., Winooski, VT) with absorbance at 450 nm minus absorbance at 550 nm.

3.3.12 Statistical analysis

Statistical analyses were performed using GraphPad Prism (GraphPad Software, Inc., San Diego, CA). Comparisons of the effect of free LE solution, LE NPs, and LE NPs-TR gels on cell viability and VEGF expression were assessed using paired t-tests with a significance level (p value) of 0.05. All experiments were carried out in triplicates (n=3) and shown as mean values ± SD.

3.4 Results

3.4.1 Nanoparticle characterization

Dynamic Pro plate reader was used to determine the size and PDI of the blank and LE -loaded NPs. The LE NPs were larger in size than the blank NPs. PDI data revealed that all NPs formulations had a normal size distribution (Table 3.1) with PDI value less than 1.

Table 3.1: Nanoparticle (NP) characterization data of particle size and polydispersity index (PDI) carried out in triplicates (n=3) and represented as the mean value ± SD.

NP Type:	Particle size (nm):	PDI:
Blank NPs	125.10 ± 43.89	0.014 ± 0.004
LE NPs	168.00 ± 23.18	0.0142 ± 0.0023

3.4.2 Drug entrapment efficiency

UV spectroscopy was used to determine the entrapment efficiency of LE by comparing the absorbance in methanol to standard dilutions of LE in methanol (r^2=0.9981) at 243 nm (λ_{max}). The LE NPs formulation showed an entrapment efficiency of 82.6 ± 0.01% which was satisfactory.

3.4.3 Scanning electron microscopy (SEM) analysis of NPs formulations

SEM was used to visualize the morphology of LE NPs. Surface analysis of NPs formulations showed that physical integrity was maintained by all samples (Figure 3.1). Size and size distribution of the NPs formulation visualized through SEM corroborated with data obtained by DLS.

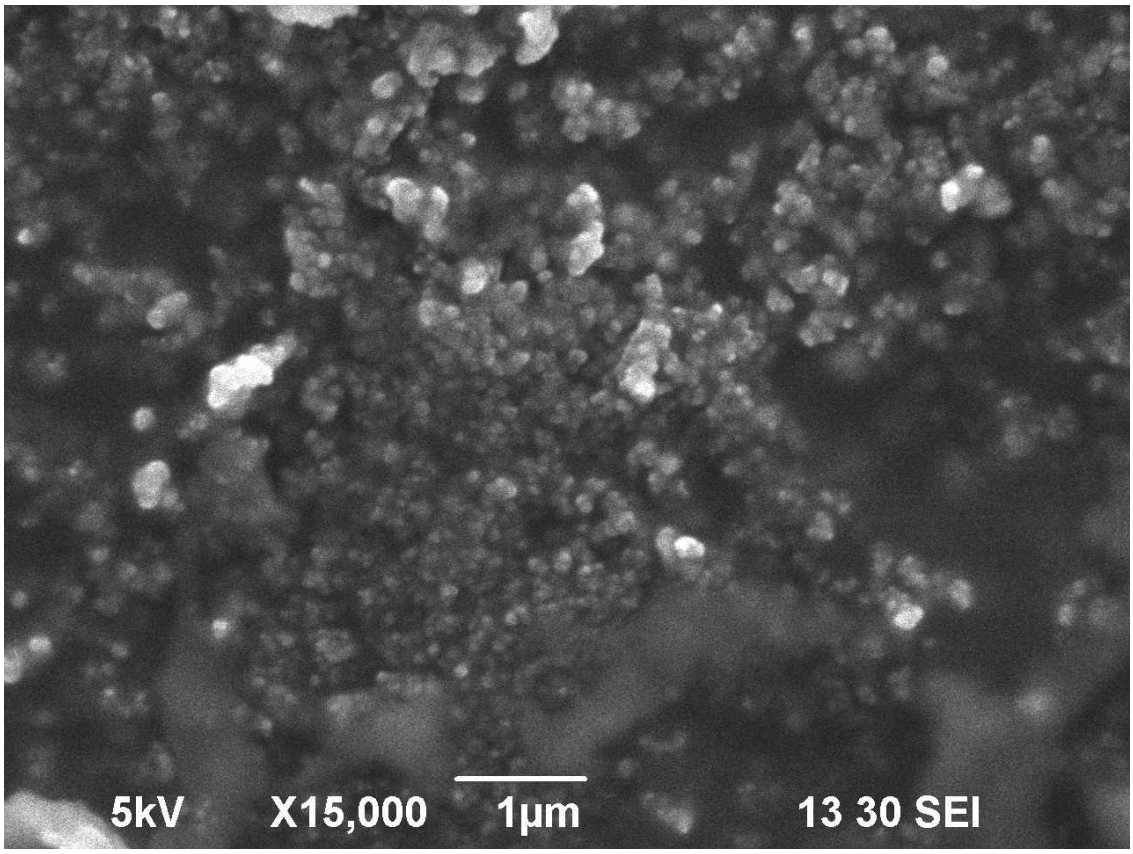

Figure 3.1: SEM visualization of loteprednol etabonate-loaded nanoparticles shows round morphology. Samples were diluted 1:10 and visualized by SEM. Samples were read at 15,000x magnification and 5kV acceleration voltage.

3.4.4 *In vitro* release

The release of LE from NPs and TR gel was conducted *in vitro* in a beaker with 100 mL of PBS at 37^{o}C. Figure 3.2 shows the cumulative release profile of the Lot NPs formulation compared to the LE NPs TR gel. At 72 hours, the LE NPs formulation had released 88% of the encapsulated

drug while the LE NPs TR gel formulation had released 5% of drug. At 168 hours, the TR gel had released 10% of drug.

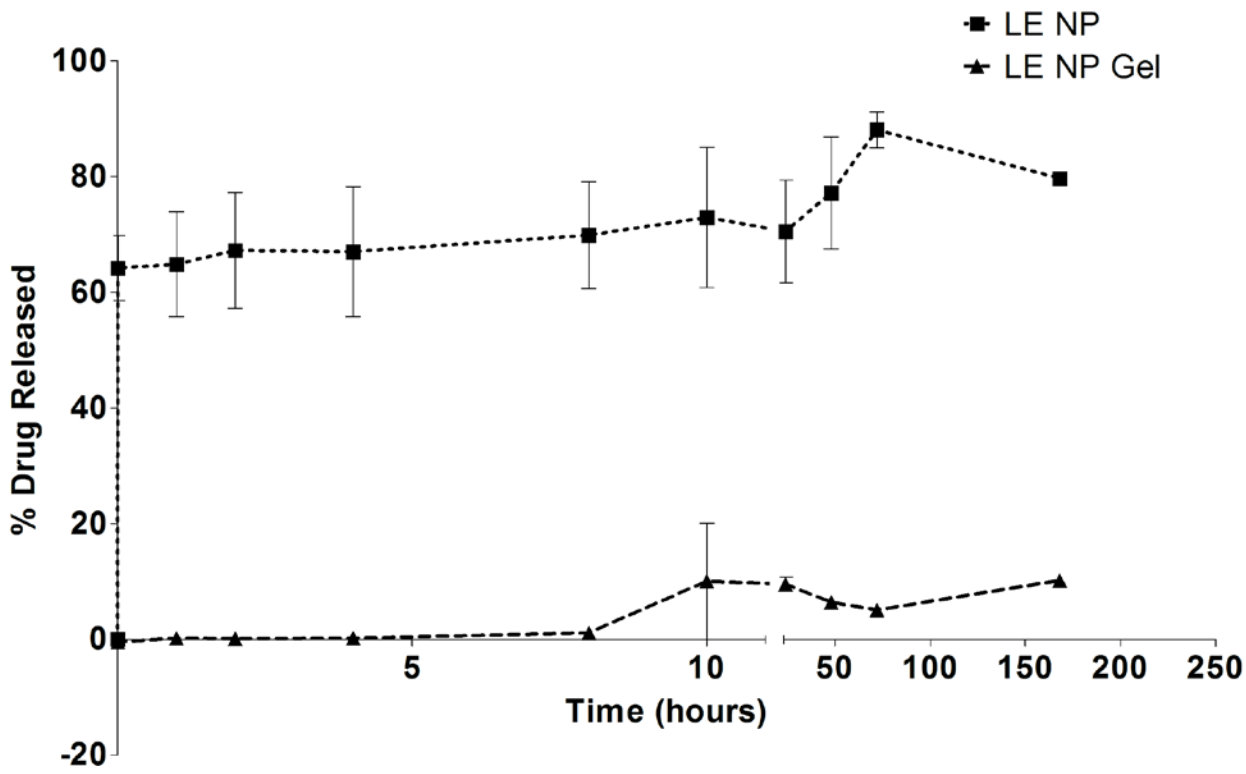

Figure 3.2: *In vitro* release data of the loteprednol etabonate nanoparticles (LE NP) compared to LE NP gel. Samples were analyzed by UV spectroscopy (243 nm, λ_{max}) at predetermined intervals over a 7-day period (*n*=3, mean value ± SD).

3.4.5 Cytotoxicity

The cytotoxicity of the DDS was investigated by MTT assay in the ARPE-19 cells to determine any possible harm related to its use. Figure 3.3 compares the cytotoxic effects of free LE with equal concentrations of the LE NPs and LE NPs in 20% w/v TR gel. Free LE had no impact on cell viability in ARPE-19 cells as compared to the untreated control cells. All other treatments were not significantly cytotoxic in ARPE-19 cells.

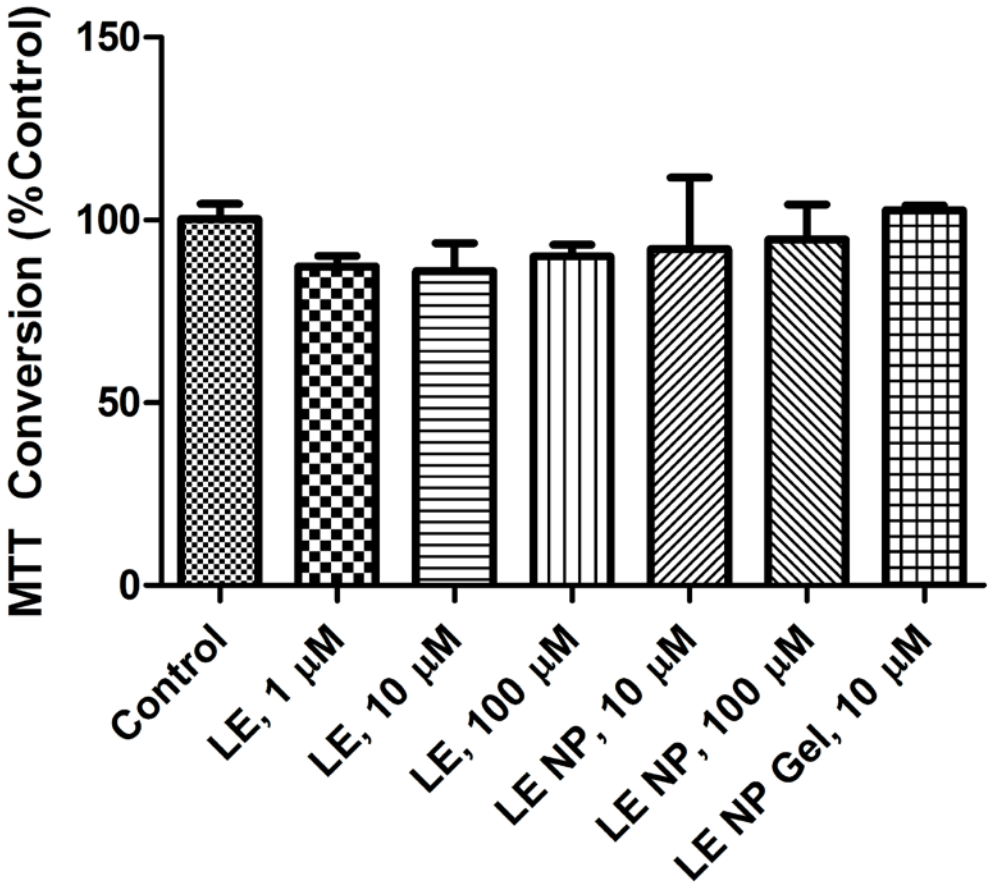

Figure 3.3: MTT cytotoxicity data in ARPE-19 cells of increasing concentrations of loteprednol etabonate (LE) free drug, LE NPs, and LE NPs in 20% w/v TR gel as compared to untreated control cells. Experiments were carried out in triplicates (*n*=3) and quantified by absorbance reading at 570 nm. Data is represented as mean ± SD.

3.4.6 Intracellular uptake of coumarin-6-loaded NPs

Figure 3.4 shows uptake of coumarin 6-loaded NPs within 2 hours. From the images, blue fluorescence from the nuclei was observed in the first panel due to DAPI labeling. Green fluorescence of the coumarin-6-loaded NPs was observed in the cytoplasm (second panel) and the cell membrane was stained with Cell Mask Deep Red in the third panel. The uptake of the

NPs by the cells is likely to have occurred *via* endocytosis. Untreated cells did not show green fluorescence (data not shown).

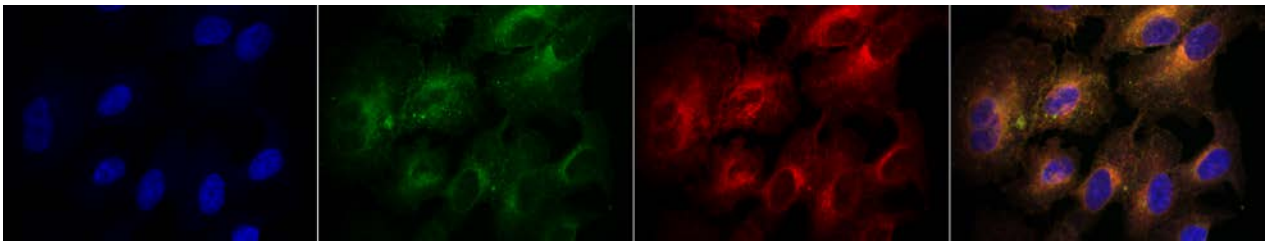

Figure 3.4: Cellular uptake of coumarin-6-loaded NPs in ARPE-19 cells. Nuclei were stained with DAPI visible in first panel. The uptake of coumarin-6-loaded NPs is depicted in second panel. Membrane staining with Cell Mask Deep Red is shown in the third panel. The final panel displays the overlaying images. Magnification of 60x.

3.4.7 VEGF secretion study

The effect of the LE DDS on VEGF secretion was studied in ARPE-19 cells. Cells were treated with different concentrations of free LE solution, LE NPs, and LE NPs in 20% w/v TR gel, for 12 and 72 hours. Figure 3.5 compares the suppression of VEGF expression between free LE solution, LE NPs and the LE NPs TR gel at 12 hours. Free LE solution at 1 μM and 10 μM showed reduction in VEGF expression compared to media control. LE NP at 10 μM was used for the VEGF expression study due to slower release characteristic of the NPs. Moreover, our preliminary data have shown better VEGF expression reduction at this concentration. LE NPs at 10 μM slightly reduced VEGF secretion while NPs TR Gel at 10 μM did not reduce VEGF secretion significantly in 12 hours compared to the control (p value <0.05) as concluded by paired t-test. However, the paired t-test results indicated that both NPs and NPs TR Gel at 10 μM significantly reduced VEGF secretion in 72 hours (p value <0.05; figure 3.6). This may be due to controlled release of the drug from NPs polymer matrix and NPs TR Gel. The VEGF

expression for NPs and NPs TR Gel at 10 μM was reduced to 90.99 ±1.29 % and 96.24 ± 1.91 % respectively. The % reduction VEGF expression of NPs TR Gel was observed as lower than NPs due to further delayed release of the drug from the gel matrix compared to NPs alone.

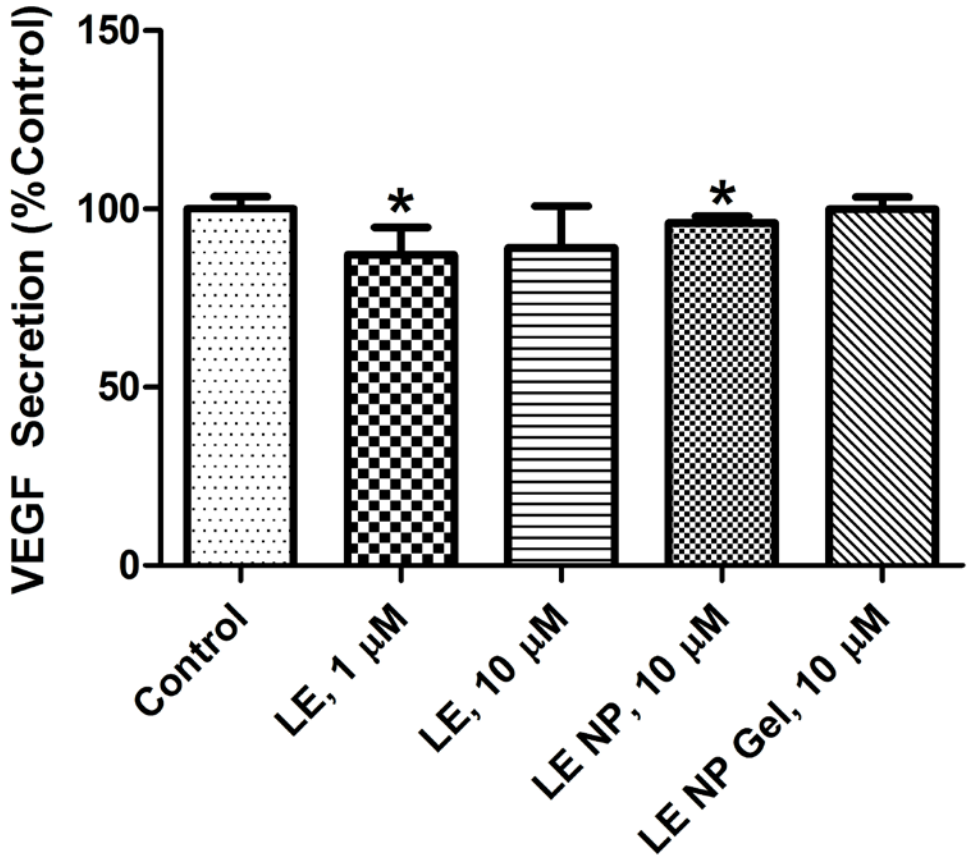

Figure 3.5: Comparative suppression of VEGF secretion in ARPE-19 cells through increasing concentrations (1, 10, μM) of loteprednol etabonate (LE) free drug, LE NPs, and LE NP gel at 12 hours. Experiments were carried out using the ELISA method (*n*=3). Data is represented by amount of VEGF secretion normalized to untreated control levels ± SD. *p<0.05 vs. Control.

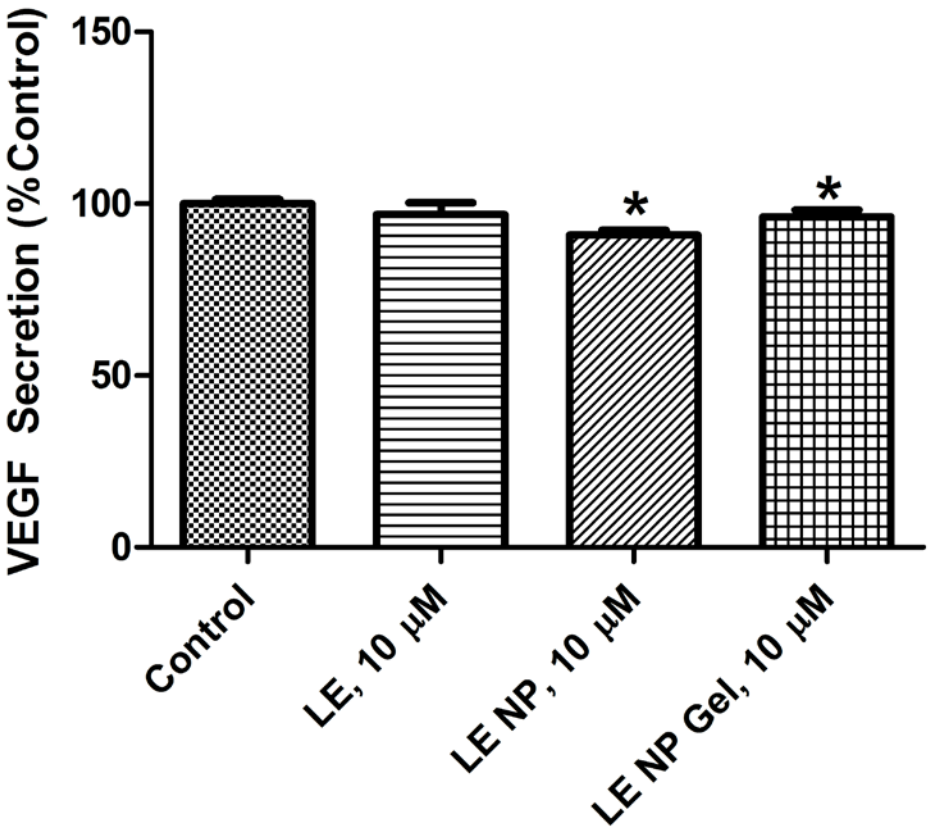

Figure 3.6: Comparative suppression of VEGF secretion in ARPE-19 cells through equal concentration treatments (10 µM) of LE free drug, LE NPs, and LE NPs in 20% w/v TR gel at 72 hours. Experiments were carried out using the ELISA method (*n*=3). Data is represented by amount of VEGF secretion normalized to untreated control levels ± SD. *p<0.05 vs. Control.

3.5 Discussion

Polymeric LE NPs were prepared by the emulsion solvent evaporation method with reproducible and satisfactory particle size and entrapment efficiency. The particle size of unloaded NPs was 125 nm while drug loaded NPs was 168 nm. Both NPs formulations showed a normal size distribution with PDI value less than 1. Particle size, PDI, and entrapment efficiency data were corroborated with previously published studies (80, 96, 97, 116).

The rate of drug release from the NPs and TR gel was measured using dialysis method in PBS at 37^{o} C over the course of 7 days. At 72 hours, the LE NPs exhibited 88% drug release while the LE NP Gel had released 5% of drug. The TR gel had released 10% of drug at 168 hours. Both formulations exhibited sustained release pattern; however, the drug release from the TR gel was further slower due to drug release via polymer degradation. Polymer matrices release encapsulated drug in two phases: the first phase of drug release occurs *via* diffusion and the second phase is by diffusion and polymer degradation (101).

MTT cytotoxicity studies in ARPE-19 cells showed no cytotoxicity after 24-hour exposure to free LE solution, LE NPs, or LE TR gel. LE was not expected to have any toxic effects as it was formulated to prevent any physiological side effects. The LE NP and LE NP incorporated TR gel DDS were observed to be safe to use in ARPE-19 cells. Additionally, the NPs were localized into the ARPE-19 cells within 2 hours as shown by confocal microscopy (figure 4). To support these data, recent *in vivo* studies have shown that NPs were localized within 6 hours at the retinal pigment epithelium of healthy rat after intravitreal injections (82). LE NPs and LE NP TR gel were able to significantly reduce VEGF expression in ARPE-19 cells at 10 μM over 72 hours more effectively than equal concentrations of LE drug solution ($p<0.05$). Free LE drug solution significantly reduced VEGF expression within 12 hours compared to control ($p<0.05$) while drug loaded NPs and NPs TR Gel exhibit their effect after 72 hours due to the extended release properties of the NPs and the gel.

3.6 Conclusions

The present study describes the potential use of a novel DDS for controlled release of LE for potential treatment of wet AMD by reducing the frequency of intravitreal injections. The proposed DDS showed sustained *in vitro* release and showed no cytotoxicity in *in vitro* experiments using ARPE-19 cells. The DDS of LE was able to significantly reduce the expression of VEGF in ARPE-19 cells over 72 hours compared to LE solution alone. The biocompatibility, low toxicity and therapeutic potential of the proposed DDS make it an ideal model for further studies investigating the experimental animal AMD models with reduced intravitreal injection frequency.

Declaration of Interest:

The authors report no declarations of interest.

Acknowledgements:

Scanning electron microscopy assistance was provided by Amanda Garces and confocal microscopy assistance was provided by Dr. Byeong "Jake" Cha, Ph.D., Lisa Muma Weitz Advanced Microscopy and Cell Imaging Core Laboratory (University of South Florida).

Chapter 4. The Effect of Corticosteroid-Nanoparticles Incorporated in a Thermoreversible Gel on Chemically Induced Choroidal Neovascularization in Mice

4.1 Introduction

Age-related macular degeneration (AMD) is the leading cause of legal blindness in the developed world. Vision reduction and blindness develop at advanced stages of the disease, especially in AMD with choroidal neovascularization (CNV) (117, 118). CNV causes accumulation of exudates in the subretinal space and underneath the retinal pigment epithelium (RPE). Visual acuity is compromised over time due to damage of the macula.

Due to the neovascularization in wet-AMD, inhibitors of angiogenesis have been widely studied and implemented clinically to deter the development of abnormal blood vessels.

Corticosteroids, such as triamcinolone acetonide and dexamethasone, are used extensively for treatment of posterior ocular disorders. This is because of their angiostatic, antipermeable, and antifibrotic properties (27). They are able to inhibit inflammatory symptoms by binding steroid receptors in cells and inducing or repressing targeted genes (such as TNF-α, IL-1β, and IL-6) (28, 119). They can also inhibit expressions of growth factors such as basic fibroblast growth factor and adhesion molecules such as ICAM-1 and decrease VEGF levels that are elevated in the process of retinal neovascularization (30, 31).

For treatment of posterior segment ocular diseases such as AMD, the biggest challenge is route of administration. Intravitreal injections allow for the most direct approach; however, the chronic nature of the disease requires consistent injections resulting in side-effects such as retinal detachment and cataract formation (24). Therefore, development of sustained release drug delivery systems (DDS) can be useful in minimizing the frequent intravitreal injections required to maintain the therapeutic drug dosage.

The DDS containing corticosteroids has been found to be effective at reducing VEGF expression *in vitro* (116). Similarly, they have been shown to reduce VEGF expression and inhibit VEGF-related permeability *in vivo* (120, 121). The ability to sustain drug release has also been shown (116). In this study, we evaluated the efficacy of the DDS (LE DDS: LE NPs in a TR gel, TA DDS: TA NPs in a TR gel) in reducing CNV in a mouse model.

4.2 Materials and Methods

4.2.1 Animals

Male C57BL/6 mice (7-9 weeks old) were purchased from Charles River (Wilmington, MA). This study was approved by the Institutional Animal Care and Use Committee of the University of South Florida. They are housed in the USF College of Medicine Vivarium under standard conditions including 12 by 12 light dark cycle and fed standard food during the whole study.

4.2.2 Study design

To investigate the effects of different corticosteroids and DDS, we divided the animals into six groups. Group 1 (control) was not treated. Group 2 was CNV-induced but left untreated. Groups 3-6 were CNV-induced and administered intravitreal injections of different treatments (LE (solution), LE DDS (LE NPs in TR gel), TA (solution), TA DDS (TA NPs in TR gel)).

4.2.3 PEG-induced choroidal neovascularization

Male C57BL/6 mice (7–9 weeks old) were administered subretinal injections of 1 mg of polyethylene glycol-8 (PEG-8). The vitreous chamber of the mouse eye was decompressed with a 27-gauge needle by inserting the needle through the conjunctiva and sclera 1 mm behind the limbus. A Hamilton syringe with a 33-gauge blunt needle was used for injections. Needle movement was stopped when light resistance was felt. An injection of 2 µl of solutions was administered (122).

4.2.4 Treatment administration

Treatments were administered one week after CNV induction. Intravitreal injection of 1 µl of each treatment containing 800 µg/ml of respective drug (LE, LE DDS, TA, or TA DDS) was administered consecutively in each eye using a dissecting microscope. A 30G ½ needle was inserted 0.5 mm posterior to the temporal limbus approximately 1.5 mm deep and angled toward the optic nerve until the needle tip was viewed in the vitreous (24).

4.2.5 Preparation of flat mounts and CNV evaluation

At two weeks and four weeks after treatment, the size of the CNV lesions was evaluated. Mice were anesthetized and perfused with 10 ml of PBS containing 50 mg/ml of fluorescein-labeled dextran. The eyes were removed and fixed in 4% paraformaldehyde for 2 hours. The cornea and lens were dissected and the entire retina was removed from the eyecup. 4-8 radial cuts were made from the edge of the eyecup to the equator and the choroid was flat-mounted in aquamount (123). Flat mounts were examined at 20x objective on an Olympus FV1000 MPE multiphoton laser scanning microscope. The percent area of neovascularization was quantified by Fiji (ImageJ) software (123).

4.2.6 Real-time reverse transcription-polymerase chain reaction (RT-PCR)

Total RNA from mouse eye was isolated and purified using mirVana miRNA Isolation Kit (Life Technologies, Carlsbad, CA) according to the protocol of the manufacturer. Quantitative real-time RT-PCR using primers synthesized at Integrated DNA Technologies were used for gene expression analysis as described previously (123-125). RT-PCR was conducted using the following primers: GAPDH (forward (F), 5'-TGAAGGTCGGTGTGAACGGATTTGGC-3'; reverse (R), 5'-CATGTAGGCC ATGAGGTCCACCAC-3'); VEGF (F, 5'-GCGGGCTGCCTCGCAGT C-3'; R, 5'-TCACCGCCTTGGCTTGTCAC- 3'). Amplification of genes was performed with Bio-Rad real-time PCR system using One-Step SYBR® Green qRT-PCR Kit and a standard thermal cycler protocol. The threshold cycle (C_T) was determined, and relative quantification was calculated by the comparative C_T method as described previously (124).

4.2.7 Statistical analysis

One-way ANOVA analysis followed by Tukey post-hoc test was performed. Additionally, when appropriate, a two-way ANOVA analysis followed by Bonferroni posttest was performed. GraphPad Prism (GraphPad Software Inc., San Diego, CA) was used for analyzing and plotting the data (n=3) and $p<0.05$ was used as a significance criteria.

4.3 Results

4.3.1 CNV induction

Figure 4.1(A) shows images of the retinal/choroidal vasculature of a control mouse and a CNV-induced mouse at 2 weeks post CNV induction. Normal blood vessels were seen in the control mouse (left panel), whereas neovascularization and leaky blood vessels were evident in the CNV-induced mouse (right panel). Figure 4.1(B) shows a comparison between the area of retinal/choroidal blood vessels in the control eye vs. the CNV-induced eye. In the control eye, vasculature comprised of 14.9% of the surface area; this value increased to 21.8% in the CNV-induced sample indicating the significant increase in retinal/choroidal blood vessels retaining fluorescein.

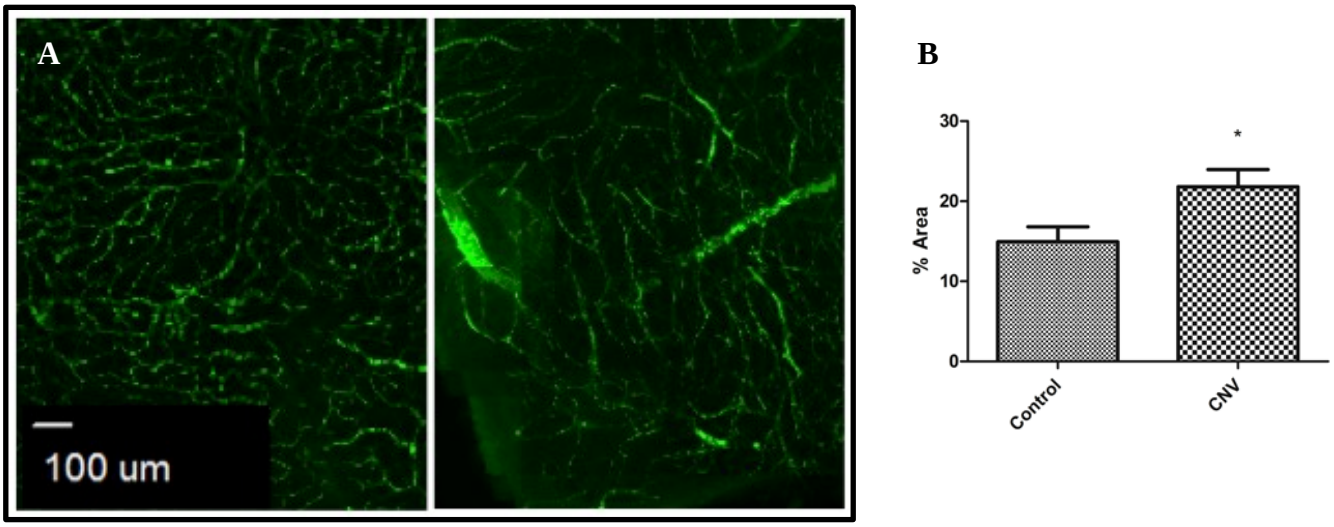

Figure 4.1: (A) FITC-dextran labeled retinal/choroidal flat-mount. Control (left) and CNV-induced eye (right). Magnification of 20x. (B) Total area of blood vessels in control and CNV-induced eye. Data is represented by mean ± SD (n=3). *p<0.05.

4.3.2 Effect of corticosteroid drug delivery systems on CNV area

Figure 4.2 shows a comparison of neovascularization in retina/choroid tissue measured for various treatment groups after 2 weeks of exposure. The untreated CNV-induced group showed a mean percentage of 20.6%. Exposure to loteprednol etabonate (LE) and LE drug delivery system (DDS) resulted in a significant decrease to 8.5% and 7.4% in the residual CNV area, respectively. There was no significant difference between LE and LE DDS. Treatment with intravitreal administration of triamcinolone acetonide (TA) solution had no effect on the CNV area; however, TA DDS displayed a significant decrease in the CNV area.

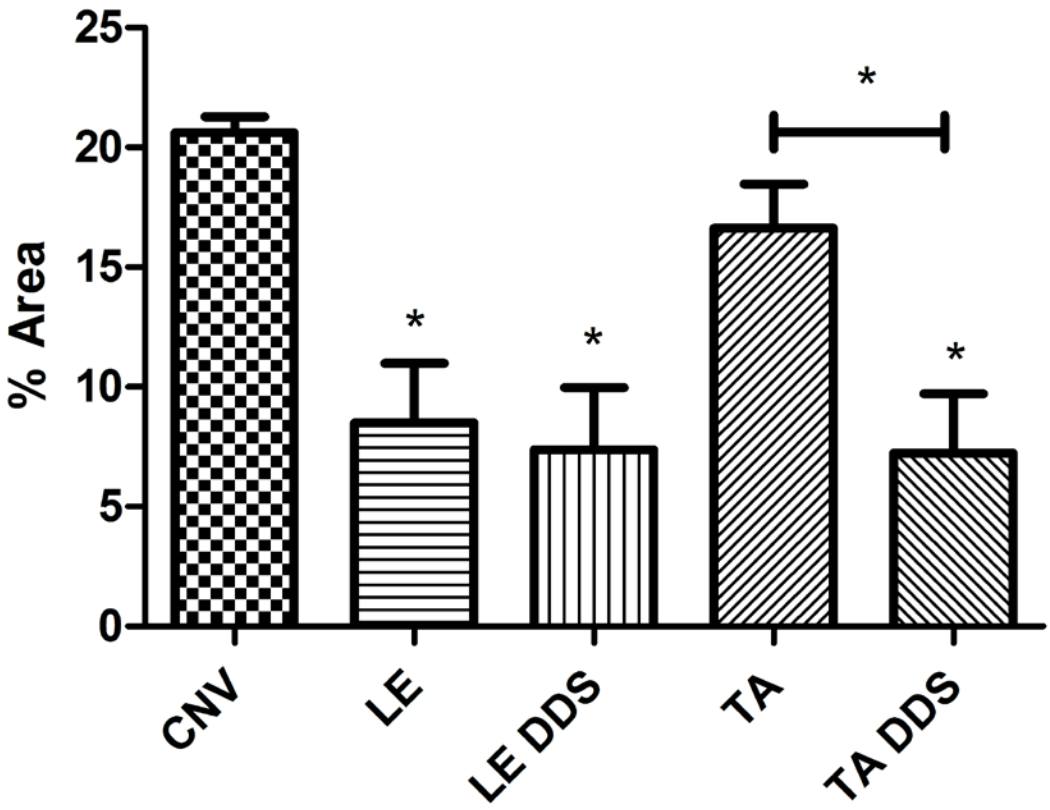

Figure 4.2: Effect of corticosteroids and corticosteroid drug delivery systems on retinal/choroidal neovascularization area at 2 weeks. Groups tested include CNV-induced (no treatment), loteprednol etabonate (LE), LE drug delivery system (DDS), triamcinolone acetonide (TA), TA DDS. Data is represented by mean ± SD (n=3). *p<0.05 vs CNV.

The effect of the corticosteroids and DDS 4 weeks post treatment is presented in Figure 4.3. Neither LE nor TA showed any significant reduction in CNV area. Exposure to LE DDS resulted in a significant decrease in CNV area to 15.7% and exposure to TA DDS to 12.0%. This was most likely due to the sustained drug release properties of the DDS.

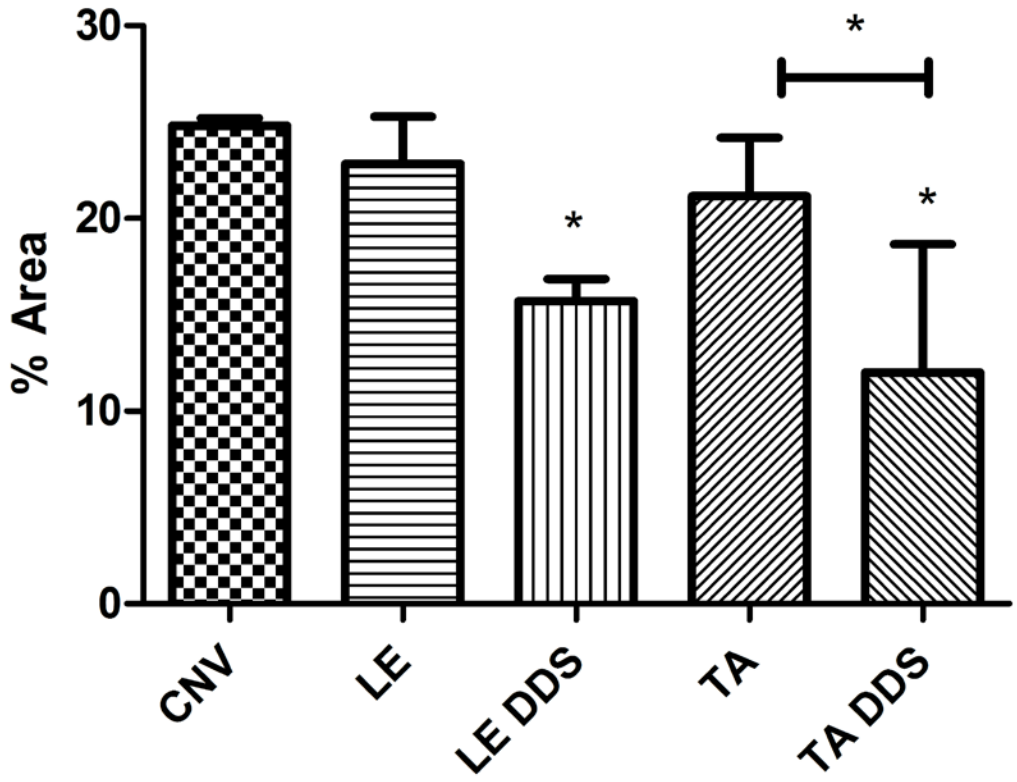

Figure 4.3: Effect of corticosteroids and corticosteroid drug delivery systems on retinal/choroidal neovascularization area at 4 weeks. Groups tested include CNV-induced (no treatment), loteprednol etabonate (LE), LE drug delivery system (DDS), triamcinolone acetonide (TA), TA DDS. Data is represented by mean ± SD (n=3). *p<0.05 vs. CNV.

To study the sustained efficacy of the DDS, the CNV area of LE and LE DDS were compared between 2 and 4 weeks (Figure 4.4). The CNV area of the LE treated group increased from 8.5% to 22.8% and the LE DDS treated groups increased from 7.3% to 15.7% over the same period of time.

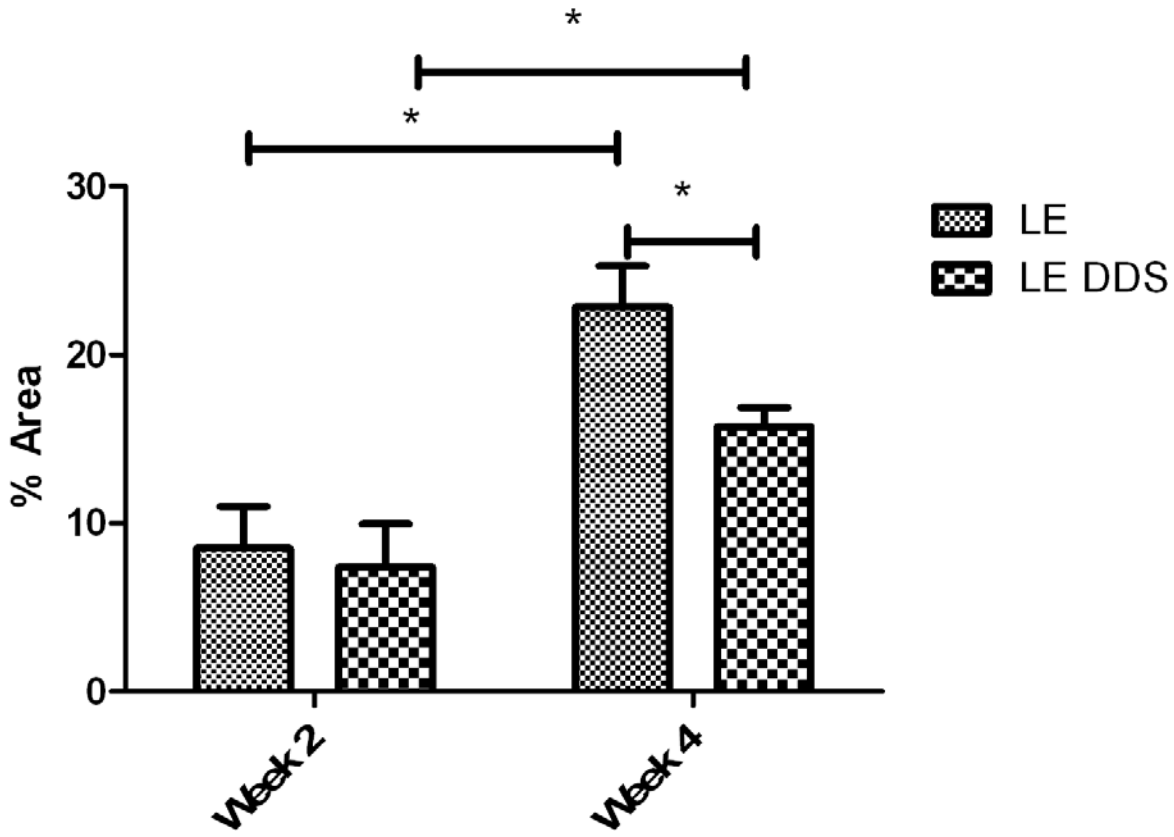

Figure 4.4: Comparison of sustained efficacy of LE and LE DDS on CNV area at 2 and 4 weeks. Effect of corticosteroids and corticosteroid drug delivery systems on retinal/choroidal neovascularization area. Data is represented by mean ± SD (n=3). *p<0.05.

In Figure 4.5, the CNV area of TA-treated group increased from 16.6% at 2 weeks post-CNV induction to 22.3% at 4 weeks. The TA DDS group increased from 7.2% to 13.6%; however, this increase was not significant ($p>0.05$).

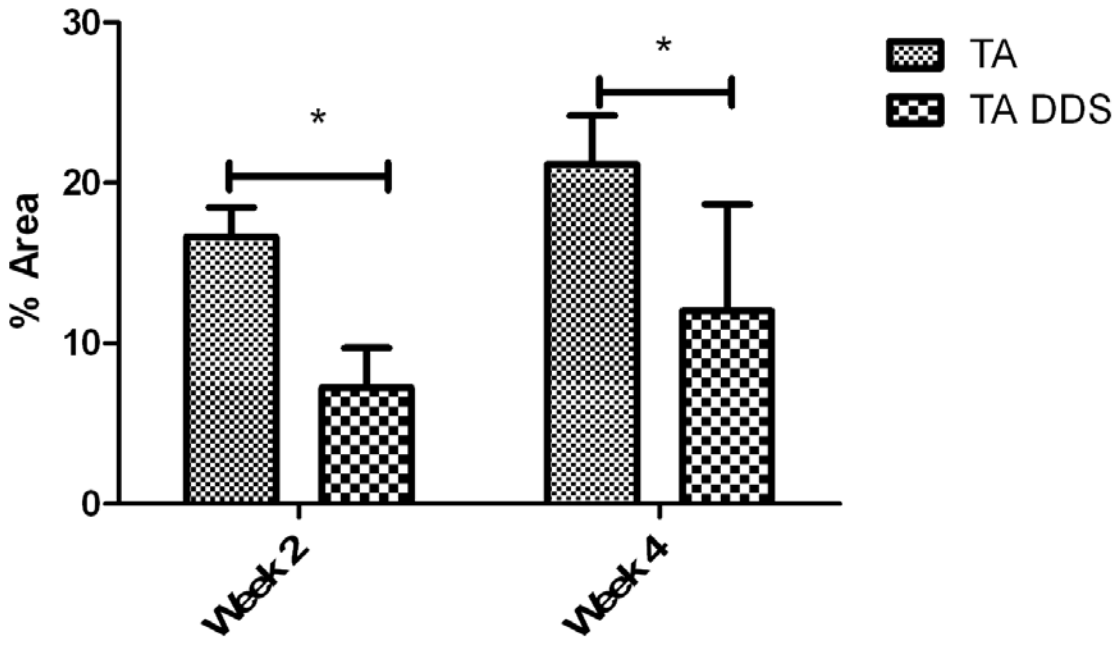

Figure 4.5: Comparison of sustained efficacy of TA and TA DDS on CNV area at 2 and 4 weeks. Effect of corticosteroids and corticosteroid drug delivery systems on retinal/choroidal neovascularization area. Data is represented by mean ± SD (n=3). *p<0.05.

4.3.3 Effect of corticosteroid drug delivery systems on VEGF expression

Gene expression of VEGF was analyzed in whole eye homogenates at 4 weeks post-treatment. Figure 4.6 shows that TA DDS significantly reduced VEGF expression as compared to the CNV-induced group.

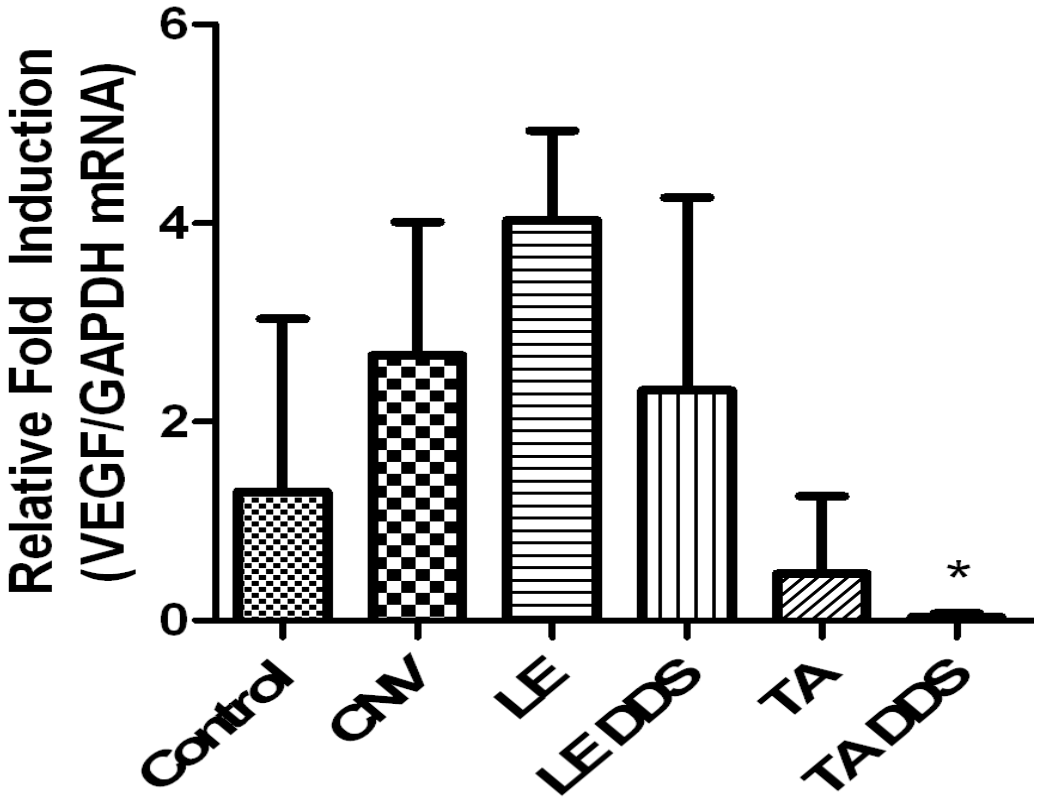

Figure 4.6: Effect of corticosteroids and corticosteroid drug delivery systems on VEGF expression at 4 weeks. Data is represented by mean ± SD (n=3). *p<0.05 vs. CNV.

4.4 Discussion

CNV is a pathophysiological characteristic of neovascular AMD. Thus, neovascular AMD is a disease which is characterized by increased levels of angiogenic factors in the retina/choroid. These factors could be designated as targets in developing effective drug delivery systems to mitigate CNV.

In this study, we evaluated the effect of corticosteroid drug delivery systems (DDS) on the VEGF levels and the extent of neovascularization estimated by an image analysis in a mouse model of CNV. Neovascularization was stimulated using a subretinal injection of PEG-8 to activate the complement system (122), which in turn induces the development of new blood vessels in the retina/choroid. A process of complement activation leading to CNV is the deposit of membrane attack complex on the RPE and choroid; this initiates production and secretion of VEGF as well as induces inflammation (122, 126, 127). Figure 4-1 depicted the FITC-dextran labeled blood vessels in a control and untreated CNV-induced eye. The control eye demonstrated regular network of blood vessels, whereas in the CNV-induced group, there was evidence of neovascularization and leaky blood vessels. Quantification of the blood vessels showed a significant increase in area from 14.9% in the control to 21.8% in the CNV-induced group.

We studied two corticosteroids with varying potencies: triamcinolone acetonide (TA) and loteprednol etabonate (LE). TA is categorized as an upper-mid strength potency steroid; it is commonly used in combination with other treatments for posterior ocular disorders (26). TA has been indicated experimentally as an alternative option for the treatment of AMD alone or combined with anti-VEGF agents (128). One additional advantage of TA is its prolonged duration of action due to its low water solubility (128). However, adverse effects such as an increase in intraocular pressure and cataract development can occur with higher potency steroids. Therefore, we also examined LE as it was designed to reduce these side effects by converting into an inactive metabolite and minimizing toxicity (107, 108). LE was reported to have a therapeutic index 20-fold better than high potency corticosteroids such as hydrocortisone or betamethasone *in vivo* (105). We tried to determine if a DDS formulation of LE would be beneficial in maintaining a balance between the active duration and lower side effects. Figures 4.2 and 4.3 showed the effect on CNV area 2 and 4 weeks post treatment, respectively. 2 weeks after treatment of CNV injury, LE and LE DDS resulted in a similar reduction of CNV area. This is most likely due to the high relative potency of LE. TA drug solution alone showed no significant change, whereas TA DDS elicited a significant reduction of CNV area, most likely due to the sustained release of the DDS. At 4 weeks after treatment, the LE and TA drug solution treatment groups no longer appeared to be suppressing the excess vasculature growth; however the LE DDS and TA DDS still showed a significant reduction.

Figures 4.4 and 4.5 compare the results between the drug solution and the DDS at two time points. While LE DDS showed a reduction in the occurrence of CNV, the comparison test between week 2 and 4 showed that there was a significant increase in vascularization by week 4. The inability of LE DDS to inhibit progression of the disease state might be due to the conversion of LE to an inactive carboxylic acid metabolite after *in vivo* interaction. Once released, it has been reported that the half-life of LE is 2.8 hours when administered systemically (129). Further testing to optimize the formulation for enhanced release rate might improve the long-term delivery. A comparison between TA and TA DDS showed no significant difference between week 2 and 4, suggesting that TA maintained its therapeutic effect in the eye over the course of one month when formulated in nanoparticles within a thermoreversible gel. These data corroborate previously reported studies in TA NPs were more effective at reducing CNV than LE NPs in a mouse CNV model (24).

Vascular endothelial growth factor (VEGF) is a well-known mediator of angiogenesis (120, 122). Figure 4.6 showed the results from gene expression analysis for VEGF levels in the eye after 4-week exposure to 4 different treatment groups. VEGF mRNA expression levels were consistent with reported literature after CNV induction in experimental models (126). Only treatment with TA DDS resulted in a significant decrease in VEGF levels. Surprisingly, LE DDS did not have an effect on VEGF expression at 4 weeks; this is most likely why the CNV area had significantly increased in the LE DDS treated groups between weeks 2 and 4.

4.5 Conclusions

Our data supports existing evidence that some corticosteroids released by DDS in the eye can inhibit the progression of neovascularization in a CNV mouse model more effectively compared to drug solutions alone.

Two corticosteroids were studied: LE, as a representative of the newer generation highly potent corticosteroids and TA, as a representative of the older generation upper mid potent corticosteroids. Our study demonstrated a significant reduction in CNV area at 2 weeks compared to the CNV-induced eye by LE, while TA failed to inhibit neovascularization in the same model. At 4 weeks, neither of the corticosteroids alone was effective in reducing the CNV area compared to CNV-induced eye without any treatment.

Both LE DDS and TA DDS exhibited significant reduction of CNV area in 2 weeks compared to CNV–induced eye. At 2 weeks, TA DDS showed significant reduction in CNV area compared to drug alone while LE DDS system showed reduction in CNV area similar to drug alone. At 4 weeks, both LE DDS and TA DDS were significantly effective in reducing CNV area compared to drug alone while LE and TA alone were ineffective. This was likely due to sustained drug release properties of the DDS.

Gene expression analysis of TA DDS indicated a significant reduction of VEGF expression compared to the CNV-induced model as well as the other treatment groups. This implies that TA could suppress angiogenesis *via* VEGF, and the DDS allows for sustained release to maintain the effects of VEGF suppression for at least 4 weeks.

TA DDS was found to be a more effective delivery system at reducing CNV area after 2 weeks and 4 weeks and consequently, reducing the need for frequent intravitreal injections of the corticosteroids.

The proposed DDS composed of PLGA-PEG nanoparticles in PLGA thermoreversible gels can be useful in delivering other anti-VEGF antibodies agents such as bevacizumamb (Avastin®), Ranizumamb (Lucentis®), and Aflibercept (Elyea®) for sustained delivery in the posterior segment of the eye and reducing the frequency of painful intravitreal injection and warrants further studies.

Chapter 5. Conclusions and Future Work

5.1. Summary and Conclusions

Macular degeneration affects 11 million people in the United States. Current anti-angiogenic treatments require frequent intravitreal injections to maintain therapeutic intraocular doses to suppress disease progression. Due to the lengthy pipeline for creation of new pharmaceuticals, it makes sense to reposition approved drugs in novel drug delivery systems to improve their sustained efficacy. In this study, we hypothesized that sustained-release corticosteroid-nanoparticles incorporated in thermoreversible gels can improve the therapeutic nature of corticosteroids for CNV in wet AMD.

In Chapter 2, "Triamcinolone Acetonide Nanoparticles Incorporated in Thermoreversible Gels for Age-Related Macular Degeneration," we prepared a DDS consisting of TA nanoparticles and a thermoreversible gel for use in mitigating VEGF overexpression *in vitro*. We characterized NPs for size and polydispersity index. The NPs were around 200 nm in size with a polydispersity index less than 1, indicative of a unimodal size distribution. The 20% w/v thermoreversible gel displayed sol-gel transition at a temperature range appropriate for physiological use. *In vitro* release assay demonstrated a sustained release; while the TA drug solution alone was completely released within 48 hours, 31.49% of the drug was released from the DDS in 10 days. The combined DDS displayed no cytotoxicity on human ARPE-19 retinal pigment epithelial cells and was able to reduce the expression of VEGF *in vitro* over 72 hours.

In Chapter 3, "Efficacy of Loteprednol Etabonate Drug Delivery System in Suppression of *in vitro* Retinal Pigment Epithelium Activation," we utilized a similar drug delivery system to deliver LE, a soft steroid that elicits lower side effects *in vivo.* The LE DDS formulation exhibited a sustained release pattern with 5% of the drug released over 10 days. Compared to LE alone, LE DDS significantly reduced the expression of VEGF in ARPE-19 cells over 72 hours. The biocompatibility, low toxicity and therapeutic potential of the DDS make it an ideal model for further investigation in a mouse CNV model.

Finally, in Chapter 4, "The Effect of Corticosteroid-Nanoparticles Incorporated in a Thermoreversible Gel on Chemically Induced Choroidal Neovascularization in Mice," the corticosteroid DDS were tested on a CNV mouse model. Our data reinforces the *in vitro* data that LE and TA in sustained DDS can inhibit the progression of neovascularization. LE DDS and TA DDS effectively reduced the CNV area over 4 weeks compared to their respective drug solution alone. These results lend themselves to further studies of clinical relevance to utilize DDS composed of PLGA-PEG nanoparticles in PLGA thermoreversible gels for posterior segment ocular disease.

5.2. Future Directions

The overall goal of this work is to produce a sustained release drug delivery system to reduce the frequency of intravitreal injections necessary to control choroidal neovascularization evident in neovascular age-related macular degeneration. The reported study has shown promising results and warrants further studies to improve efficacy of the DDS. Further extensions of the work presented would involve 1) investigation of factors that would alter drug release from the nanoparticles, such as drug loading, particle size, ratio of polymers; 2) analysis of molecular mechanisms affected by DDS; and 3) utilization of combination therapy with anti-VEGF agents to enhance therapeutic effect of DDS.

5.2.1. Effect of factors that would alter drug release from DDS

Different parameters can affect the size of NPs, such as drug/polymer ratio, stabilizer and homogenization (47) and a change in polymer mixture or ratio can affect the drug release characteristics (94). In preliminary studies, we optimized the drug/polymer ratio to obtain NPs that would be an appropriate size range for localization within the RPE. Additionally, the NPs dispersed in the thermoreversible gel show a sustained release for up to one month. Other studies have shown that polymer blending including PLGA of different molecular weights can allow for higher drug entrapment due to closer packing of the polymers (94). This parameters can be altered to incorporate more drug and further lengthen the sustained release effects of the DDS.

5.2.2. Effect of DDS on molecular mechanisms of CNV

The *in vivo* study was designed to investigate the sustained efficacy of the DDS on the incidence of CNV and effect on VEGF expression. However, it does not include analysis of other angiogenic and inflammatory mediators that are involved in the progression of CNV. CNV is associated with increased production of VEGF, TGF-β, and β-FGF (125). Therefore, it would be important to investigate if exposure to the DDS results in a reduction of these angiogenic factors by measuring mRNA and protein expression. Additionally, analysis of inflammatory mediators such as MMPs, IL-6, TNF-α that are indicated in CNV as well as inhibitors of angiogenesis such as angiostatin, endostatin, pigment epithelium-derived factor (PEDF) would give valuable insight into the mechanisms by which our DDS affects a response (14).

5.2.3. Combination therapy with corticosteroid DDS and anti-vascular endothelial growth factor (VEGF) for an enhanced anti-angiogenic effect

Clinical therapy for neovascular macular degeneration is targeted against the vascular component of choroidal neovascularization. Primary treatment includes anti-VEGF agents that can halt the progression of angiogenesis as well as reduce vascular permeability. The anti-angiogenic drugs currently used in the treatment of neovascular AMD work by binding VEGF-A isoforms: ranibizumab (Lucentis), bevacizumab (Avastin), pegaptanib sodium (Macugen) (7, 19-21). Corticosteroids are sometimes used to supplement these drugs to enhance the anti-inflammatory effects (14). The DDS can include similar combination therapy by utilizing both one of the anti-VEGF agents and either TA or LE. This system will be more specific towards angiogenesis and have an enhanced anti-angiogenic effect as compared to monotherapy (130). Effect on choroidal neovascularization area, drug concentration in ocular tissue and effect on gene and protein expression would be measured.

References

1. Prevalence of Adult Vision Impairment and Age-Related Eye Diseases in America Bethesda, MD: National Eye Institue; 2014 [cited 2014 04/01/14]. Available from: http://www.nei.nih.gov/eyedata/adultvision_usa.asp.
2. Regatieri CV, Dreyfuss JL, Nader HB. Experimental Treatments for Neovascular Age-Related Macular Degeneration Ying G, editor. Shanghai, China: InTech; 2012. p. 83-98.
3. Thrimawithana TR, Young S, Bunt CR, Green C, Alany RG. Drug delivery to the posterior segment of the eye. Drug Discovery Today. 2011 Mar;16(5-6):270-7. PubMed PMID: 21167306.
4. Nirmal HB, Bakliwal SR, Pawar SP. In-situ gel: new trends in controlled and sustained drug delivery system. International Journal of PharmTech Research. 2010;2(2):1398-408.
5. Choi BG, Park MH, Cho SH, Joo MK, Oh HJ, Kim EH, et al. In situ thermal gelling polypeptide for chondrocytes 3D culture. Biomaterials. 2010 Dec;31(35):9266-72. PubMed PMID: 20864172.
6. Tamboli V, Mishra G, Mitra A. Biodegradable polymers for ocular drug delivery. In: Mitra A, editor. Advances in Ocular Drug Delivery2012. p. 65-86.
7. Bylsma GW, Guymer RH. Treatment of age-related macular degeneration. Clinical & Experimental Optometry: Journal of the Australian Optometrical Association. 2005 Sep;88(5):322-34. PubMed PMID: 16255691.
8. Normal Macula Clarksburg, MD: BrightFocus Foundation; 2000 [cited 2014 April 4, 2014]. Available from: http://www.brightfocus.org/macular/about/understanding/normal-macula.html.
9. Rofagha S, Bhisitkul RB, Boyer DS, Sadda SR, Zhang K, Group S-US. Seven-year outcomes in ranibizumab-treated patients in ANCHOR, MARINA, and HORIZON: a multicenter cohort study (SEVEN-UP). Ophthalmology. 2013 Nov;120(11):2292-9. PubMed PMID: 23642856.
10. Heier JS, Brown DM, Chong V, Korobelnik JF, Kaiser PK, Nguyen QD, et al. Intravitreal aflibercept (VEGF trap-eye) in wet age-related macular degeneration. Ophthalmology. 2012 Dec;119(12):2537-48. PubMed PMID: 23084240.
11. Park YG, Rhu HW, Kang S, Roh YJ. New approach of anti-VEGF agents for age-related macular degeneration. Journal of Ophthalmology. 2012;2012:637316. PubMed PMID: 22496964. Pubmed Central PMCID: 3307057.
12. Ferrara N, Gerber HP, LeCouter J. The biology of VEGF and its receptors. Nature Medicine. 2003 Jun;9(6):669-76. PubMed PMID: 12778165.
13. Verteporfin In Photodynamic Therapy Study G. Verteporfin therapy of subfoveal choroidal neovascularization in age-related macular degeneration: two-year results of a randomized clinical trial including lesions with occult with no classic choroidal neovascularization--verteporfin in photodynamic therapy report 2. American Journal of Ophthalmology. 2001 May;131(5):541-60. PubMed PMID: 11336929.
14. Campa C, Costagliola C, Incorvaia C, Sheridan C, Semeraro F, De Nadai K, et al. Inflammatory mediators and angiogenic factors in choroidal neovascularization: pathogenetic interactions and therapeutic implications. Mediators of Inflammation. 2010;2010. PubMed PMID: 20871825. Pubmed Central PMCID: 2943126.

15. Group MPS. Laser photocoagulation of subfoveal neovascular lesions of age-related macular degeneration: updated findings from two clinical trials. Archives of ophthalmology. 1993;111(9):1200.
16. Ishikawa M, Jin D, Sawada Y, Abe S, Yoshitomi T. Future therapies of wet age-related macular degeneration. Journal of Ophthalmology. 2015;2015:138070. PubMed PMID: 25802751. Pubmed Central PMCID: 4354726.
17. Smith AG, Kaiser PK. Emerging treatments for wet age-related macular degeneration. Expert Opinion on Emerging Drugs. 2014 Mar;19(1):157-64. PubMed PMID: 24555421.
18. Kaiser PK. Emerging therapies for neovascular age-related macular degeneration: drugs in the pipeline. Ophthalmology. 2013 May;120(5 Suppl):S11-5. PubMed PMID: 23642781.
19. Rosenfeld PJ, Brown DM, Heier JS, Boyer DS, Kaiser PK, Chung CY, et al. Ranibizumab for neovascular age-related macular degeneration. The New England Journal of Medicine. 2006 Oct 5;355(14):1419-31. PubMed PMID: 17021318.
20. Melnikova I. Wet age-related macular degeneration. Nature Reviews Drug discovery. 2005 Sep;4(9):711-2. PubMed PMID: 16178119.
21. Vadlapudi AD, Ashaben P, Kishore C, Ashim KM. Recent patents on emerging therapeutics for the treatment of glaucoma, age-related macular degeneration and uveitis. Recent Patents on Biomedical Engineering. 2012;5(1):83-101.
22. Chen G, Li W, Tzekov R, Jiang F, Mao S, Tong Y. Bevacizumab versus ranibizumab for neovascular age-related macular degeneration: a meta-analysis of randomized controlled trials. Retina. 2015 Feb;35(2):187-93. PubMed PMID: 25105318.
23. Chen G, Li W, Tzekov R, Jiang F, Mao S, Tong Y. Ranibizumab monotherapy or combined with laser versus laser monotherapy for diabetic macular edema: a meta-analysis of randomized controlled trials. PloS ONE. 2014;9(12):e115797. PubMed PMID: 25541937. Pubmed Central PMCID: 4277392.
24. Mudunuri K. Intravitreal delivery of corticosteroid nanoparticles [Ph.D.]. Gainesville, FL: University of Florida; 2008.
25. Samudre SS, Lattanzio FA, Jr., Williams PB, Sheppard JD, Jr. Comparison of topical steroids for acute anterior uveitis. Journal of Ocular Pharmacology and Therapeutics. 2004 Dec;20(6):533-47. PubMed PMID: 15684812.
26. Wang Y, Wang VM, Chan CC. The role of anti-inflammatory agents in age-related macular degeneration (AMD) treatment. Eye. 2011 Feb;25(2):127-39. PubMed PMID: 21183941. Pubmed Central PMCID: 3044916.
27. Ciulla TA, Walker JD, Fong DS, Criswell MH. Corticosteroids in posterior segment disease: an update on new delivery systems and new indications. Current Opinion in Ophthalmology. 2004 Jun;15(3):211-20. PubMed PMID: 15118508.
28. Sherif Z, Pleyer U. Corticosteroids in ophthalmology: past-present-future. Ophthalmologica Journal International D'ophtalmologie. 2002 Sep-Oct;216(5):305-15. PubMed PMID: 12424394.
29. Wu WS, Wang FS, Yang KD, Huang CC, Kuo YR. Dexamethasone induction of keloid regression through effective suppression of VEGF expression and keloid fibroblast proliferation. The Journal of Investigative Dermatology. 2006 Jun;126(6):1264-71. PubMed PMID: 16575391.

30. Penfold PL, Wen L, Madigan MC, Gillies MC, King NJ, Provis JM. Triamcinolone acetonide modulates permeability and intercellular adhesion molecule-1 (ICAM-1) expression of the ECV304 cell line: implications for macular degeneration. Clinical and Experimental Immunology. 2000 Sep;121(3):458-65. PubMed PMID: 10971511. Pubmed Central PMCID: 1905725.
31. Wang YS, Friedrichs U, Eichler W, Hoffmann S, Wiedemann P. Inhibitory effects of triamcinolone acetonide on bFGF-induced migration and tube formation in choroidal microvascular endothelial cells. Graefe's Archive for Clinical and Experimental Ophthalmology. 2002 Jan;240(1):42-8. PubMed PMID: 11954780.
32. Sendrowski DP, Jaanus SD, Semes LP, Stern ME. Anti-inflammatory drugs. 5th ed. Bartlett JD, Jaanus SD, editors. New York, NY: Elsevier Health Sciences; 2008. 816 p.
33. McGhee CN, Dean S, Danesh-Meyer H. Locally administered ocular corticosteroids: benefits and risks. Drug safety: an International Journal of Medical Toxicology and Drug Experience. 2002;25(1):33-55. PubMed PMID: 11820911.
34. Tzekov R, Lin T, Zhang KM, Jackson B, Oyejide A, Orilla W, et al. Ocular changes after photodynamic therapy. Investigative Ophthalmology & Visual Science. 2006 Jan;47(1):377-85. PubMed PMID: 16384988.
35. Kaiser PK, Boyer DS, Cruess AF, Slakter JS, Pilz S, Weisberger A, et al. Verteporfin plus ranibizumab for choroidal neovascularization in age-related macular degeneration: twelve-month results of the DENALI study. Ophthalmology. 2012 May;119(5):1001-10. PubMed PMID: 22444829.
36. Gambhire S, Bhalerao K, Singh S. In situ hydrogel: different approaches to ocular drug delivery. International Journal of Pharmacy and Pharmaceutical Sciences. 2013;5(2):27-36.
37. Zhang W, Prausnitz MR, Edwards A. Model of transient drug diffusion across cornea. Journal of Controlled Release. 2004 Sep 30;99(2):241-58. PubMed PMID: 15380634.
38. Urtti A. Challenges and obstacles of ocular pharmacokinetics and drug delivery. Advanced Drug Delivery Reviews. 2006 Nov 15;58(11):1131-5. PubMed PMID: 17097758.
39. Kleinberg TT, Tzekov RT, Stein L, Ravi N, Kaushal S. Vitreous substitutes: a comprehensive review. Survey of Ophthalmology. 2011 Jul-Aug;56(4):300-23. PubMed PMID: 21601902.
40. Peyman GA, Lad EM, Moshfeghi DM. Intravitreal injection of therapeutic agents. Retina. 2009 Jul-Aug;29(7):875-912. PubMed PMID: 19584648.
41. Pahuja P, Arora S, Pawar P. Ocular drug delivery system: a reference to natural polymers. Expert Opinion on Drug Delivery. 2012 Jul;9(7):837-61. PubMed PMID: 22703523.
42. Yasukawa T, Ogura Y, Tabata Y, Kimura H, Wiedemann P, Honda Y. Drug delivery systems for vitreoretinal diseases. Progress in Retinal and Eye Research. 2004 May;23(3):253-81. PubMed PMID: 15177203.
43. Saraiya NV, Goldstein DA. Dexamethasone for ocular inflammation. Expert Opinion on Pharmacotherapy. 2011 May;12(7):1127-31. PubMed PMID: 21457057.
44. Gaudana R, Ananthula HK, Parenky A, Mitra AK. Ocular drug delivery. The AAPS Journal. 2010 Sep;12(3):348-60. PubMed PMID: 20437123. Pubmed Central PMCID: 2895432.

45. Zhou HY, Hao JL, Wang S, Zheng Y, Zhang WS. Nanoparticles in the ocular drug delivery. International Journal of Ophthalmology. 2013;6(3):390-6. PubMed PMID: 23826539. Pubmed Central PMCID: 3693026.
46. Patel A, Cholkar K, Agrahari V, Mitra AK. Ocular drug delivery systems: An overview. World Journal of Pharmacology. 2013;2(2):47-64.
47. Sabzevari A, Adibkia K, Hashemi H, Hedayatfar A, Mohsenzadeh N, Atyabi F, et al. Polymeric triamcinolone acetonide nanoparticles as a new alternative in the treatment of uveitis: in vitro and in vivo studies. European Journal of Pharmaceutics and Biopharmaceutics. eV. 2013 May;84(1):63-71. PubMed PMID: 23295645.
48. Bu HZ, Gukasyan HJ, Goulet L, Lou XJ, Xiang C, Koudriakova T. Ocular disposition, pharmacokinetics, efficacy and safety of nanoparticle-formulated ophthalmic drugs. Current Drug Metabolism. 2007 Feb;8(2):91-107. PubMed PMID: 17305490.
49. Bourges JL, Gautier SE, Delie F, Bejjani RA, Jeanny JC, Gurny R, et al. Ocular drug delivery targeting the retina and retinal pigment epithelium using polylactide nanoparticles. Investigative Ophthalmology and Visual Science. 2003 Aug;44(8):3562-9. PubMed PMID: 12882808.
50. Bala I, Hariharan S, Kumar MN. PLGA nanoparticles in drug delivery: the state of the art. Critical Reviews in Therapeutic Drug Carrier Systems. 2004;21(5):387-422. PubMed PMID: 15719481.
51. Geldenhuys W, Mbimba T, Bui T, Harrison K, Sutariya V. Brain-targeted delivery of paclitaxel using glutathione-coated nanoparticles for brain cancers. Journal of Drug Targeting. 2011 Nov;19(9):837-45. PubMed PMID: 21692650.
52. Carroll RT, Bhatia D, Geldenhuys W, Bhatia R, Miladore N, Bishayee A, et al. Brain-targeted delivery of Tempol-loaded nanoparticles for neurological disorders. Journal of Drug Targeting. 2010 Nov;18(9):665-74. PubMed PMID: 20158436.
53. Kreppel F, Kochanek S. Modification of adenovirus gene transfer vectors with synthetic polymers: a scientific review and technical guide. Molecular Therapy. 2008 Jan;16(1):16-29. PubMed PMID: 17912234.
54. Li F, Hurley B, Liu Y, Leonard B, Griffith M. Controlled release of bevacizumab through nanospheres for extended treatment of age-related macular degeneration. The Open Ophthalmology Journal. 2012;6:54-8. PubMed PMID: 22798970. Pubmed Central PMCID: 3394187.
55. Park D, Shah V, Rauck BM, Friberg TR, Wang Y. An anti-angiogenic reverse thermal gel as a drug-delivery system for age-related wet macular degeneration. Macromolecular Bioscience. 2013 Apr;13(4):464-9. PubMed PMID: 23316011.
56. Rauck BM, Friberg TR, Mendez CAM, Park D, Shah V, Bilonick RA, et al. Biocompatible reverse thermal gel sustains the release of intravitreal bevacizumab in vivo. Investigative Ophthalmology and Visual Science. 2014 Jan;55(1):469-76. PubMed PMID: WOS:000331877200055. English.
57. Vodithala S, Khatry S, Shastri N, Sadanandam DM. Development and evaluation of thermoreversible ocular gels of ketorolac tromethamine. International Journal of Biopharmaceutics. 2010;1(1):39-45.
58. Sutariya V, Miladore N, Geldenhuys W, Bhatia D, Wehrung D, Nakamura H. Thermoreversible gel for delivery of activin receptor-like kinase 5 inhibitor SB-505124 for glaucoma filtration surgery. Pharmaceutical Development and Technology. 2013 Jul-Aug;18(4):957-62. PubMed PMID: 22206499.

59. Gopal L, Sharma T. Use of intravitreal injection of triamcinolone acetonide in the treatment of age-related macular degeneration. Indian Journal of Ophthalmology. 2007;55(6):431.
60. Sherif Z, Pleyer U. Corticosteroids in ophthalmology: past–present–future. Ophthalmologica Journal International D'ophtalmologie. 2002;216(5):305-15.
61. Wu WS, Wang FS, Yang KD, Huang C-C, Kuo Y-R. Dexamethasone induction of keloid regression through effective suppression of VEGF expression and keloid fibroblast proliferation. Journal of Investigative Dermatology. 2006;126(6):1264-71.
62. Wang YS, Friedrichs U, Eichler W, Hoffmann S, Wiedemann P. Inhibitory effects of triamcinolone acetonide on bFGF-induced migration and tube formation in choroidal microvascular endothelial cells. Graefe's Archive for Clinical and Experimental Ophthalmology. 2002;240(1):42-8.
63. Ciulla TA, Criswell MH, Danis RP, Hill TE. Intravitreal triamcinolone acetonide inhibits choroidal neovascularization in a laser-treated rat model. Archives of Ophthalmology. 2001;119(3):399-404.
64. Spaide RF, Sorenson J, Maranan L. Combined photodynamic therapy with verteporfin and intravitreal triamcinolone acetonide for choroidal neovascularization. Ophthalmology. 2003;110(8):1517-25.
65. McGhee CN, Dean S, Danesh-Meyer H. Locally administered ocular corticosteroids. Drug Safety. 2002;25(1):33-55.
66. Fernández-Robredo P, Sancho A, Johnen S, Recalde S, Gama N, Thumann G, et al. Current treatment limitations in age-related macular degeneration and future approaches based on cell therapy and tissue engineering. Journal of Ophthalmology. 2014;2014:1-13.
67. Nowak JZ. Age-related macular degeneration (AMD): pathogenesis and therapy. Pharmacological Reports. 2006;58(3):353-63.
68. Regatieri C, Dreyfuss J, Nader H. Experimental treatments for neovascular age-related macular degeneration. In: Ying G-S, editor. Age Related Macular Degeneration - The Recent Advances in Basic Research and Clinical Care. Rijeka, Croatia: InTech 2012. p. 83-98.
69. Buschini E, Piras A, Nuzzi R, Vercelli A. Age related macular degeneration and drusen: neuroinflammation in the retina. Progress in Neurobiology. 2011;95(1):14-25.
70. Bylsma GW, Guymer RH. Treatment of age‐related macular degeneration. Clinical and Experimental Optometry. 2005;88(5):322-34.
71. R Thrimawithana T, Young S, R Bunt C, R Green C, G Alany R. Drug delivery to the posterior segment of the eye: challenges and opportunities. Drug Delivery Letters. 2011;1(1):40-4.
72. Park YG, Rhu HW, Kang S, Roh YJ. New Approach of Anti-VEGF Agents for Age-Related Macular Degeneration. Journal of ophthalmology. 2012;2012.
73. Ferrara N, Gerber H-P, LeCouter J. The biology of VEGF and its receptors. Nature Medicine. 2003;9(6):669-76.
74. Zhang W, Prausnitz MR, Edwards A. Model of transient drug diffusion across cornea. Journal of Controlled Release. 2004;99(2):241-58.
75. Urtti A. Challenges and obstacles of ocular pharmacokinetics and drug delivery. Advanced Drug Delivery Reviews. 2006;58(11):1131-5.

76. Gambhire S, Bhalerao K, Singh S. In situ hydrogel: different approaches to ocular drug delivery. International Journal of Pharmacy & Pharmaceutical Sciences. 2013;5(2):27-36.
77. Gaudana R, Ananthula HK, Parenky A, Mitra AK. Ocular drug delivery. The AAPS Journal. 2010;12(3):348-60.
78. Zhou HY, Hao JL, Wang S, Zheng Y, Zhang WS. Nanoparticles in the ocular drug delivery. International Journal of Ophthalmology. 2013;6(3):390.
79. Patel A, Cholkar K, Agrahari V, Mitra AK. Ocular drug delivery systems: an overview. World. 2013;2(2):47-64.
80. Sabzevari A, Adibkia K, Hashemi H, Hedayatfar A, Mohsenzadeh N, Atyabi F, et al. Polymeric triamcinolone acetonide nanoparticles as a new alternative in the treatment of uveitis: In vitro and in vivo studies. European Journal of Pharmaceutics and Biopharmaceutics. 2013;84(1):63-71.
81. Bu H-Z, Gukasyan HJ, Goulet L, Lou X-J, Xiang C, Koudriakova T. Ocular disposition, pharmacokinetics, efficacy and safety of nanoparticle-formulated ophthalmic drugs. Current Drug Metabolism. 2007;8(2):91-107.
82. Bourges J-L, Gautier SE, Delie F, Bejjani RA, Jeanny J-C, Gurny R, et al. Ocular drug delivery targeting the retina and retinal pigment epithelium using polylactide nanoparticles. Investigative Ophthalmology and Visual Science. 2003;44(8):3562-9.
83. Bala I, Hariharan S, Kumar MR. PLGA nanoparticles in drug delivery: the state of the art. Critical Reviews™ in Therapeutic Drug Carrier Systems. 2004;21(5):387-422.
84. Geldenhuys W, Mbimba T, Bui T, Harrison K, Sutariya V. Brain-targeted delivery of paclitaxel using glutathione-coated nanoparticles for brain cancers. Journal of Drug Targeting. 2011;19(9):837-45.
85. Carroll RT, Bhatia D, Geldenhuys W, Bhatia R, Miladore N, Bishayee A, et al. Brain-targeted delivery of Tempol-loaded nanoparticles for neurological disorders. Journal of Drug Targeting. 2010;18(9):665-74.
86. Kreppel F, Kochanek S. Modification of adenovirus gene transfer vectors with synthetic polymers: a scientific review and technical guide. Molecular Therapy. 2008;16(1):16-29.
87. Li F, Hurley B, Liu Y, Leonard B, Griffith M. Controlled release of bevacizumab through nanospheres for extended treatment of age-related macular degeneration. The Open Ophthalmology Journal. 2012;6:54.
88. Nirmal H, Bakliwal S, Pawar S. In-Situ gel: New trends in controlled and sustained drug delivery system. International Journal of PharmTech Research. 2010;2(2):1398-408.
89. Choi BG, Park MH, Cho S-H, Joo MK, Oh HJ, Kim EH, et al. In situ thermal gelling polypeptide for chondrocytes 3D culture. Biomaterials. 2010;31(35):9266-72.
90. Park D, Shah V, Rauck BM, Friberg TR, Wang Y. An anti‐angiogenic reverse thermal gel as a drug‐delivery system for age‐related wet macular degeneration. Macromolecular Bioscience. 2013;13(4):464-9.
91. Vodithala S, Khatry S, Shastri N, Sadanandam M. Development and evaluation of thermoreversible ocular gels of ketorolac tromethamine. International Journal of Biopharmaceutics. 2010;1(1):39-45.
92. Sutariya V, Miladore N, Geldenhuys W, Bhatia D, Wehrung D, Nakamura H. Thermoreversible gel for delivery of activin receptor-like kinase 5 inhibitor SB-505124 for

glaucoma filtration surgery. Pharmaceutical Development and Technology. 2013;18(4):957-62.
93. Majithiya RJ, Ghosh PK, Umrethia ML, Murthy RS. Thermoreversible-mucoadhesive gel for nasal delivery of sumatriptan. AAPS PharmSciTech. 2006;7(3):E80-E6.
94. Duvvuri S, Janoria KG, Mitra AK. Development of a novel formulation containing poly (d, l-lactide-co-glycolide) microspheres dispersed in PLGA–PEG–PLGA gel for sustained delivery of ganciclovir. Journal of Controlled Release. 2005;108(2):282-93.
95. Moghimipour E, Tafaghodi M, Balouchi A, Handali S. Formulation and in vitro evaluation of topical liposomal gel of triamcinolone acetonide. Research Journal of Pharmaceutical, Biological and Chemical Sciences. 2013;4(1):101-7.
96. Gómez-Gaete C, Tsapis N, Besnard M, Bochot A, Fattal E. Encapsulation of dexamethasone into biodegradable polymeric nanoparticles. International Journal of Pharmaceutics. 2007;331(2):153-9.
97. Budhian A, Siegel SJ, Winey KI. Haloperidol-loaded PLGA nanoparticles: systematic study of particle size and drug content. International Journal of Pharmaceutics. 2007;336(2):367-75.
98. Patel SP, Vaishya R, Mishra GP, Tamboli V, Pal D, Mitra AK. Tailor-made pentablock copolymer based formulation for sustained ocular delivery of protein therapeutics. Journal of Drug Delivery. 2014;2014:401747. PubMed PMID: 25045540. Pubmed Central PMCID: 4090486.
99. Tamboli V, Mishra GP, Mitra AK. Novel pentablock copolymer (PLA-PCL-PEG-PCL-PLA) based nanoparticles for controlled drug delivery: Effect of copolymer compositions on the crystallinity of copolymers and in vitro drug release profile from nanoparticles. Colloid and Polymer Science. 2013 May 1;291(5):1235-45. PubMed PMID: 23626400. Pubmed Central PMCID: 3633208.
100. Suen WL, Chau Y. Specific uptake of folate-decorated triamcinolone-encapsulating nanoparticles by retinal pigment epithelium cells enhances and prolongs antiangiogenic activity. Journal of Controlled Release. 2013 Apr 10;167(1):21-8. PubMed PMID: 23313961.
101. Yoncheva K, Lambov N. Development of biodegradable poly (alpha-methylmalate) microspheres. Die Pharmazie. 2000;55(2):148-50.
102. Yasukawa T, Ogura Y, Tabata Y, Kimura H, Wiedemann P, Honda Y. Drug delivery systems for vitreoretinal diseases. Progress in Retinal and Eye Research. 2004;23(3):253-81.
103. Kadam RS, Tyagi P, Edelhauser HF, Kompella UB. Influence of choroidal neovascularization and biodegradable polymeric particle size on transscleral sustained delivery of triamcinolone acetonide. International Journal of Pharmaceutics. 2012 Sep 15;434(1-2):140-7. PubMed PMID: 22633904. Pubmed Central PMCID: 3573139.
104. Coffey MJ, DeCory HH, Lane SS. Development of a non-settling gel formulation of 0.5% loteprednol etabonate for anti-inflammatory use as an ophthalmic drop. Clinical Ophthalmology. 2013;7:299-312.
105. Comstock TL, Decory HH. Advances in corticosteroid therapy for ocular inflammation: loteprednol etabonate. International Journal of Inflammation. 2012;2012:789623. PubMed PMID: 22536546. Pubmed Central PMCID: 3321285.
106. Comstock TL, Paterno MR, Singh A, Erb T, Davis E. Safety and efficacy of loteprednol etabonate ophthalmic ointment 0.5% for the treatment of inflammation and pain following

cataract surgery. Clinical Ophthalmology. 2011;5:177-86. PubMed PMID: 21383946. Pubmed Central PMCID: 3045067.
107. Bodor N, Bodor N, Wu WM. A comparison of intraocular pressure elevating activity of loteprednol etabonate and dexamethasone in rabbits. Current Eye Research. 1992 Jun;11(6):525-30. PubMed PMID: 1505197.
108. Bodor N, Loftsson T, Wu WM. Metabolism, distribution, and transdermal permeation of a soft corticosteroid, loteprednol etabonate. Pharmaceutical Research. 1992 Oct;9(10):1275-8. PubMed PMID: 1448425.
109. Ilyas H, Slonim CB, Braswell GR, Favetta JR, Schulman M. Long-term safety of loteprednol etabonate 0.2% in the treatment of seasonal and perennial allergic conjunctivitis. Eye and Contact Lens. 2004 Jan;30(1):10-3. PubMed PMID: 14722462.
110. Controlled evaluation of loteprednol etabonate and prednisolone acetate in the treatment of acute anterior uveitis. American Journal of Ophthalmology. 1999 5//;127(5):537-44.
111. Bourges JL, Gautier SE, Delie F, Bejjani RA, Jeanny JC, Gurny R, et al. Ocular drug delivery targeting the retina and retinal pigment epithelium using polylactide nanoparticles. Investigative Ophthalmology and Visual Science. 2003;44:3562-9.
112. Bejjani RA, BenEzra D, Cohen H, Rieger J, Andrieu C, Jeaanny JC, et al. Nanoparticles for gene delivery to retinal pigment epithelial cells. Molecular Vision. 2005;11:124-32.
113. Normand N, Valamanesh F, Savoldelli M, Mascarelli F, BenEzra D, Courtois Y, et al. VP22 light controlled delivery of oligonucleotides to ocular cells in vitro and in vivo. Molecular Vision. 2005;11:184-91.
114. Kassem MA, AbdelRahman AA, Ghorab MM, Ahmed MB, Khalil RM. Nanosuspensions as an ophthalmic delivery system for certain glucocorticoid drugs. Internation Journal of Pharmaceutics. 2007;340:126-33.
115. Silva GRd, Fialho SL, Siqueira RC, Jorge R, Junior AdSC. Implants as drug delivery devices for the treatment of eye diseases. Brazillian Journal of Pharmaceutical Sciences. 2010;46(3):585-95.
116. Hirani A, Grover A, Lee YW, Pathak Y, Sutariya V. Triamcinolone acetonide nanoparticles incorporated in thermoreversible gels for age-related macular degeneration. Pharmaceutical Development and Technology. 2014 Sep 26:1-7. PubMed PMID: 25259682.
117. Coleman HR, Chan CC, Ferris FL, 3rd, Chew EY. Age-related macular degeneration. Lancet. 2008 Nov 22;372(9652):1835-45. PubMed PMID: 19027484. Pubmed Central PMCID: 2603424.
118. Campochiaro PA. Retinal and choroidal neovascularization. Journal of Cellular Physiology. 2000 Sep;184(3):301-10. PubMed PMID: 10911360.
119. Necela BM, Cidlowski JA. Mechanisms of glucocorticoid receptor action in noninflammatory and inflammatory cells. Proceedings of the American Thoracic Society. 2004;1(3):239-46. PubMed PMID: 16113441.
120. Zhang X, Bao S, Lai D, Rapkins RW, Gillies MC. Intravitreal triamcinolone acetonide inhibits breakdown of the blood-retinal barrier through differential regulation of VEGF-A and its receptors in early diabetic rat retinas. Diabetes. 2008 Apr;57(4):1026-33. PubMed PMID: 18174522. Pubmed Central PMCID: 2836241.
121. Zhang X, Wang N, Schachat AP, Bao S, Gillies MC. Glucocorticoids: structure, signaling and molecular mechanisms in the treatment of diabetic retinopathy and diabetic

macular edema. Current Molecular Medicine. 2014 Mar;14(3):376-84. PubMed PMID: 24467200.
122. Lyzogubov VV, Tytarenko RG, Liu J, Bora NS, Bora PS. Polyethylene glycol (PEG)-induced mouse model of choroidal neovascularization. The Journal of Biological Chemistry. 2011 May 6;286(18):16229-37. PubMed PMID: 21454496. Pubmed Central PMCID: 3091230.
123. Lambert V, Lecomte J, Hansen S, Blacher S, Gonzalez ML, Struman I, et al. Laser-induced choroidal neovascularization model to study age-related macular degeneration in mice. Nature Protocols. 2013 Nov;8(11):2197-211. PubMed PMID: 24136346. Epub 2013/10/19.
124. Lee WH, Sonntag WE, Mitschelen M, Yan H, Lee YW. Irradiation induces regionally specific alterations in pro-inflammatory environments in rat brain. International Journal of Radiation Biology. 2010 Feb;86(2):132-44. PubMed PMID: 20148699. Pubmed Central PMCID: 2827151.
125. Bora PS, Sohn JH, Cruz JM, Jha P, Nishihori H, Wang Y, et al. Role of complement and complement membrane attack complex in laser-induced choroidal neovascularization. Journal of Immunology. 2005 Jan 1;174(1):491-7. PubMed PMID: 15611275.
126. Lyzogubov VV, Tytarenko RG, Jha P, Liu J, Bora NS, Bora PS. Role of ocular complement factor H in a murine model of choroidal neovascularization. The American Journal of Pathology. 2010 Oct;177(4):1870-80. PubMed PMID: 20813971. Pubmed Central PMCID: 2947282.
127. Anderson DH, Radeke MJ, Gallo NB, Chapin EA, Johnson PT, Curletti CR, et al. The pivotal role of the complement system in aging and age-related macular degeneration: hypothesis re-visited. Progress in Retinal and Eye Research. 2010 Mar;29(2):95-112. PubMed PMID: 19961953. Pubmed Central PMCID: 3641842.
128. Sarao V, Veritti D, Boscia F, Lanzetta P. Intravitreal steroids for the treatment of retinal diseases. The Scientific World Journal. 2014;2014:989501. PubMed PMID: 24526927. Pubmed Central PMCID: 3910383.
129. Hochhaus G, Chen LS, Ratka A, Druzgala P, Howes J, Bodor N, et al. Pharmacokinetic characterization and tissue distribution of the new glucocorticoid soft drug loteprednol etabonate in rats and dogs. Journal of Pharmaceutical Sciences. 1992 Dec;81(12):1210-5. PubMed PMID: 1491342.
130. Stewart MW. PDGF: Ophthalmology's Next Great Target. Expert Reviews in Ophthalmology. 2013;8(6):527-37.

Appendix A: Ocular Toxicity of Nanoparticles

Anjali Hirani[1,2*] and Aditya Grover[1], Yong W. Lee[2], Vijaykumar Sutariya[1], Yashwant Pathak[1]

[1] Department of Pharmaceutical Sciences, College of Pharmacy, University of South Florida, Tampa, FL 33612

[2] School of Biomedical Engineering and Sciences, Virginia Tech, Blacksburg, VA 24060

*A. Grover and A. Hirani are equal contributors to this work

Corresponding Author: Yashwant Pathak

Published: Hirani A, Grover A, Lee YW, Sutariya V, Pathak Y. (2014). Ocular Toxicity of Nanoparticles In V. Sutariya and Y. Pathak (Eds.), *Biointeraction of Nanomaterials* (pp. 347-352) Boca Raton, FL: CRC Press Taylor & Francis Group.

Contents

1.1 Use of Nanoparticles in Ocular Therapy

The application of biodegradable nanoparticles in ocular therapies is of utmost importance to the field of ocular medicine. The enhancement of current methods of therapy could mean a drastic change in the quality of life of people suffering from a number of degenerative posterior eye disorders. Currently, the most common form of ocular therapy involved topical treatment in the form of eye drops due to its ease of use, minimal risk of infection, and patient compliability (1). This method is limited in its effect, as natural processes in the eye flush the drug out of the tissue within the first minute of application; lacrimation is one such example (1, 2). The structural barriers in ocular tissue combined with the difficulty in drug delivery make the posterior eye chamber a potentially neglected site of therapy (1).

To directly target the posterior eye chamber, a common method of therapy is intravitreal injection (IVT) to deliver drugs to the retina (1, 2). This method is not without any adverse side effects, common ones of which include tissue damage and infections (1). Nonbiodegradable forms of treatment are also used, by which a nano-sized device is surgically implanted at the site of therapy (3). The drawbacks of such a method are the relative large sized incision required to implant a device and the repeated implantations of a new device once the previous one has exhausted its drug supply; neglecting removal of the device may cause it to be encapsulated by fibrous tissue (3). Possible complications with this type of therapy include retinal detachment, vitreous hemorrhage, and dissolution of the device, among others (3).

It behooves pharmaceutical researchers to develop nanotechnologies that bypass these invasive methods. Such particles improve tissue penetration, bypassing IVT, and provide sustained drug or gene therapy, a possible advantage that would bypass the need for viral gene therapy, a method that is not without its own risk of infection and hemorrhagic complications (2, 4, 5). By being able to control the dramatic increase in surface area to volume ratio of nanoparticles as compared to comparable macroscopic devices, researchers would be able to enhance tissue penetration and drug delivery systems directly to the effected tissue (4, 6).

The accessibility of the eye makes it a great target for nanoparticle therapy (2). However, such technologies are not without their own drawbacks. Nanoparticles may be coated with toxic

chemicals which could be released into the body during therapies or may build up into tissues and cause blockages leading to an increase in interocular pressure (3, 4). The retina and optic neural tissue are very sensitive to toxic materials, which may cause unforeseen complications due to seepage of toxic materials during therapy (2, 5, 6).

The most common forms of nanoparticle toxicity that are expressed in ocular tissue are oxidative stress, counteractions with cell membranes, and inflammation (2). These parameters were tested in the trials conducted with the following nanoparticles outlined in this section of the chapter. Because the rabbit is the most common animal model used for ocular toxicity studies, most of the studies cited used this animal to obtain toxicity data (2). The large lens of the mouse and rat make them poor models, as administrating intraocular injections proves difficult (2). In addition, a number of ocular complications arise in the mouse or rat by even the slightest touch of the eye by the needle, including inflammation or the development of cataracts (2). Monkeys' eyes provide the best model for studying ocular toxicity of nanoparticles, but none of the following studies cited used the monkey as a model for the respective toxicity studies; it is unsure why not (2).

1.1.1 Nanoceria

One of the causes of retinal degenerative diseases, such as diabetic retinopathy, is oxidative damage due to reactive oxygen radical species (6). Cerium oxide nanoparticles, also known as nanoceria, have been developed as antioxidants and free radical scavengers as a potential therapy for such neurodegenerative diseases (6). When these nanoparticles are synthesized in the 3-5 nm range, they mimic the effects of the antioxidant enzymes, such as superoxide dismutase and catalase, which neutralize superoxide anions and hydrogen peroxides, respectively (6-8).

The primary method of administration for the nanoceria particles was via IVT. After injection, the retinal tissue accumulated the greatest concentration of nanoparticles and 70% of the particles were retained 120 days post-injection (6). Nanoceria was not actively eliminated from the eye, as 90% of the injected nanoceria was retained in the eye 120 days post-injection (6). The experimental half-life yield of the nanoceria in the retina was 414 days with a half-life

of 525 days in the eye. Studies by the Asati et al. showed that the polymer coating of the nanoceria particles may induce a charge on the particles, varying the rates of uptake in different tissues and inducing localization in certain tissues (6, 9). They also found that positively charged nanoceria particles could be taken up by more cell types than negatively charged particles (9).

Previous studies showed that weekly injected nanoceria did not have cytotoxic effects in heart, kidney, brain, lung, spleen, and liver; cytotoxic studies in ocular tissue also showed that nanoceria did not have toxic effects on healthy retinal tissue over a range of doses (6). Investigations of four types of retinal tissue – superior and inferior central retina and superior and inferior peripheral retina – 9 days post-IVT injection showed that there was no reduction in the thickness of these layers. This finding along with the lack of observable change in retinal function post nanoceria IVT injection as compared to saline injected eyes further suggests that nanoceria does not have any short- or long-term cytotoxic effects on retinal tissue (6). In addition, nanoceria particles were shown to be nontoxic to optical neural tissue up to 120 days post-injection (6).

However, there may be some drawbacks to using nanoceria particles. Synthesis of nanoceria particles through use of hexamethylenetetramine (HMT) may induce cytotoxic effects in ocular tissue (6). In addition, some cell culture studies with nanoceria have yielded results of particle aggregation, which may negatively affect ocular tissue (10). Given these possible negative effects of nanoceria particles, there are no negative effects on healthy retinal cells with enhanced redox nanoceria capacity (6). The minimal cytotoxic effects of nanoceria particles on retinal tissue make it a great candidate for possible widespread ocular drug therapies.

1.1.2 CK30PEG

Recombinant adeno-associated viruses (AAV) have been extensively used in ocular tissue as a gene therapeutic method by which long-term gene expression can be induced, thereby offering therapeutic intervention for defects in large genes (11, 12). Plasmid DNA compacted with polyethylene glycol (PEG)-substituted polylysine (CK30PEG) nanoparticles offer a promising alternative to AAV gene therapies (13, 14). Subretinal injections of CK30PEG nanoparticles were able to induce persistent gene expression in mice for up to a year, opening up

doors to efficiently deliver up to 20 kbp plasmid vectors efficiently to dividing and post-mitotic cells (11, 13, 15). These nanoparticles have been shown to be safe and effective in human clinical trials, thereby allowing for the direct targeting of molecular markers in photoreceptors and retinal pigment epithelium cells for gene therapies (11). Similar therapeutic results have been shown in mouse models expressing the retinitis pigmentosa phenotype (16).

Histological examination showed that the subretinal delivery of CK30PEG nanoparticles did not induce infiltration of inflammatory cells in the eye (13). Injected eyes did not show the proliferation of polymorphonuclear leukocytes (PMN), an early response to toxicity (13). Myeloperoxidase (MPO) immunoreactivity, an activator of inflammatory signaling cascades, was not detected in injected eyes, nor was F4/80 microglia/macrophage marker, a response to ischemia-induced retinopathy (13). PMN, MPO, and F4/80 markers were histologically expressed in positive experimental controls (13). The lack of such expression in CK30PEG injected eyes suggests that these nanoparticles do not cause an inflammatory cascade in injected eyes (13).

Enzyme-linked immunosorbent assay (ELISA) and Real-time reverse-transcription PCR (qRT-PCR) were used to detect the presence of interleukin-8 (IL-8), monocyte chemotactic protein-1 (MCP-1), and tumor necrosis factor-□ (TNF-α) proteins and mRNA, respectively, in CK30PEG injected eyes, saline injected eyes, and Bacillus cereus endophthalmitis eyes as a positive control (13). IL-8 can be produced in response to inflammatory stimuli and is involved in the initiation and amplification of acute inflammatory response processes (13). B. cereus eyes expressed elevated levels of IL-8 protein and mRNA, with lack of elevation of either expressed by nanoparticle and saline injected eyes (13). MCP-1 is a member of the chemokine family and recruits monocytes to sites of injury and infection (13). Eyes injected with CK30PEG nanoparticles showed transient elevations in MCP-1 mRNA and protein which returned to saline-injected control levels after 1 day (13). B. cereus positive control eye samples expressed markedly elevated levels of MCP-1 protein and mRNA (13). TNF-α is produced by macrophages and monocytes as a part of the inflammation cascade pathway and apoptotic cell death (13). There was no detectable increase in TNF-α levels following subretinal injection of CK30PEG, compared to significantly increased TNF-α levels in endophthalimitis positive control eyes.

The lack in expression of inflammatory cascade proteins in eyes with subretinally-injected CK30PEG suggests that this gene therapy model is nontoxic in ocular tissue, thereby safely inducing sustained gene expression in necessary tissues (13).

1.1.3 Magnetic Nanoparticles (MNP)

DNA-tethered magnetic nanoparticles are FDA-approved MRI contrast agents able to successfully deliver genes to targeted ocular tissues (2, 4, 5). These nanoparticles are nontoxic to retinal tissue; apart from successfully transfecting ocular cells, eyes treated with MNP did not show signs of inflammation nor did they induce white blood cell infiltration, both intravitreally and subretinally (5). Intraocular pressure in MNP treated eyes remained the same as PBS treated eyes, suggesting that the particles did not disturb any intraocular meshwork (4).

Histological analysis of MNP treated ocular tissue did not yield any signs of iron oxide toxicity by the nanoparticles (4). MTT cytotoxicity assays showed the biocompatibility of MNP coated with polyethylenoxide copolymers, suggesting that these nanoparticles are safe for intraocular injection (4). In addition, the iron oxide was not shown to cause oxidative stress in vivo (2).

The use of uncoated MNP could lead to aggregation and oxidation in vivo, thus natural, biocompatible and biodegradable polymers are used to coat the nanoparticles (4). Adaptation of the surface of the particle could enhance product delivery to tissues and could target specific tissues by the polymer coat used on the MNP (4). Because iron oxide is a component of the MNP, exposure to external magnetic fields could be harmful to body tissues, however this data was not provided (4). In addition, iron could damage photoreceptors in the eye, thereby causing a serious side effect (4, 17). However, the low iron load in the MNP and the protective polymer coating prevented iron from leaking out into the tissue and showed no great amplitude difference in electroretinography (ERG) waveforms as compared to tissues injected with PBS (4). Because MNP causes no major cytotoxicity issues in vivo for up to 5 months post-injection, MNP is one of the safest nanoparticle gene delivery mechanisms currently available (2, 4).

1.1.4 Chitosan

Chitosan, a biocompatible and nontoxic deacetylated form of chitin derived from crustacean shells, is one of the least expensive and most widely used nanomaterial in ocular therapies (2, 5). The positively-charged surface of the nanoparticles helps it interact well with the negatively-charged corneal surface and has been successful in delivering drugs and genes to ocular tissue (2, 5).

Given these benefits, chitosan is a biomaterial that has different effects in different ocular tissues, making it compatible in some and incompatible in others (2, 5). Topically, chitosan shows biocompatibility and efficient gene delivery with little to none tolerance issues nor any tissue necrosis up to 24 hours post treatment (2). However, chitosan induces acute inflammatory responses when injected intravitreally (2, 5). The severe inflammatory response caused a vitreous haze and membranous opacities caused by infiltration of a large number of monocytes to phagocytize the foreign polysachharide-based chitosan nanoparticles, suggesting that the immunomodulatory hyalocytes in the vitreous humor are particularly sensitive to chitosan (2, 5). There were signs of retinal degradation at the sites of most severe inflammation (5). The dichotomy in biological interaction of chitosan with different tissues suggests that chitosan is a promising nanoparticle for topical ocular therapy but a poor intraocular therapeutic nanoparticle.

1.1.5 Polylactic-C-glycolic Acid (PLGA)

PLGA is a copolymer of polylactic acid (PLA) and polyglycolic acid (PGA) (3). This biodegradable, biocompatible copolymer is one of the most studied polymers and is a popular choice for the treatment of choroidal neovascularization (2, 3). The ratio of PLA and PGA in the synthesis of PLGA can be altered to change the therapeutic effects of the copolymer in biological systems by changing the total surface area, rate of drug release, and rate of polymer degradation (3). Because PGA is synthesized using toxic solvents, improper formulations may cause toxicity in biological systems (3). Furthermore, PLGA can be synthesized by emulsification in acetone and methylene chloride, also chemicals that may induce cytotoxicity (2). However, dose-dependent studies of PLGA in biological systems did not yield any signs of cytotoxic effects on ocular tissues (2). With no reports of cytotoxicity in the eye, PLGA remains one of the most widely used, FDA-approved nanoparticles for experimental nanotherapies (2).

1.1.6 Other Nanoparticles

1.1.6.1 Poly(alkyl-cyanoacrylate) (PACA)

PACA is a colloidal suspension of nanoparticles shown to prolong the corneal penetration of hydrophilic and lipophilic drugs in the eye (18). These compounds have a strong shelf life, as they maintained their mean size and appeared unchanged when stored at room temperature for 6 months (18). The corneal penetration may be due to their colloidal nature, however its therapeutic application may be hindered by the disruption caused to the corneal cell membrane (18).

1.1.6.2 Poly-ε-caprolactone (PECL) nanoparticles and nanocapsules

PECL is a hydrophobic, biodegradable, and biocompatible polymer of ε-caprolactone (3). PECL nanoparticles are slowly broken down in biological systems by the hydrolysis of ester linkages but the nanoparticles can be mixed with more hydrophilic polymers to form copolymers that can be broken down at faster rates (3, 19). Experimental studies in rabbit eyes showed that the nanoparticles are well tolerated without any signs of inflammation in anterior and posterior segments of the eye (20).

PECL nanocapsules enhance the penetration of lipophilic drugs in ocular tissues without damaging the cell membranes, with penetration rates more favorable than PECL nanoparticles (18). The sizes of nanocapsules did not change after 6 months at room temperature, suggesting that the polymer coating imparts stability to the nanocapsules (18).

1.1.6.3 Nanomicelles

Nanomicelles, up to 100 nm in size, are a low-toxicity colloidal dispersion of molecules with a hydrophobic core and hydrophilic shell (1, 21). These molecules provide an excellent method by which to solubilize hydrophobic drugs with therapeutic concentrations and administer them to hydrophilic tissues, thereby lowering drug degradation and enhancing permeability (1). Because the hydrophilic sclera is an efficient therapeutic pathway to the posterior eye, nanomicelles make it easier for hydrophobic drugs to efficiently diffuse to the posterior eye with minimal degradation (1). In addition, the hydrophilicity of the nanomicelle shell may confer

resistance against systemic circulation washout via ocular blood and lymphatic vessels (1). This relatively new nanotherapeutic molecule has shown little toxicity in biological systems, but more toxicological studies are warranted before its widespread use (1).

1.1.6.4 Poly[(cholesteryl oxocarbonylamido ethyl) methyl bis(ethylene) ammonium iodide] (PCEP)

PCEP is a DNA-condensing agent with gene therapy potential in the eye (5). Similarly to MNP, PCEP did not induce inflammation when injected intravitreally or subretinally (5). These relatively harmless molecules did not attract white blood cells to the site of injection (5). Because of its inert, biodegradability, and low toxicity, it serves as a potential ocular nanoparticle transfection agent (5).

1.1.6.5 Acrylate polymers (Eudragit)

Eudragit is a nanoparticle that improves drug stability and maximizes drug dosages and effects (2). The biological activity of eudragit can be directly manipulated by the choice of polymer used to make the eudragit copolymer (2). There were no reports of ocular toxicity after 10 minutes of application, with mild irritation in the first 10 minutes reported by 20-30% of subjects (2). Because of its low- to nontoxicity, eudragit serves as an ocular topically therapeutic nanoparticle.

1.1.6.6 Solid lipid nanoparticles (SLN)

SLN, ranging in size up to 400 nm, are biodegradable and biocompatible, and have been used as nanoparticles since the 1990s (2). The advantage of these nanoparticles is their advanced drug load that they can carry (2). However, due to the nature of its synthesis, a potential source of toxicity may be the presence of excipients on the nanoparticle (2). In addition, some surfactants dissociate from the nanoparticle during sterilization due to the high temperatures, another potential source of toxicity; there is no dissociation of surfactants at body temperature (2).

1.2 References

1. Vadlapudi AD, Mitra AK. Nanomicelles: an emerging platform for drug delivery to the eye. Therapeutic Delivery. 2013;4(1):1-3.

2. Prow TW. Toxicity of nanomaterials to the eye. Wiley Interdisciplinary Reviews: Nanomedicine and Nanobiotechnology. 2010;2(4):317-33.

3. Christoforidis JB, Chang S, Jiang A, Wang J, Cebulla CM. Intravitreal devices for the treatment of vitreous inflammation. Mediators of Inflammation. 2012;2012.

4. Raju HB, Hu Y, Vedula A, Dubovy SR, Goldberg JL. Evaluation of magnetic micro-and nanoparticle toxicity to ocular tissues. PLoS One. 2011;6(5):e17452.

5. Prow TW, Bhutto I, Kim SY, Grebe R, Merges C, McLeod DS, et al. Ocular nanoparticle toxicity and transfection of the retina and retinal pigment epithelium. Nanomedicine: Nanotechnology, Biology and Medicine. 2008;4(4):340-9.

6. Wong LL, Hirst SM, Pye QN, Reilly CM, Seal S, McGinnis JF. Catalytic nanoceria are preferentially retained in the rat retina and are not cytotoxic after intravitreal injection. PLoS One. 2013;8(3):e58431.

7. Jessica E. Nanoceria exhibit redox state-dependent catalase mimetic activity. Chemical Communications. 2010;46(16):2736-8.

8. Self WT, Seal S. Nanoparticles of cerium oxide having superoxide dismutase activity. Google Patents; 2009.

9. Asati A, Santra S, Kaittanis C, Perez JM. Surface-charge-dependent cell localization and cytotoxicity of cerium oxide nanoparticles. ACS Nano. 2010;4(9):5321-31.

10. Verma A, Stellacci F. Effect of surface properties on nanoparticle–cell interactions. Small. 2010;6(1):12-21.

11. Han Z, Conley SM, Makkia R, Guo J, Cooper MJ, Naash MI. Comparative analysis of DNA nanoparticles and AAVs for ocular gene delivery. PLoS One. 2012;7(12):e52189.

12. Amado D, Mingozzi F, Hui D, Bennicelli JL, Wei Z, Chen Y, et al. Safety and efficacy of subretinal readministration of a viral vector in large animals to treat congenital blindness. Science Translational Medicine. 2010;2(21):21ra16.

13. Ding X-Q, Quiambao AB, Fitzgerald JB, Cooper MJ, Conley SM, Naash MI. Ocular delivery of compacted DNA-nanoparticles does not elicit toxicity in the mouse retina. PLoS One. 2009;4(10):e7410.

14. Liu G, Li D, Pasumarthy MK, Kowalczyk TH, Gedeon CR, Hyatt SL, et al. Nanoparticles of compacted DNA transfect postmitotic cells. Journal of Biological Chemistry. 2003;278(35):32578-86.

15. Fink T, Klepcyk P, Oette S, Gedeon C, Hyatt S, Kowalczyk T, et al. Plasmid size up to 20 kbp does not limit effective in vivo lung gene transfer using compacted DNA nanoparticles. Gene Therapy. 2006;13(13):1048-51.

16. Cai X, Conley SM, Nash Z, Fliesler SJ, Cooper MJ, Naash MI. Gene delivery to mitotic and postmitotic photoreceptors via compacted DNA nanoparticles results in improved phenotype in a mouse model of retinitis pigmentosa. The FASEB Journal. 2010;24(4):1178-91.

17. Declercq SS, Meredith P, Rosenthal AR. Experimental siderosis in the rabbit: correlation between electroretinography and histopathology. Archives of Ophthalmology. 1977;95(6):1051-8.

18. Calvo P, Vila‐Jato JL, Alonso MJ. Comparative in vitro evaluation of several colloidal systems, nanoparticles, nanocapsules, and nanoemulsions, as ocular drug carriers. Journal of Pharmaceutical Sciences. 1996;85(5):530-6.

19. Pitt C. Poly-e-caprolactone and its copolymers. In: Langer MCaRS, editor. Biodegradable Polymers as Drug Delivery Systems. New York, NY: Marcel Dekker; 1990. p. 71.

20. Silva-Cunha A, Fialho, SL., Naud, MC., Behar-Cohen, F. Poly-e-caprolactone intravitreous devices: an in vivo study. Investigative Ophthalmology Visual Science. 2009;50(5):2312-8.

21. Trivedi R, Kompella UB. Nanomicellar formulations for sustained drug delivery: strategies and underlying principles. Nanomedicine. 2010;5(3):485-505.

Appendix B: Nanotechnology for Omics-based Ocular Drug Delivery

Anjali Hirani[1,2,*], Aditya Grover[1,*], Yong Woo Lee[2], Yashwant Pathak[1], Vijaykumar Sutariya[1]

[1] Department of Pharmaceutical Sciences, USF College of Pharmacy, University of South Florida, Tampa, FL 33612.

[2] School of Biomedical Engineering and Sciences, Virginia Tech-Wake Forest University, Blacksburg, VA 24061.

[*] These authors contributed equally to this work.

This chapter/paper appears in *Handbook of Research on Diverse Application of Nanotechnology in Biomedicine, Chemistry and Engineering* edited by S. Soni, A. Salhotra, and M. Suar

Published: Hirani A, Lee YW, Pathak YV, Sutariya V. (2014). Nanotechnology for Omics-based Ocular Drug Delivery In S. Soni, A. Salhotra, and M. Suar (Eds.), *Handbook of Research on Diverse Application of Nanotechnology in Biomedicine, Chemistry and Engineering* (pp. 152-166) Hershey, PA: IGI Global.

ABSTRACT

Millions of people suffer from ocular diseases that impair vision and can lead to blindness. Advances in genomics and proteomics have revealed a number of different molecular markers specific for different ocular diseases, thereby optimizing the processes of drug development and discovery. Nanotechnology can increase the throughput of data obtained in omics-based studies and allows for more sensitive diagnostic techniques as well more efficient drug delivery systems. Biocompatible and biodegradable nanomaterials developed through omics-based research are able to target reported molecular markers for different ocular diseases and offer novel alternatives to conventional drug therapy. In this chapter, we review the pathophysiology, current genomic and proteomic information and current nanomaterial-based therapies of four ocular diseases: glaucoma, uveal melanoma, age-related macular degeneration, and diabetic retinopathy. Omics-based research can be used to elucidate specific genes and proteins and develop novel nanomedicine formulations to prevent, halt, or cure ocular diseases at the transcriptional or translational level.

OCULAR DISEASE

Approximately 140 million Americans over the age of 40 suffer from a variety of ocular diseases that impair vision and may lead to blindness (NEI, 2012). The prevalence of ocular disorders will continue to increase with the worldwide aging population. Although current treatments do exist, there is a need for better diagnostics and more efficient therapies that can arrest the progression and/or even reverse damage of ocular diseases. Currently, more information is needed to understand the pathogenesis of ocular disease as well as determining new drug targets to enhance ocular drug discovery or repositioning current drugs for more efficacious therapy.

Limitations in Treatment for Ocular Diseases

Currently, therapies exist to delay progression of some ocular diseases; however, a better understanding of pathogenic processes is needed to find more effective treatments. Some of the common ocular diseases presented later in this chapter possess a complex interplay of genetic factors that are challenging to treat. Discovery of genes responsible for ocular disorders can aid in the development of new therapeutic agents. Clinically, we are merely treating symptoms and not targeting the actual disease mechanisms. More research needs to be completed to elucidate these mechanisms.

A number of barriers for ocular drug delivery exist, such as nasolacrimal drainage and the blood-aqueous and blood-retinal barriers. This restricts administration of potential therapeutics. Drug can be delivered by a variety of routes including topical ocular, periocular injection, intravitreal injection, and systemic administration. The topical route is a convenient method of drug delivery to the anterior segment; however, a model of transient diffusion has shown that less than 5% of a lipophilic drug and 0.5% of a hydrophilic drug penetrate the cornea (W. Zhang, Prausnitz, & Edwards, 2004), and the remainder is cleared through nasolacrimal drainage and systemic absorption(Gambhire, Bhalerao, & Singh, 2013) . The amount of available drug that permeates across the sclera is reduced with cationic and lipophilic solutes and the RPE has tight intercellular junctions for hydrophilic molecules (Urtti, 2006). Additionally, the lymphatic system, blood vessels and active transporters all work to clear drugs administered through transscleral routes. Systemic administration of drugs requires high doses that are potentially toxic to obtain a therapeutic concentration across the blood ocular barriers (Geroski & Edelhauser,

2000; Sigurdsson, Konraethsdottir, Loftsson, & Stefansson, 2007). Intravitreal injections circumvent physiological barriers and maintain therapeutic doses without damage to bystander tissues; however, frequent injections can lead to complications like retinal detachment, increase in ocular pressure, and hemorrhage (Peyman, Lad, & Moshfeghi, 2009). Given the presence of these physiological barriers, the development of therapies utilizing nanotechnology that efficiently deliver drugs and extend drug release to the eye would be beneficial to the progression of ocular disease treatment. Due to the lengthy pipeline in gaining FDA approval, newly repositioned drugs can be utilized to expand current disease therapy.

Omics-based nanotechnology

The goal of omics-based nanotechnology is to use nanoscale technology to enhance early detection, gain an understanding of pathophysiology, as well as find better treatments for eye disease. Nanogenomics refers to a new approach for medical diagnostics and therapy (Nicolini, 2006). Nanoproteomics allows us to evaluate expression of ocular proteins, identify novel therapeutic targets study the pharmacological effects of therapeutics (Steely & Clark, 2000). These new techniques can improve the current understanding of ocular diseases and aid in the discovery of therapies targeting genes responsible for ocular disease.

APPLICATION TO OCULAR DISEASES

Glaucoma

Pathophysiology:

Glaucoma causes blindness in about 7 million people every year, only 10% of the people affected by glaucoma worldwide (Quigley, 1996). A number of risk factors have been identified for glaucoma, including hypertension, family history, and age, among others (Abbot F Clark & Thomas Yorio, 2003). Glaucoma is caused by progressive damage to the trabecular meshwork, optic nerve head, and retinal ganglion cells; however, the exact mechanism behind the nerve damage is yet unknown (Abbot F Clark & Thomas Yorio, 2003; Frank S Ong et al., 2013). Glaucoma can usually be diagnosed as open- or closed-angle and primary or secondary based on the degree of ocular hypertension (Abbot F Clark & Thomas Yorio, 2003). Elevated intraocular pressure (IOP) is characteristic of primary open-angle glaucoma (POAG), the most common type of glaucoma, and is the most common target of treatment.

Current genomic and proteomic information:

A number of genetic markers that play a role in multiple different types of glaucomas have been identified.

MYOC was one of the first genes identified for juvenile and adult-onset POAG (Stone et al., 1997). Its associated protein, myocilin, has been associated with the trabecular meshwork and may be associated with increased outflow resistance, leading to an increase in IOP pressure (Fautsch, Bahler, Jewison, & Johnson, 2000; WuDunn, 2002; Z. Zhou & Vollrath, 1999).

Reiger syndrome is a genetic disorder which manifests itself in craniofacial and umbilical abnormalities (Amendt, Semina, & Alward, 2000). The varied phenotypes associated with Reiger syndrome are associated with different mutations in the PITX2 gene and the PITX2 transcription factor for which it codes. More than half of the individuals diagnosed with Reiger syndrome develop glaucoma, making the mutant PITX2 gene a risk factor and molecular marker for glaucoma (WuDunn, 2002).

Primary congenital glaucoma has been traced to mutations in CYP1B1 gene. CYP1B1 codes for the CYP1B1 protein from the cytochrome P450 family, but its mechanism in ocular pathology is not yet fully understood (Stoilov, Jansson, Sarfarazi, & Schenkman, 2001). Studies of various ethnic populations affected with congenital glaucoma revealed multiple mutations of the CYP1B1 gene responsible for the disease in Western- and Middle Eastern as well as Japanese populations (Michels-Rautenstrauss et al., 2001).

Six genes (GLC1A-GLC1F) have been identified through pedigree analysis of families affected by hereditary POAG. PCOLCE2 has also been identified as a possible indicator of glaucoma because of its association with the trabecular meshwork and the GLC1C locus, but no mutations in PCOLCE2 were identified in patients with GLC1C-induced POAG (WuDunn, 2002). Population studies in Estonian POAG patients also showed a significantly higher association between individuals positive for the glutathione S-transferase (GSTM1) protein with POAG as compared to a control population. Smoking increased this risk (Juronen et al., 2000).

Reductions in the outflow of aqueous humor from the anterior chamber of the eye have been implicated in glaucoma pathology due to its association to IOP. Imbalances in the expression levels of matrix metalloproteinases (MMPs) and tissue inhibitors of MMPs (TIMPs), which remodel the extracellular matrix (ECM) of the trabecular meshwork, may account for the differences in aqueous humor outflow in patients with glaucoma (Wong et al., 2002). Disruption

of trabecular meshwork ECM was also revealed as a result of increased TGF-beta levels in glaucoma patients (Zhao, Ramsey, Stephan, & Russell, 2004). Prostaglandins increase the activity of MMPs in ciliary smooth muscle cells, which effects the outflow of aqueous humor, and can lead to a decrease in the high IOP pressure characteristic of POAG (Weinreb, Kashiwagi, Kashiwagi, Tsukahara, & Lindsey, 1997). In addition, cochlin protein has been identified as an elevator of IOP pressure in glaucoma patients by disrupting the trabecular meshwork (Bhattacharya et al., 2005).

Current therapies:

A number of current nanomedicine therapies have been investigated in the treatment of glaucoma physiology. The benefits that nanomedicines offer are their biodegradability, sustained release of drugs, and targeting of necessary tissues and molecular pathways.

Chu et al. investigated the activity of 7-hydroxy-2-dipropylaminotetralin (7-OH-DPAT)-loaded calcium phosphate nanoparticles (CAP) in the reduction of IOP and aqueous flow rate in glaucomatic rabbits. 7-OH-DPAT in CAP showed a hypotensive, therefore therapeutic, effect in the glaucomatic model; however, raclopride, a dopamine D2/D3 receptor agonist, was shown to reduce the effect of 7-OH-DPAT in CAP. The data suggests that dopamine D2/D3 receptors may play a role in modulating IOP and that CAP may potentially be a therapeutic agent for glaucoma. In addition, further investigations of the role of the dopamine D2/D3 receptor in glaucoma may elucidate further directed therapies for the modulation of glaucomatic IOP (Chu, He, & Potter, 2002).

Wadhwa et al. revealed the IOP-reducing effects of hyaluronic acid (HA)-conjugated chitosan (CS) nanoparticles (CS-HP-NPs) loaded with dorzolamide hydrochloride and timolol maleate, 2 drugs used in glaucoma treatment. CS-NPs have been used as nanomedicine carriers due to their biodegrability and drug availability, but conjugation with HA synergistically increases the mucoadhesion of CS-NPs. In vivo studies in rabbits revealed a significant IOP reduction in rabbits treated with CS-HA-NPs as opposed to the free drug solution, suggesting its potential use against glaucoma (Wadhwa, Paliwal, Paliwal, & Vyas, 2010).

Jiang et al. reported the neuroprotective role of glial cell-line derived neurotrophic factor (GDNF) loaded into poly DL-lactide-co-glycolide (PLGA) microspheres in elevated IOP-induced rats. Intravitreal injections of the GDNF-PLGA microspheres were significantly better in

the neuroprotection of retinal ganglion cells (RGCs) in chronically elevated IOP through the analysis of glial fibrillary acidic protein (GFAP) production compared to the blank PLGA microspheres and GDNF alone (Jiang et al., 2007). It is reasonable to believe that the nanomedicine administration of various other genes and RNA inhibitors of proteins may be able to provide further neuroprotection to RGCs after injury or surgery (Zarbin, Montemagno, Leary, & Ritch, 2013). Indeed, as a potential post-operative therapy to protect against scarring after glaucoma surgery, Dos Santos et al. investigated the role of nanosized complexes of antisense TGF-beta2 phosphorothiorate oligonucleotides (PS-ODN) with polyethylenimine (PEI) encapsulated in PLGA microspheres. Subconjunctival injections in rabbits significantly improved bleb survival and increased the intracellular penetration of PS-ODN, revealing the microspheres' potential therapeutic role (Gomes dos Santos et al., 2006).

The incorporation of drugs, genes, or oligonucleotides into biodegradable and biocompatible nanomedicine vectors may provide novel therapeutic potentials in the prevention and treatment of glaucoma. The size range of nanomedicines make these vectors compatible for endocytosis into effected cells and also offer sustained release of the compounds associated with the vectors. These compounds may be able to directly influence the genetic and molecular pathways that influence the glaucoma phenotype.

Uveal Melanoma

Pathophysiology:

Uveal melanoma (UM) is one of the most common ocular cancers in adults, with 7 cases per million each year and over 20 cases per million in those over the age of 70 (Ramasamy et al., 2014; Singh & Topham, 2003). Over ninety percent of UM cases arise in the choroid and have the worst prognosis, followed by the ciliary body and iris, with the best prognosis (Ramasamy et al., 2014). Over half of UM cases result in metastasis, 40% of which result in death even after primary tumor treatment (Bedikian, 2006). Close to 90% of UM metastatic cases result in metastasis to the liver; the skin, bones, and lungs are other common sites of metastasis following metastasis to the liver (Lorigan, Wallace, & Mavligit, 1991; Singh & Borden, 2005).

Current genomic and proteomic information:

Heat shock protein 27 (HSP-27) is a cytoplasmic protein involved in cell migration, cytoskeletal structure, cell survival, and tumor progression (Kostenko & Moens, 2009). It plays different roles in a number of different cancers; HSP-27 is over expressed in gastric, prostate, and node-negative breast carcinoma and indicates a poor prognosis in each, but over-expression of HSP-27 indicates good prognosis in non-small-cell lung- and ovarian carcinomas (Ramasamy et al., 2014). Proteomic analysis of primary UM tissue revealed a down regulation of HSP-27 in monosomy 3 tumors, with a significantly lower expression in monosomy 3 tumors as opposed to disomy 3 tumors (Coupland et al., 2010). In addition, Jmor et al. showed that a significantly reduced expression of HSP-27 in UM tissue correlated with a predicted survival of less than 8 years (Jmor, Kalirai, Taktak, Damato, & Coupland, 2012). Investigations in a human cuteanous melanoma cell line revealed that the over expression of HSP-27 inhibited cell proliferation and reduced cell invasiveness, which suggests that the under expression of HSP-27 might induce greater cell migration in UM (Aldrian et al., 2002).

Two-dimensional difference gel electrophoresis (2D DIGE) followed up by immunohistochemical studies in primary UM tumor samples also identified the over expression of fatty acid-binding protein heart type (FABP3) and triosephosphate isomerase (TPI1). In addition, siRNA knockdowns of these 2 proteins in a primary UM cell line revealed significantly reduced levels of cell invasion and migration (Linge et al., 2012). FABPs are thought to play a number of metabolic roles in cells, including growth, differentiation, and apoptosis (Lichtenfels et al., 2009). Investigation of the over expression of FABP in small cell lung cancer implicate its role in mitosis and cell growth (L. Zhang, Cilley, & Chinoy, 2000). FABP has also been linked with poor prognosis and tumor aggressiveness in human gastric carcinoma (Hashimoto et al., 2004). TPI1 plays a role in the cell's glycolysis and gluconeogenesis pathways, high rates of which are required for tumor cells (Albery & Knowles, 1976; Bui & Thompson, 2006). TPI1 has been reported to be associated with the aggressiveness of breast cancer, and its under expression was found to induce apoptosis in the HeLa cell line (Lee et al., 2010; Selicharova et al., 2008). However, its over expression in lung cancer tissue, cell lines, and plasma, as well as in prostate cancer implicates its role in the progression of disease and as biomarkers (Chen et al., 2002; Kim, Koo, Kim, Sohn, & Park, 2008; Qian et al., 2010). The identification of these genetic markers in UM and their varied roles in a number of different types of cancers suggests that their

over expression in primary UM tumors may contribute to the oncogeneity of the tissue. Further investigations of the roles of FABP3 and TPI1 in UM may reveal novel pathways for therapeutic intervention as well as screening techniques in preventing the progression of UM.

Proteomic analyses of primary tumors and cell lines have revealed the above-mentioned proteins as potential biomarkers for UM; however, further such studies are required to elucidate more proteins for the identification of UM. There is a lack of genomic and proteomic analysis of UM tissues in available literature, but such studies would greatly increase the understanding of the molecular mechanisms behind the induction and progression of the disease. The proteins and biomarkers identified by future studies would provide researchers with genomic and molecular pathways to target through nanotechnological intervention.

Current therapies:

The relatively low incidences of UM and the considerable lack of extensive genomic and proteomic studies of UM tissues contribute to low number of nanomedicines to target UM. However, the versatile nature of nanomedicines suggests its possible successes in treating UM.

Wang et al. investigated the role of dendrimer nanoparticle transfection therapy in the human choroidal melanoma cell line (OCM-1) as a potential treatment (Yingchih Wang, Mo, Wei, & Shi, 2013). The dendrimer nanoparticles were complexed with recombinant DNA plasmids of tumor necrosis factor-a (TNFa) and herpes simplex virus thymidine kinase (HSV-TK), both constructed with the promoter sequence of early growth response-1 (Egr1). Dendrimer nanoparticles are biocompatible and are formed from nanoparticle polymers with sizes of less than 100 nm, physiologically relevant when treating ocular diseases. The polymer is composed of amino groups which are protonated at physiological pH levels, allowing electrostatic interactions with oligonucleotides and their compaction and protection during transfection. The transfection complex is able to be endocytosed by the cell, allowing the oligonucleotide complex to be released into the cell and enter the nucleus for transcriptional regulation. Dendrimer-based nanoparticle transfection complexes offer biocompatibility and the protection of associated nucleic acids (Yingchih Wang et al., 2013).

Molecular studies in various tumors have identified the HSV-TK suicide gene as a promising and successful cancer treatment by killing infected cells and surrounding uninfected cells when administered in conjunction with other drugs or compounds (Rainov, 2000). Wang et

al. administered HSV-TK with TNF-a due to the natural anti-tumor properties exhibited by TNF-a, including the ability to activate immune responses and cause hemorrhaging and necrosis in tumoric tissues (Ha Thi et al., 2013; Kearney et al., 2013). HSV-TK and TNF-a were complexed with Egr1 promoter due to Egr1's revealed anti-tumor properties when associated with target genes (Y. Zhou et al., 2010) and the hypothesis that irradiation with 125I may activate the Egr1 promoter complex and induce the transcription and translation of TNF-a and HSV-TK (Yingchih Wang et al., 2013).

Wang et al. radiated the successfully-transfected tissues with 125I and found a significantly elevated expression of TNF-a and HSV-TK through western blot and ELISA analysis after radiation as compared to before, thought to be due to the activation of Egr1 transcription. Transmission electron microscopy (TEM) analysis of irradiated TNF-TK transfected tissues revealed an increased number of cells in the necrotic state along with the inhibition of cell growth and proliferation. The successful coupling of radiation with gene therapy revealed that targeted gene therapy through the Egr1 promoter and radiation could provide for a novel therapeutic route against UM (Yingchih Wang et al., 2013).

Future proteomic studies that reveal a number of other proteins involved in UM pathological pathways may also become similar targets for in vitro and in vivo experiments such as the one conducted by Wang et al. Coupling nanomedicine gene therapy with standard radiation therapy reveals a synergistic therapeutic effect in treated tissues, and may lead to clinical breakthroughs and better therapies.

Age-Related Macular Degeneration

Pathophysiology:

Age-related macular degeneration (AMD) is a disease that destroys sharp, central vision. It affects the central region of the retina known as the macula, which is responsible for fine vision. It is characterized by the presence of drusen and area of hyperpigmentation on the retinal pigment epithelium (RPE). Advanced AMD is characterized by choroidal neovascularization (CNV), the growth of abnormal blood vessels beneath the RPE or between the RPE and the retina(Bylsma & Guymer, 2005). It is accompanied by fluid and blood rupturing Bruch's membrane into the subretinal space, leading to irregularities of the retina.

Current genomic and proteomic information:

Case studies have provided evidence for a variety of genetic markers involved in the occurrence of AMD, namely in the formation of drusen and degeneration of macula. Docosahexaenoic acid (DHA) is present in photoreceptor cell membranes in the retina. It is extremely sensitive to oxidative damage and cleavage results in the production of carboxyethylpyrrole (CEP), an oxidative protein (Gu et al., 2010). CEP has been found to be abundant in ocular tissue of patients presenting with AMD. While a genetic marker of oxidative damage, CEPs promote the growth of capillaries and can contribute to neovascularization (Lu et al., 2009).

Due to the neovascularization present in AMD, anti-angiogenic therapy is useful to slow the progression of the disease. Vascular endothelial growth factor A (VEGF-A) is the most potent promoter of angiogenesis and vascular permeability and its role in the pathogenesis of neovascular AMD is well recognized (Ferrara, Gerber, & LeCouter, 2003; Park, Rhu, Kang, & Roh, 2012; Verteporfin In Photodynamic Therapy Study, 2001). VEGF levels and vitreous levels are elevated in human CNV in compared to healthy controls (Sendrowski, Jaanus, Semes, & Stern, 2008). Due to the implication of VEGF in the progression of AMD, anti-angiogenic drugs have been recently pursued to block the development and leakage of new, abnormal blood vessels.

Current therapies:

Three anti-angiogenic drugs are currently being used in the treatment of AMD: ranibizumab (Lucentis), bevacizumab (Avastin), and pegaptanib (Macugen)(Bylsma & Guymer, 2005). Ranibizumab is a human recombinant antibody fragment that displays high binding affinity towards all VEGF isoforms. Clinical trials have shown that ranibizumab helps maintain stable vision without further progression of the disease; however, because of the high cost of the drug, the use of the drug worldwide is limited (Rosenfeld et al., 2006). Bevacizumab has been used more recently as an ‘off label’ therapy. It is a full-length human recombinant monoclonal antibody, which binds all VEGF isoforms. It is FDA approved for colorectal, lung, and breast cancer, but is used in clinical trials for AMD due to lower patient cost. Pegaptanib is a pegylated aptamer that acts as an anti-VEGF agent. It binds the VEGF165 isoform and inhibits angiogenesis (Vadlapudi, Ashaben, Kishore, & Ashim, 2012). For these anti-angiogenic drugs, the biggest challenge is route of administration. Intravitreal injections allow for the most direct

approach; however, the chronic nature of the disease requires consistent injections resulting in side-effects such as retinal detachment and cataract formation (Mudunuri, 2008). Recent studies using nanoemulsions and polymeric micelles containing anti-VEGF bevacizumab result in sustained delivery. Additional research has shown that pDNA encapsulated by micelles can ameliorate choroidal neovascularization in AMD (F. S. Ong et al., 2013). These nanoemulsions and polymeric micelles used for delivery offer more effective drug delivery by their ability to maintain therapeutic concentrations of the active drug molecule over a longer duration than previous methods.

Diabetic Retinopathy

Pathophysiology:

Diabetic retinopathy (DR) is a consequence of diabetes, usually developing within 5-10 years. The disease is associated with progressive retinal ischemia (A. F. Clark & T. Yorio, 2003). It is characterized by loss of pericytes in retinal capillaries and subsequent thickening of capillary basement membranes and local ischemia. This induces the expression of VEGF, which can cause vessel leakage and formation of abnormal blood vessels, similar to AMD. The majority of vision loss from DR is due to macular edema. Other factors such as proliferation of fibrovascular membranes can lead to retinal detachment (A. F. Clark & T. Yorio, 2003).

Current genomic and proteomic information:

DR has been studied by proteomic analysis of the vitreous humor. Mass spectroscopy based studies have shown that elevated levels of extracellular carbonic anhydrase-I and kallikrein are present in patients with DR. This suggests that retinal hemorrhage contribute to the DR proteomic information. Studies displaying intravitreal injection of carbonic anhydrase-I in rats lead to increased retinal vessel leakage and edema (Gao et al., 2007).

Current therapies:

Current therapies include photocoagulation therapy and pharmacological agents that block VEGF signaling, such as ruboxistaurin mesylate which is a protein kinase C-□ inhibitor. Additionally, corticosteroids are also being evaluated for their angiostatic, antipermeable and antifibrotic properties (Samudre, Lattanzio, Williams, & Sheppard, 2004; Y. Wang, Wang, & Chan, 2011). Triamcinolone acetonide and dexamethasone are used in combination with other

treatments for posterior ocular disorders. They act by binding steroid receptors in cells to induce or repress targeted genes, thereby inhibiting inflammatory symptoms like edema and vascular permeability (Sherif & Pleyer, 2002). Corticosteroids act on VEGF by inhibiting VEGF secretion and inhibiting cytokine production (Wu, Wang, Yang, Huang, & Kuo, 2006). Corticosteroids can also inhibit basic fibroblast growth factor and ICAM-1 expression and decrease VEGF levels that are evident in neovascularization (Penfold et al., 2000; Y. S. Wang, Friedrichs, Eichler, Hoffmann, & Wiedemann, 2002). As with AMD, nanoparticles have gained attention as a drug delivery system to overcome the blood-retinal barriers. Recent studies have encapsulated current therapies in nanoemulsions to sustain drug delivery. Alternatively AuNPs alone have been shown to inhibit retinal neovascularization by suppressing VEGF receptor activation. It is believed that AuNP bind to the heparin-binding proteins of certain VEGF isoforms (Jo, Lee, & Kim, 2011).

CONCLUSIONS AND FUTURE PERSPECTIVES

Genomic and proteomic analyses consist of a number of different techniques to help identify the molecular basis behind diseases. Because the eyes act as our window to the world around us, measures taken to protect the eyes from damage would be of great benefit to all people.

We have described a number of different ocular diseases, ranging in severity from slight discomfort caused by IOP in glaucomatic patients, to partial blindness in AMD patients, leading to death in patients of UM. We have described a number of molecular markers, genomic and proteomic, that act as indicators for their respective diseases. These genes and proteins are involved in a multitude of pathways in ocular tissues and may play different roles in different diseases, but elucidating their role in ocular diseases helps in developing therapies against those diseases. However, the data obtained from genomic and proteomic analyses in ocular tissues available in current literature is not exhaustive; further research needs to be conducted to identify many more omics-related markers in all kinds of ocular tissues and diseases.

What has been reported so far in regards to genomic and proteomic biomarkers of ocular diseases have been useful in the development of nanomedicine for those diseases. Nanomedicine offers a number of advantages when compared to conventional drug therapy, including small sizes, tissue-targeting, sustained release of the drug, low toxicity, biocompatibility, and biodegradability. Nanomedicine is between 1-999 nm in size, but most are around 100-200 nm in

size, sizes that are tolerated in ocular tissues. The sizes and targeting of tissues through surface conjugations of the nanomedicine vectors enable their endocytosis into the cell. Once in the cell, nanomedicine exhibits a steady and sustained release of the drug compound over days, weeks, and even months. Most nanomedicine vectors are made from organic compounds that are well tolerated in ocular tissues, such as PLGA, and can be broken down into harmless compounds by catabolismand eventually excreted. The ability to deliver novel drug, nucleic acid, protein, and herbal compounds through complexing or encapsulating them within nanomedicine allows for the direct targeting of the molecular pathways indicated by omics analysis specific for that disease. Through directly targeting specific proteins, the disease can be prevented, arrested, or even cured at the transcriptional or translational level. Further and continued omics-based research will have a direct impact on the well-being and prognosis of degenerative ocular diseases through the development of novel nanomedicine formulations.

REFERENCES

Albery, W John, & Knowles, Jeremy R. (1976). Free-energy profile for the reaction catalyzed by triosephosphate isomerase. Biochemistry, 15(25), 5627-5631.

Aldrian, Silke, Trautinger, Franz, Fröhlich, Ilse, Berger, Walter, Micksche, Michael, & Kindas-Mügge, Ingela. (2002). Overexpression of Hsp27 affects the metastatic phenotype of human melanoma cells in vitro. Cell stress & chaperones, 7(2), 177.

Amendt, BA, Semina, EV, & Alward, WLM. (2000). Rieger syndrome: a clinical, molecular, and biochemical analysis. Cellular and Molecular Life Sciences CMLS, 57(11), 1652-1666.

Bedikian, Agop Y. (2006). Metastatic uveal melanoma therapy: current options. International ophthalmology clinics, 46(1), 151-166.

Bhattacharya, Sanjoy K, Rockwood, Edward J, Smith, Scott D, Bonilha, Vera L, Crabb, John S, Kuchtey, Rachel W, . . . Crabb, John W. (2005). Proteomics reveal Cochlin deposits associated with glaucomatous trabecular meshwork. Journal of Biological Chemistry, 280(7), 6080-6084.

Bui, Thi, & Thompson, Craig B. (2006). Cancer's sweet tooth. Cancer cell, 9(6), 419-420.

Bylsma, G. W., & Guymer, R. H. (2005). Treatment of age-related macular degeneration. Clin Exp Optom, 88(5), 322-334.

Chen, Guoan, Gharib, Tarek G, Huang, Chiang-Ching, Thomas, Dafydd G, Shedden, Kerby A, Taylor, Jeremy MG, . . . Iannettoni, Mark D. (2002). Proteomic analysis of lung adenocarcinoma identification of a highly expressed set of proteins in tumors. Clinical Cancer Research, 8(7), 2298-2305.

Chu, Teh-Ching, He, Qing, & Potter, David E. (2002). Biodegradable calcium phosphate nanoparticles as a new vehicle for delivery of a potential ocular hypotensive agent. Journal of ocular pharmacology and therapeutics, 18(6), 507-514.

Clark, A. F., & Yorio, T. (2003). Ophthalmic drug discovery. Nat Rev Drug Discov, 2(6), 448-459. doi: 10.1038/nrd1106

Clark, Abbot F, & Yorio, Thomas. (2003). Ophthalmic drug discovery. Nature Reviews Drug Discovery, 2(6), 448-459.

Coupland, Sarah E, Vorum, Henrik, Mandal, Nakul, Kalirai, Helen, Honoré, Bent, Urbak, Steen Fiil, . . . Damato, Bertil. (2010). Proteomics of uveal melanomas suggests HSP-27 as a possible surrogate marker of chromosome 3 loss. Investigative ophthalmology & visual science, 51(1), 12-20.

Fautsch, Michael P, Bahler, Cindy K, Jewison, David J, & Johnson, Douglas H. (2000). Recombinant TIGR/MYOC increases outflow resistance in the human anterior segment. Investigative ophthalmology & visual science, 41(13), 4163-4168.

Ferrara, N., Gerber, H. P., & LeCouter, J. (2003). The biology of VEGF and its receptors. Nat Med, 9(6), 669-676. doi: 10.1038/nm0603-669

Gambhire, S., Bhalerao, K., & Singh, S. (2013). In situ hydrogel: Different approaches to ocular drug delivery. Int. J. Pharm. Pharm Sci., 5(2), 27-36.

Gao, B. B., Clermont, A., Rook, S., Fonda, S. J., Srinivasan, V. J., Wojtkowski, M., . . . Feener, E. P. (2007). Extracellular carbonic anhydrase mediates hemorrhagic retinal and cerebral vascular permeability through prekallikrein activation. Nat Med, 13(2), 181-188. doi: 10.1038/nm1534

Geroski, D. H., & Edelhauser, H. F. (2000). Drug delivery for posterior segment eye disease. Invest Ophthalmol Vis Sci, 41(5), 961-964.

Gomes dos Santos, Ana L, Bochot, Amélie, Doyle, Aoife, Tsapis, Nicolas, Siepmann, Juergen, Siepmann, Florence, . . . Fattal, Elias. (2006). Sustained release of nanosized complexes of polyethylenimine and anti-TGF-β2 oligonucleotide improves the outcome of glaucoma surgery. Journal of controlled release, 112(3), 369-381.

Gu, J., Pauer, G. J., Yue, X., Narendra, U., Sturgill, G. M., Bena, J., . . . Proteomic, A. M. D. Study Group. (2010). Proteomic and genomic biomarkers for age-related macular degeneration. Adv Exp Med Biol, 664, 411-417. doi: 10.1007/978-1-4419-1399-9_47

Ha Thi, Huyen Trang, Lim, Hee-Sun, Kim, Jooyoung, Kim, Young-Mi, Kim, Hye-Youn, & Hong, Suntaek. (2013). Transcriptional and post-translational regulation of Bim is essential for TGF-β and TNF-α-induced apoptosis of gastric cancer cell. Biochimica et Biophysica Acta (BBA)-General Subjects, 1830(6), 3584-3592.

Hashimoto, Takeaki, Kusakabe, Takashi, Sugino, Takashi, Fukuda, Takeaki, Watanabe, Kazuo, Sato, Yukio, . . . Fujii, Hiroshi. (2004). Expression of heart-type fatty acid-binding

protein in human gastric carcinoma and its association with tumor aggressiveness, metastasis and poor prognosis. Pathobiology, 71(5), 267-273.

Jiang, Caihui, Moore, Michael J, Zhang, Xinmei, Klassen, Henry, Langer, Robert, & Young, Michael. (2007). Intravitreal injections of GDNF-loaded biodegradable microspheres are neuroprotective in a rat model of glaucoma. Mol Vis, 13, 1783-1792.

Jmor, Fidan, Kalirai, Helen, Taktak, Azzam, Damato, Bertil, & Coupland, Sarah E. (2012). HSP‐27 protein expression in uveal melanoma: correlation with predicted survival. Acta ophthalmologica, 90(6), 534-539.

Jo, D. H., Lee, T. G., & Kim, J. H. (2011). Nanotechnology and nanotoxicology in retinopathy. Int J Mol Sci, 12(11), 8288-8301. doi: 10.3390/ijms12118288

Juronen, Erkki, Tasa, Gunnar, Veromann, Siiri, Parts, Lii, Tiidla, Anne, Pulges, Riina, . . . Mikelsaar, Aavo-Valdur. (2000). Polymorphic glutathione S-transferase M1 is a risk factor of primary open-angle glaucoma among Estonians. Experimental eye research, 71(5), 447-452.

Kearney, Conor J, Sheridan, Clare, Cullen, Sean P, Tynan, Graham A, Logue, Susan E, Afonina, Inna S, . . . Martin, Seamus J. (2013). Inhibitor of apoptosis proteins (IAPs) and their antagonists regulate spontaneous and tumor necrosis factor (TNF)-induced proinflammatory cytokine and chemokine production. Journal of Biological Chemistry, 288(7), 4878-4890.

Kim, Jung Eun, Koo, Kyung Hee, Kim, Yeul Hong, Sohn, Jeongwon, & Park, Yun Gyu. (2008). Identification of potential lung cancer biomarkers using an in vitro carcinogenesis model. Experimental & molecular medicine, 40(6), 709-720.

Kostenko, Sergiy, & Moens, Ugo. (2009). Heat shock protein 27 phosphorylation: kinases, phosphatases, functions and pathology. Cellular and molecular life sciences, 66(20), 3289-3307.

Lee, Won-Hee, Choi, Joon-Seok, Byun, Mi-Ran, Koo, Kyo-tan, Shin, Soona, Lee, Seung-Ki, & Surh, Young-Joon. (2010). Functional inactivation of triosephosphate isomerase through phosphorylation during etoposide-induced apoptosis in HeLa cells: Potential role of Cdk2. Toxicology, 278(2), 224-228.

Lichtenfels, Rudolf, Dressler, Sven P, Zobawa, Monica, Recktenwald, Christian V, Ackermann, Angelika, Atkins, Derek, . . . Lottspeich, Friedrich. (2009). Systematic Comparative

Protein Expression Profiling of Clear Cell Renal Cell Carcinoma A PILOT STUDY BASED ON THE SEPARATION OF TISSUE SPECIMENS BY TWO-DIMENSIONAL GEL ELECTROPHORESIS. Molecular & Cellular Proteomics, 8(12), 2827-2842.

Linge, Annett, Kennedy, Susan, O'Flynn, Deirdre, Beatty, Stephen, Moriarty, Paul, Henry, Michael, . . . Meleady, Paula. (2012). Differential expression of fourteen proteins between uveal melanoma from patients who subsequently developed distant metastases versus those who did not. Investigative ophthalmology & visual science, 53(8), 4634-4643.

Lorigan, JG, Wallace, S, & Mavligit, GM. (1991). The prevalence and location of metastases from ocular melanoma: imaging study in 110 patients. AJR. American journal of roentgenology, 157(6), 1279-1281.

Lu, L., Gu, X., Hong, L., Laird, J., Jaffe, K., Choi, J., . . . Salomon, R. G. (2009). Synthesis and structural characterization of carboxyethylpyrrole-modified proteins: mediators of age-related macular degeneration. Bioorg Med Chem, 17(21), 7548-7561. doi: 10.1016/j.bmc.2009.09.009

Michels-Rautenstrauss, Karin G, Mardin, Christian Y, Zenker, Martin, Jordan, Nicole, Gusek-Schneider, Gabriele-Charlotte, & Rautenstrauss, Bernd W. (2001). Primary congenital glaucoma: three case reports on novel mutations and combinations of mutations in the GLC3A (CYP1B1) gene. Journal of glaucoma, 10(4), 354-357.

Mudunuri, K. (2008). Intravitreal Delivery of Corticosteroid Nanoparticles. (Ph.D. Ph.D.), University of Florida, Gainesville, FL. Retrieved from http://ufdc.ufl.edu/UFE0022065/00001

NEI. (2012). Prevalence of Adult Vision Impairment and Age-Related Eye Diseases in America. Retrieved 11/20/13, 2013

Nicolini, C. (2006). Nanogenomics for medicine. Nanomedicine (Lond), 1(2), 147-152. doi: 10.2217/17435889.1.2.147

Ong, F. S., Kuo, J. Z., Wu, W. C., Cheng, C. Y., Blackwell, W. L., Taylor, B. L., . . . Wong, T. Y. (2013). Personalized Medicine in Ophthalmology: From Pharmacogenetic Biomarkers to Therapeutic and Dosage Optimization. J Pers Med, 3(1), 40-69. doi: 10.3390/jpm3010040

Ong, Frank S, Kuo, Jane Z, Wu, Wei-Chi, Cheng, Ching-Yu, Blackwell, Wendell-Lamar B, Taylor, Brian L, . . . Wong, Tien Y. (2013). Personalized Medicine in Ophthalmology: From Pharmacogenetic Biomarkers to Therapeutic and Dosage Optimization. Journal of Personalized Medicine, 3(1), 40-69.

Park, Y. G., Rhu, H. W., Kang, S., & Roh, Y. J. (2012). New Approach of Anti-VEGF Agents for Age-Related Macular Degeneration. J Ophthalmol, 2012, 637316. doi: 10.1155/2012/637316

Penfold, P. L., Wen, L., Madigan, M. C., Gillies, M. C., King, N. J., & Provis, J. M. (2000). Triamcinolone acetonide modulates permeability and intercellular adhesion molecule-1 (ICAM-1) expression of the ECV304 cell line: implications for macular degeneration. Clin Exp Immunol, 121(3), 458-465.

Peyman, G. A., Lad, E. M., & Moshfeghi, D. M. (2009). Intravitreal injection of therapeutic agents. Retina, 29(7), 875-912. doi: 10.1097/IAE.0b013e3181a94f01

Qian, Xiao-Long, Shi, Qing-Guo, Pang, Bo, Wu, Rui-Qin, Yu, Lan, Li, Shan-Hu, . . . Zhou, Jian-Guang. (2010). [Identification and expression of two new secretory proteins associated with prostate cancer]. Yi chuan= Hereditas/Zhongguo yi chuan xue hui bian ji, 32(3), 235-241.

Quigley, Harry A. (1996). Number of people with glaucoma worldwide. British Journal of Ophthalmology, 80(5), 389-393.

Rainov, Nicolai G. (2000). A phase III clinical evaluation of herpes simplex virus type 1 thymidine kinase and ganciclovir gene therapy as an adjuvant to surgical resection and radiation in adults with previously untreated glioblastoma multiforme. Human gene therapy, 11(17), 2389-2401.

Ramasamy, Pathma, Murphy, Conor C, Clynes, Martin, Horgan, Noel, Moriarty, Paul, Tiernan, Damien, . . . Meleady, Paula. (2014). Proteomics in uveal melanoma. Experimental eye research, 118, 1-12.

Rosenfeld, P. J., Brown, D. M., Heier, J. S., Boyer, D. S., Kaiser, P. K., Chung, C. Y., . . . Group, Marina Study. (2006). Ranibizumab for neovascular age-related macular degeneration. N Engl J Med, 355(14), 1419-1431. doi: 10.1056/NEJMoa054481

Samudre, S. S., Lattanzio, F. A., Jr., Williams, P. B., & Sheppard, J. D., Jr. (2004). Comparison of topical steroids for acute anterior uveitis. J Ocul Pharmacol Ther, 20(6), 533-547. doi: 10.1089/jop.2004.20.533

Selicharova, Irena, Sanda, Miloslav, Miadkova, J, Ohri, Sujata Saraswat, Vashishta, Aruna, Fusek, Martin, . . . Vetvicka, Vaclav. (2008). 2-DE analysis of breast cancer cell lines 1833 and 4175 with distinct metastatic organ-specific potentials: comparison with parental cell line MDA-MB-231. Oncology reports, 19(5), 1237-1244.

Sendrowski, D.P., Jaanus, S.D., Semes, L.P., & Stern, M.E. (2008). Anti-Inflammatory Drugs (5th ed.). New York, NY: Elsevier Health Sciences.

Sherif, Z., & Pleyer, U. (2002). Corticosteroids in ophthalmology: past-present-future. Ophthalmologica, 216(5), 305-315. doi: 66189

Sigurdsson, H. H., Konraethsdottir, F., Loftsson, T., & Stefansson, E. (2007). Topical and systemic absorption in delivery of dexamethasone to the anterior and posterior segments of the eye. Acta Ophthalmol Scand, 85(6), 598-602. doi: 10.1111/j.1600-0420.2007.00885.x

Singh, Arun D, & Borden, Ernest C. (2005). Metastatic uveal melanoma. Ophthalmology clinics of North America, 18(1), 143-150, ix.

Singh, Arun D, & Topham, Allan. (2003). Survival rates with uveal melanoma in the United States: 1973–1997. Ophthalmology, 110(5), 962-965.

Steely, H. T., Jr., & Clark, A. F. (2000). The use of proteomics in ophthalmic research. Pharmacogenomics, 1(3), 267-280. doi: 10.1517/14622416.1.3.267

Stoilov, I, Jansson, Ingela, Sarfarazi, M, & Schenkman, John B. (2001). Roles of cytochrome p450 in development. Drug metabolism and drug interactions, 18(1), 33-56.

Stone, Edwin M, Fingert, John H, Alward, Wallace LM, Nguyen, Thai D, Polansky, Jon R, Sunden, Sara LF, . . . Nichols, Brian E. (1997). Identification of a gene that causes primary open angle glaucoma. Science, 275(5300), 668-670.

Urtti, A. (2006). Challenges and obstacles of ocular pharmacokinetics and drug delivery. Adv Drug Deliv Rev, 58(11), 1131-1135. doi: 10.1016/j.addr.2006.07.027

Vadlapudi, A.D., Ashaben, P. , Kishore, C., & Ashim, K.M. (2012). Recent Patents on Emerging Therapeutics for the Treatment of Glaucoma, Age Related Macular Degeneration and Uveitis. Recent Pat Biomed Eng, 5(1), 83-101.

Verteporfin In Photodynamic Therapy Study, Group. (2001). Verteporfin therapy of subfoveal choroidal neovascularization in age-related macular degeneration: two-year results of a randomized clinical trial including lesions with occult with no classic choroidal neovascularization--verteporfin in photodynamic therapy report 2. Am J Ophthalmol, 131(5), 541-560.

Wadhwa, Sheetu, Paliwal, Rishi, Paliwal, Shivani R, & Vyas, SP. (2010). Hyaluronic acid modified chitosan nanoparticles for effective management of glaucoma: development, characterization, and evaluation. Journal of drug targeting, 18(4), 292-302.

Wang, Y. S., Friedrichs, U., Eichler, W., Hoffmann, S., & Wiedemann, P. (2002). Inhibitory effects of triamcinolone acetonide on bFGF-induced migration and tube formation in choroidal microvascular endothelial cells. Graefes Arch Clin Exp Ophthalmol, 240(1), 42-48.

Wang, Y., Wang, V. M., & Chan, C. C. (2011). The role of anti-inflammatory agents in age-related macular degeneration (AMD) treatment. Eye (Lond), 25(2), 127-139. doi: 10.1038/eye.2010.196

Wang, Yingchih, Mo, Li, Wei, Wenbin, & Shi, Xuehui. (2013). Efficacy and safety of dendrimer nanoparticles with coexpression of tumor necrosis factor-α and herpes simplex virus thymidine kinase in gene radiotherapy of the human uveal melanoma OCM-1 cell line. International journal of nanomedicine, 8, 3805.

Weinreb, Robert N, Kashiwagi, Kenji, Kashiwagi, Fumiko, Tsukahara, Shigeo, & Lindsey, James D. (1997). Prostaglandins increase matrix metalloproteinase release from human ciliary smooth muscle cells. Investigative ophthalmology & visual science, 38(13), 2772-2780.

Wong, Tina TL, Sethi, Charanjit, Daniels, Julie T, Limb, G Astrid, Murphy, Gillian, & Khaw, Peng T. (2002). Matrix metalloproteinases in disease and repair processes in the anterior segment. Survey of ophthalmology, 47(3), 239-256.

Wu, W. S., Wang, F. S., Yang, K. D., Huang, C. C., & Kuo, Y. R. (2006). Dexamethasone induction of keloid regression through effective suppression of VEGF expression and keloid fibroblast proliferation. J Invest Dermatol, 126(6), 1264-1271. doi: 10.1038/sj.jid.5700274

WuDunn, Darrell. (2002). Genetic basis of glaucoma. Current opinion in ophthalmology, 13(2), 55-60.

Zarbin, Marco Attilio, Montemagno, Carlo, Leary, James Francis, & Ritch, Robert. (2013). Nanomedicine for the treatment of retinal and optic nerve diseases. Current opinion in pharmacology, 13(1), 134-148.

Zhang, Li, Cilley, Robert E, & Chinoy, Mala R. (2000). Suppression subtractive hybridization to identify gene expressions in variant and classic small cell lung cancer cell lines. Journal of Surgical Research, 93(1), 108-119.

Zhang, W., Prausnitz, M. R., & Edwards, A. (2004). Model of transient drug diffusion across cornea. J Control Release, 99(2), 241-258. doi: 10.1016/j.jconrel.2004.07.001

Zhao, Xiujun, Ramsey, Keri E, Stephan, Dietrich A, & Russell, Paul. (2004). Gene and protein expression changes in human trabecular meshwork cells treated with transforming growth factor-β. Investigative ophthalmology & visual science, 45(11), 4023-4034.

Zhou, Yixiong, Song, Xin, Jia, Renbin, Wang, Haibo, Dai, Liyan, Xu, Xiaofang, . . . Fan, Xianqun. (2010). Radiation ‐ inducible human tumor necrosis factor ‐ related apoptosis ‐ inducing ligand (TRAIL) gene therapy: a novel treatment for radioresistant uveal melanoma. Pigment cell & melanoma research, 23(5), 661-674.

Zhou, Zhaohui, & Vollrath, Douglas. (1999). A cellular assay distinguishes normal and mutant TIGR/myocilin protein. Human molecular genetics, 8(12), 2221-2228.